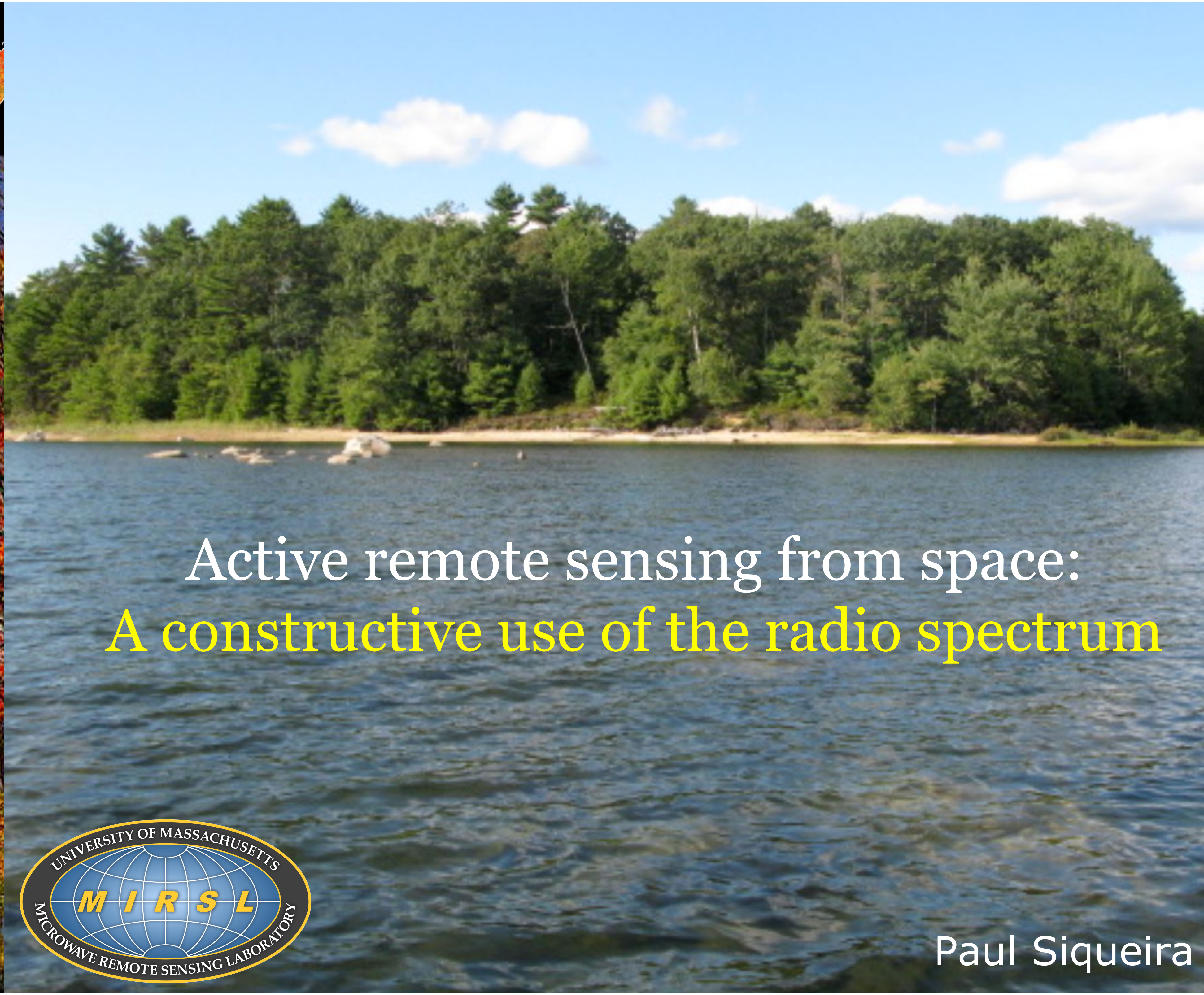

Active remote sensing from space:
A constructive use of the radio spectrum

UNIVERSITY OF MASSACHUSETTS
MIRSL
MICROWAVE REMOTE SENSING LABORATORY

Paul Siqueira

The Vantage Point of Space

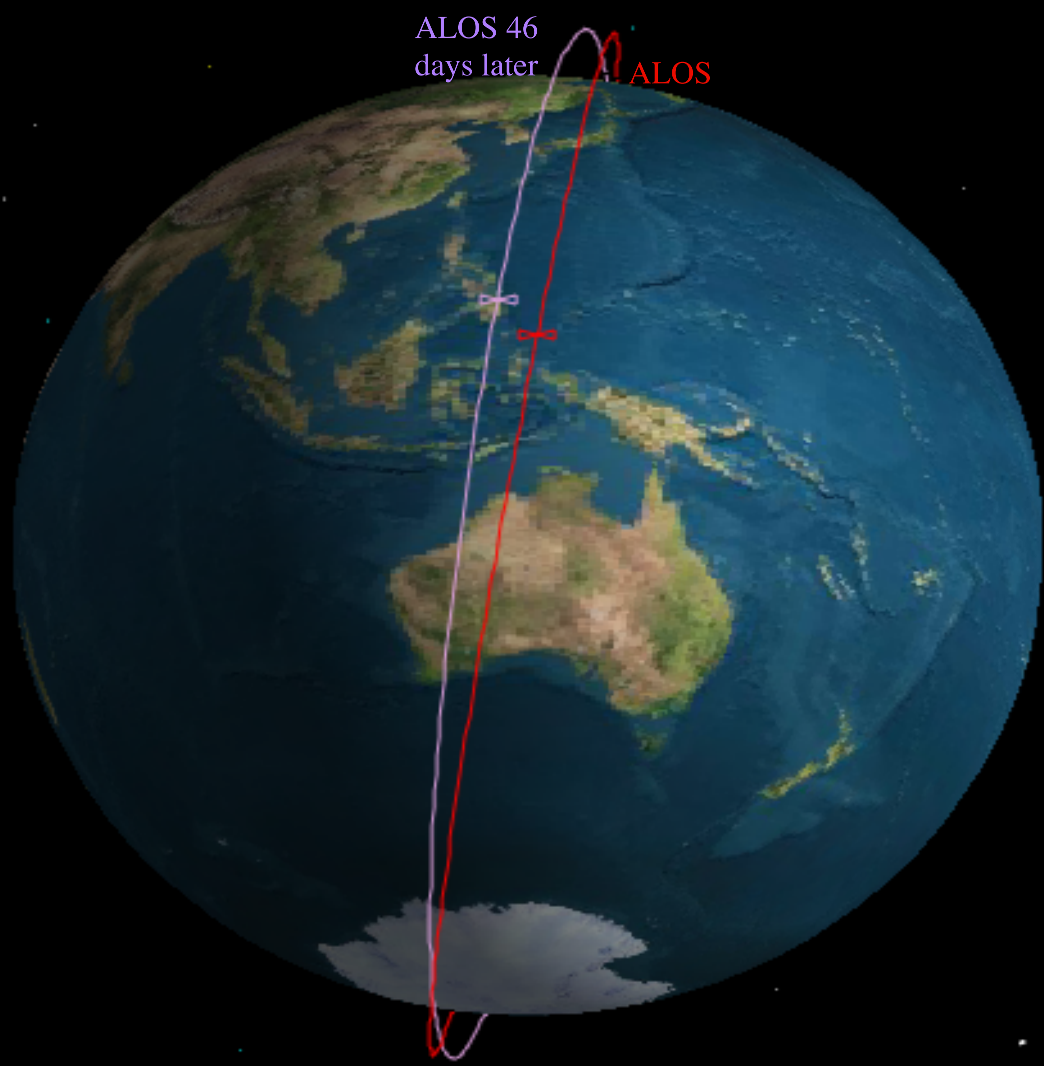

The Water and Energy Cycles

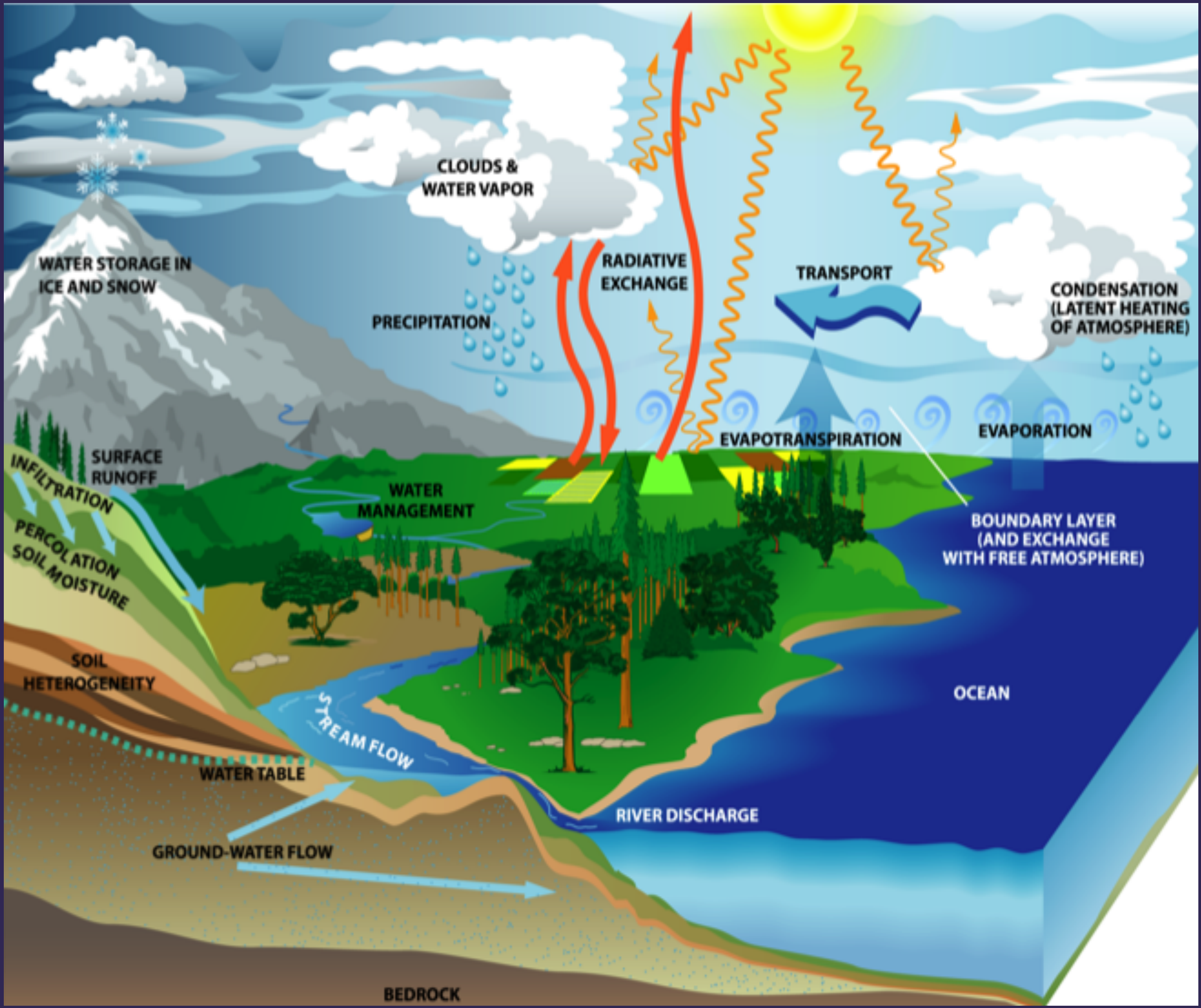

The Carbon Cycle

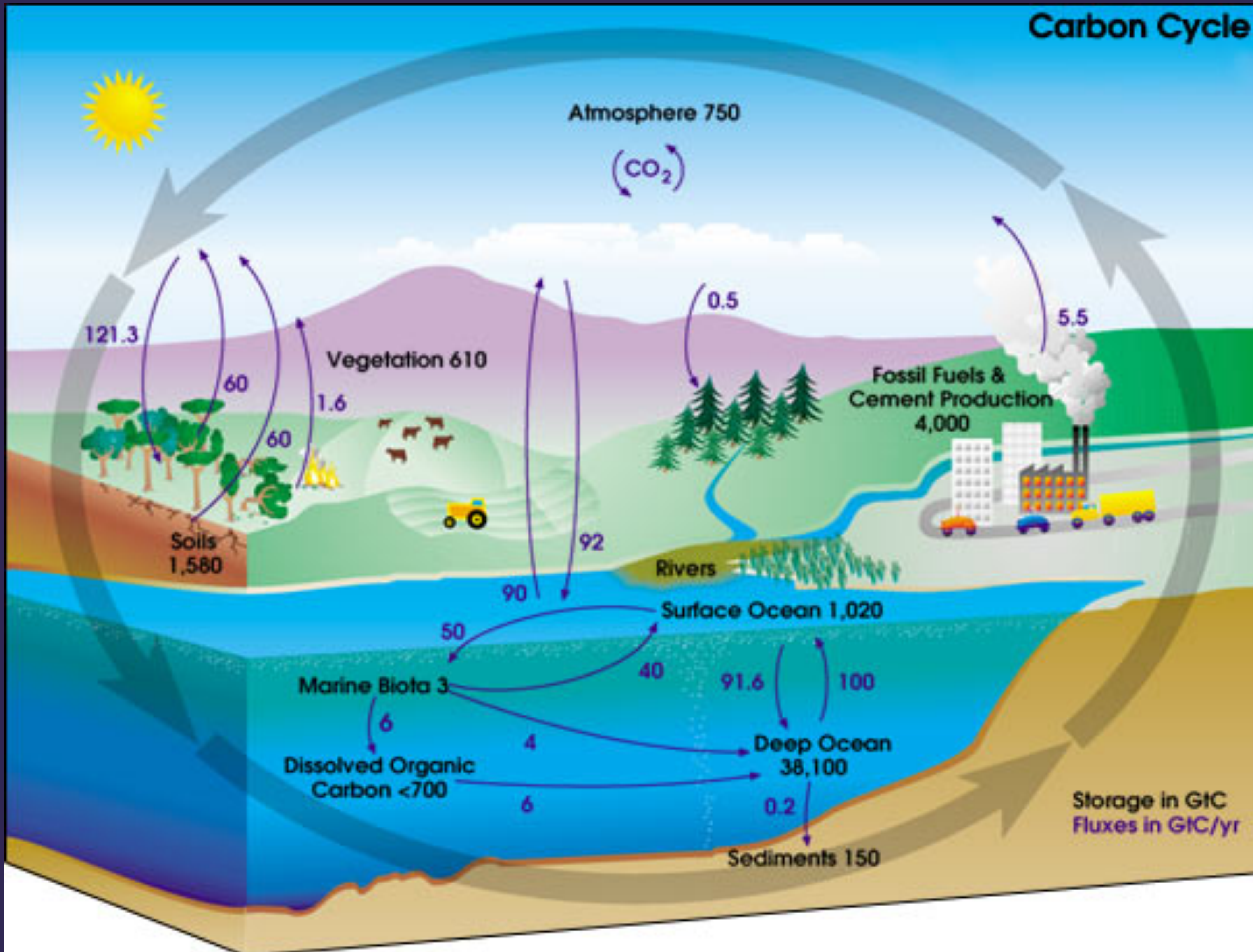

In any given year, tens of billions of tons of carbon move between the atmosphere, hydrosphere, and geosphere. Human activities add about 5.5 billion tons per year of carbon dioxide to the atmosphere. The illustration above shows total amounts of stored carbon in black, and annual carbon fluxes in purple. (Illustration courtesy NASA Earth Science Enterprise)

Human induced effects on Global Warming

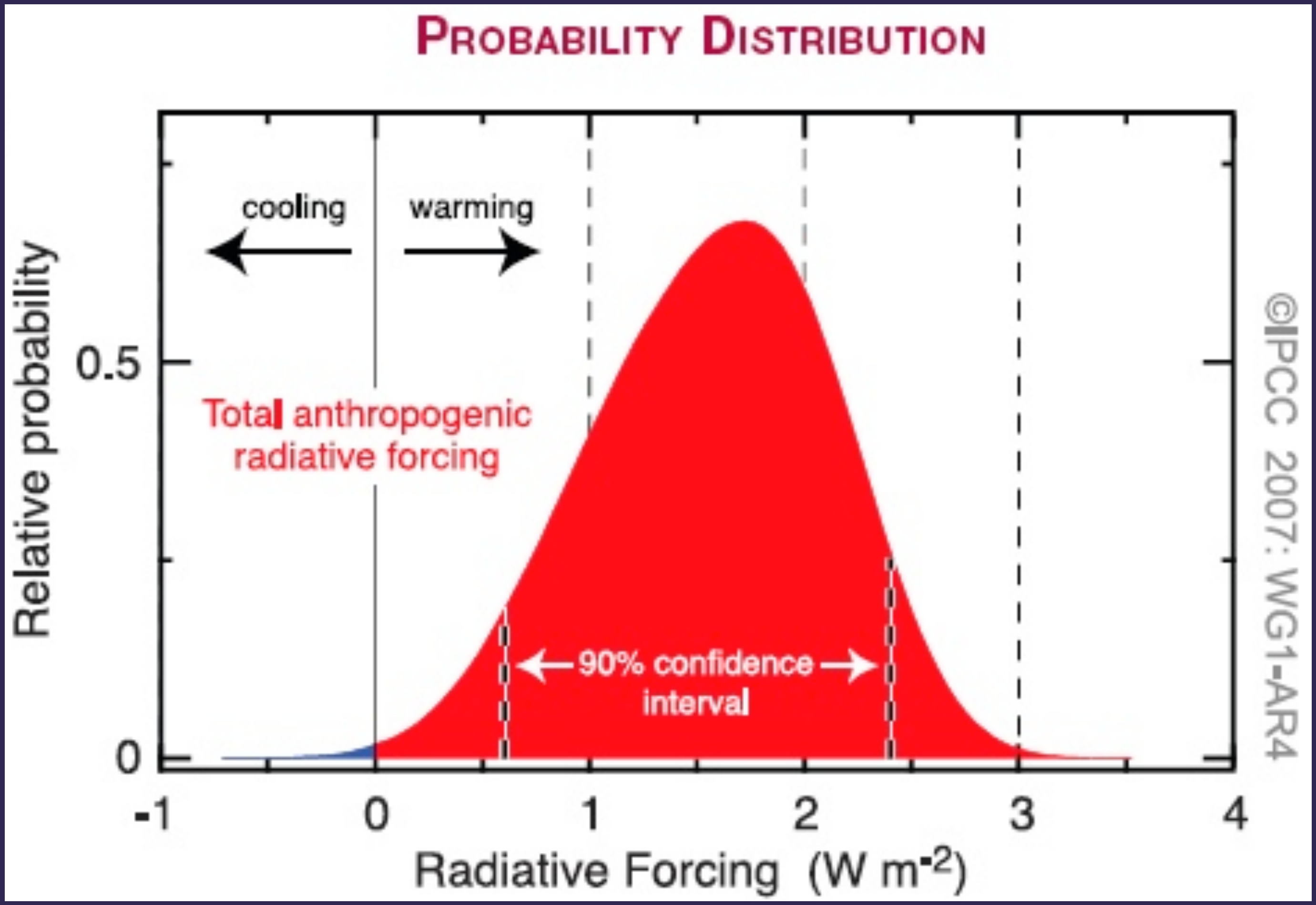

The need for measurement accuracy

Penzias &
Wilson 1968

Vegetation and Terrestrial Carbon Storage

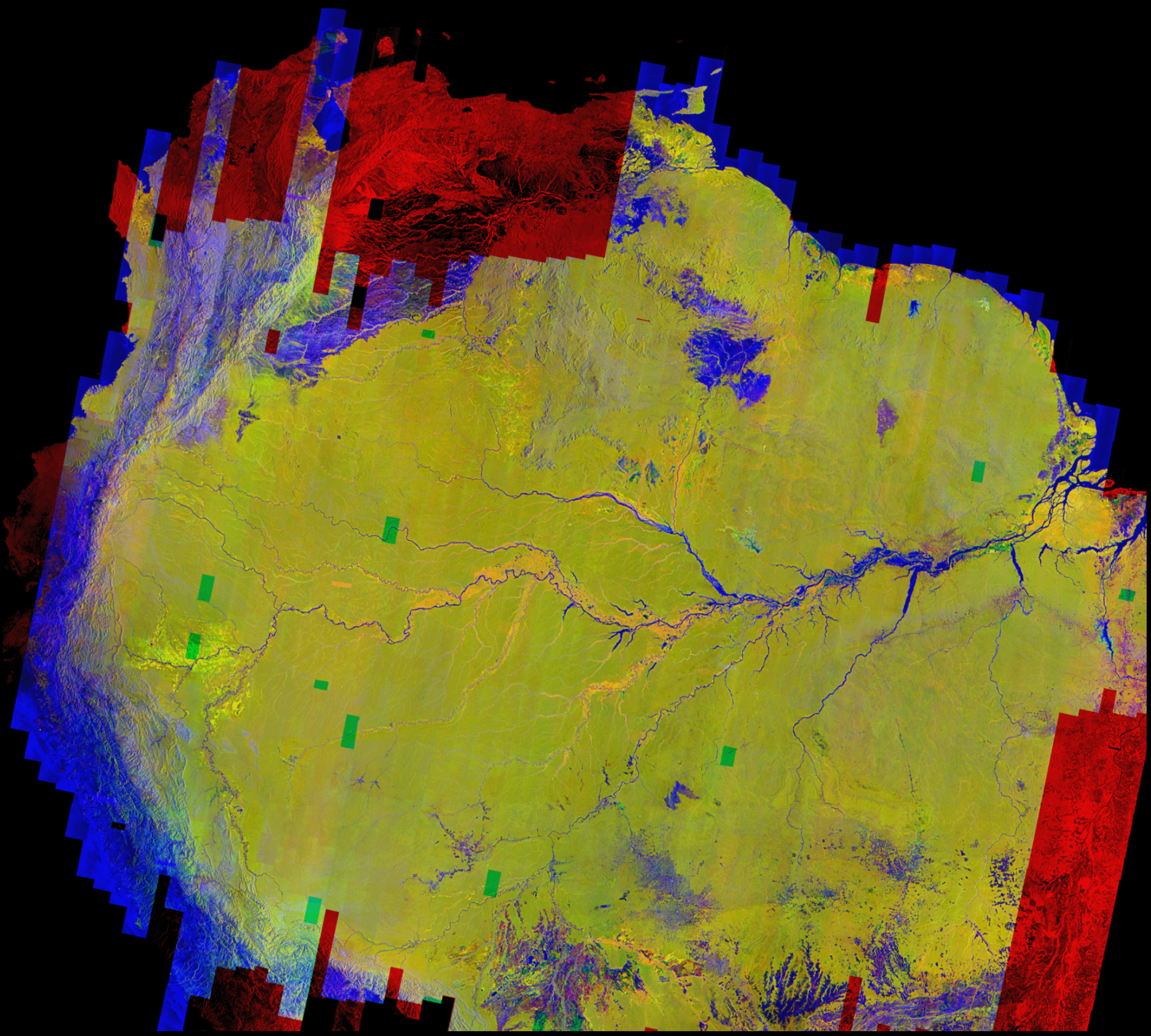

Building Blocks

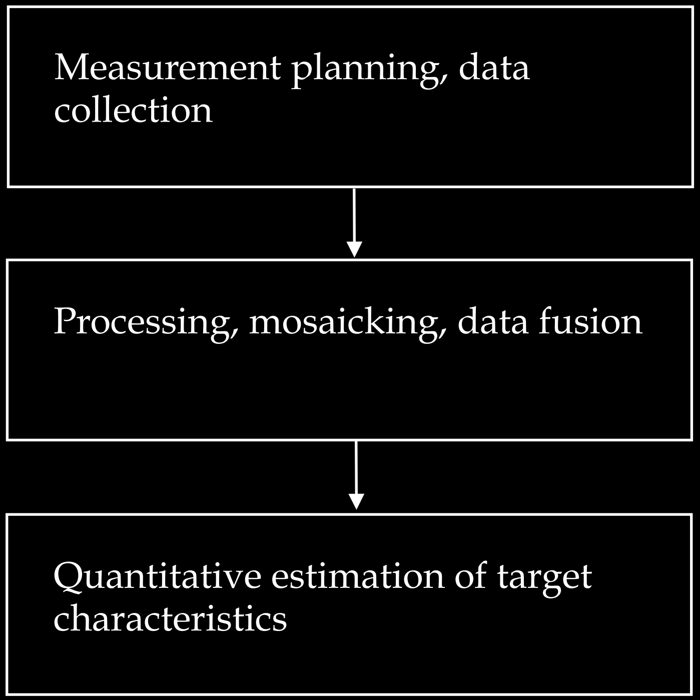

The Connecticut River Valley

Ikonos

L-Band SAR

Microwaves are primarily senstive to structure and water content

25m L-band SAR coverage of Earth Surfaces (JERS-1; 1995)

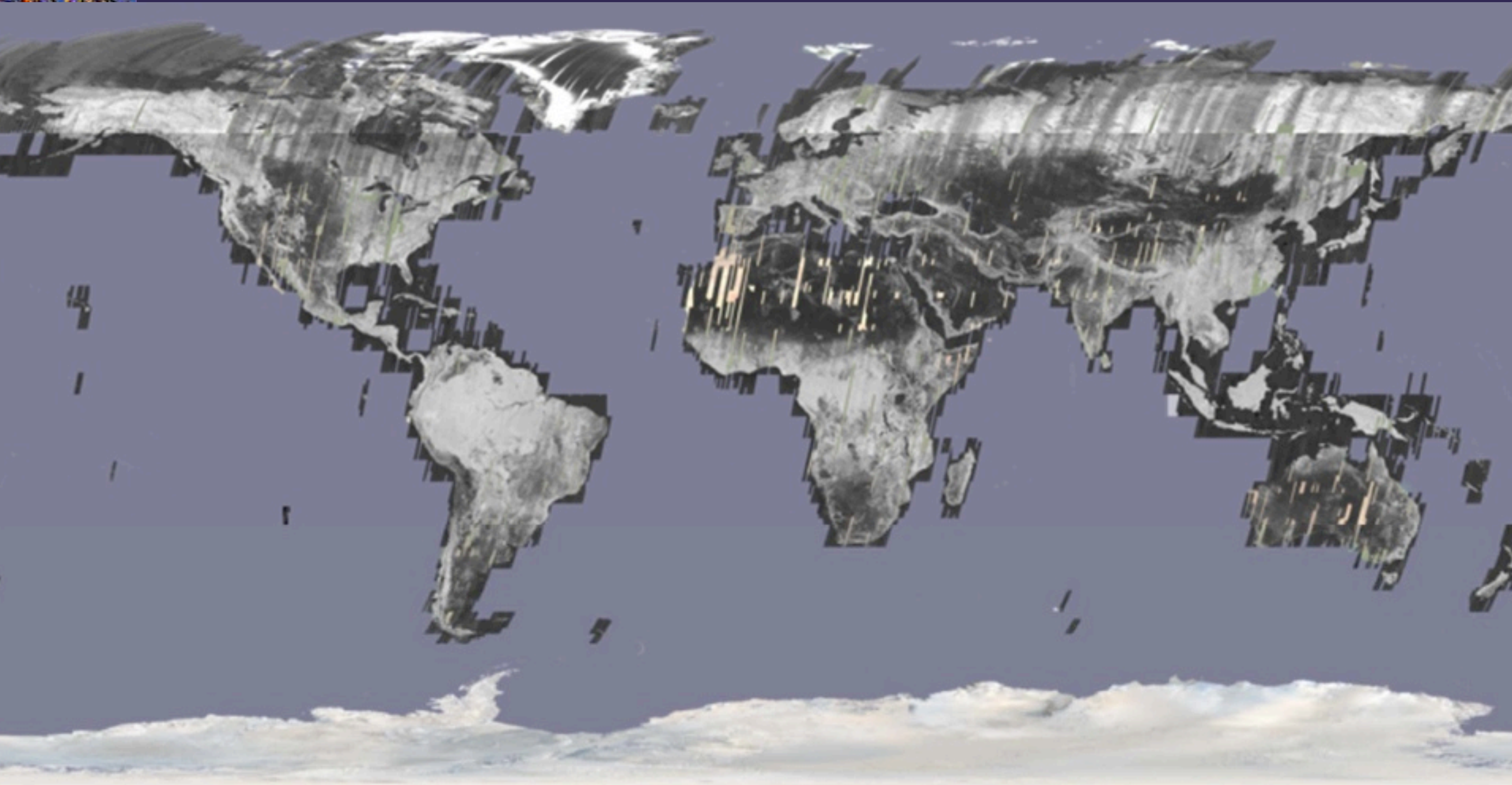

How Synthetic Aperture Radar Works

getting high resolution from a far distance

Range Resolution

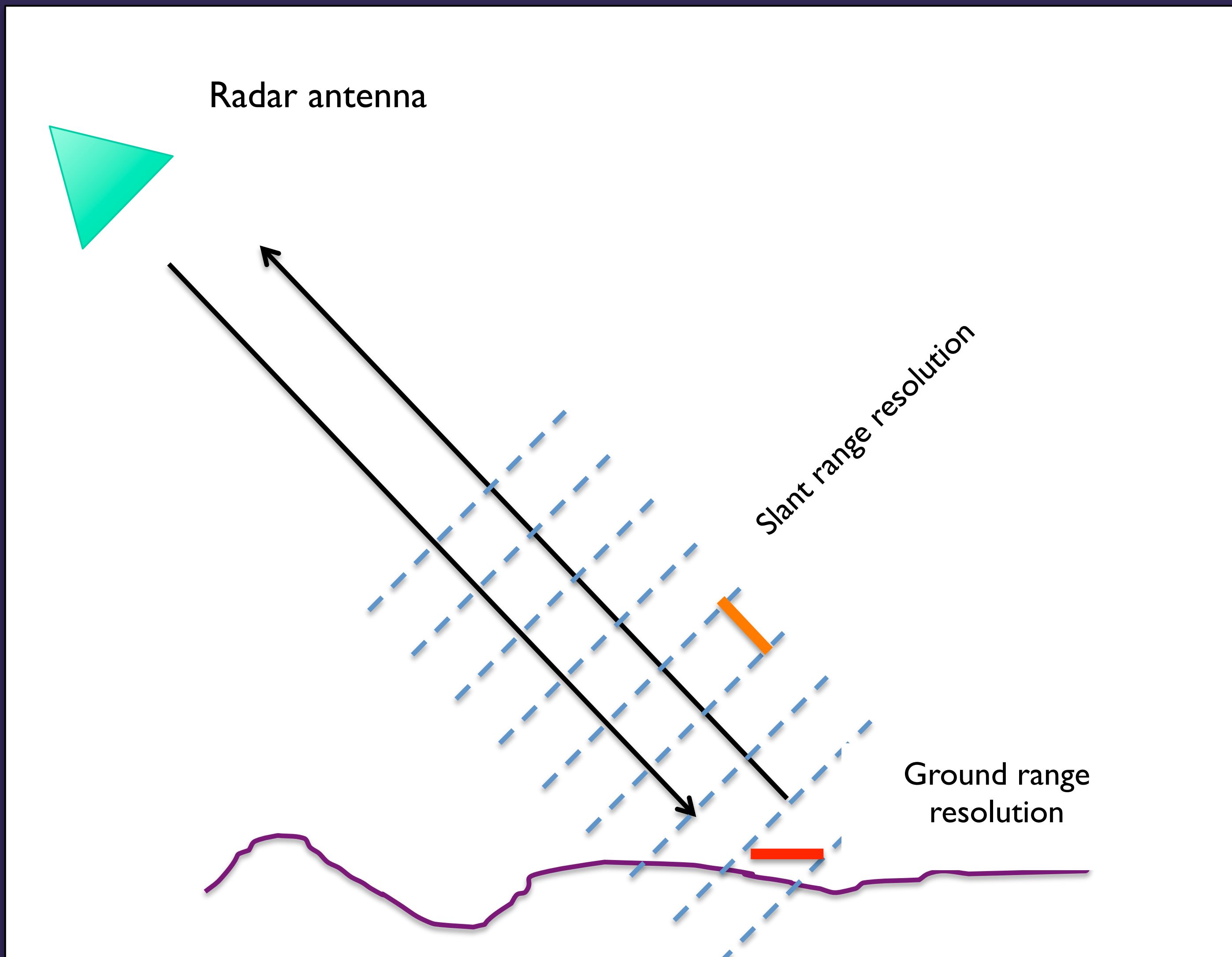

Synthesizing an Aperture to Improve Azimuth Resolution

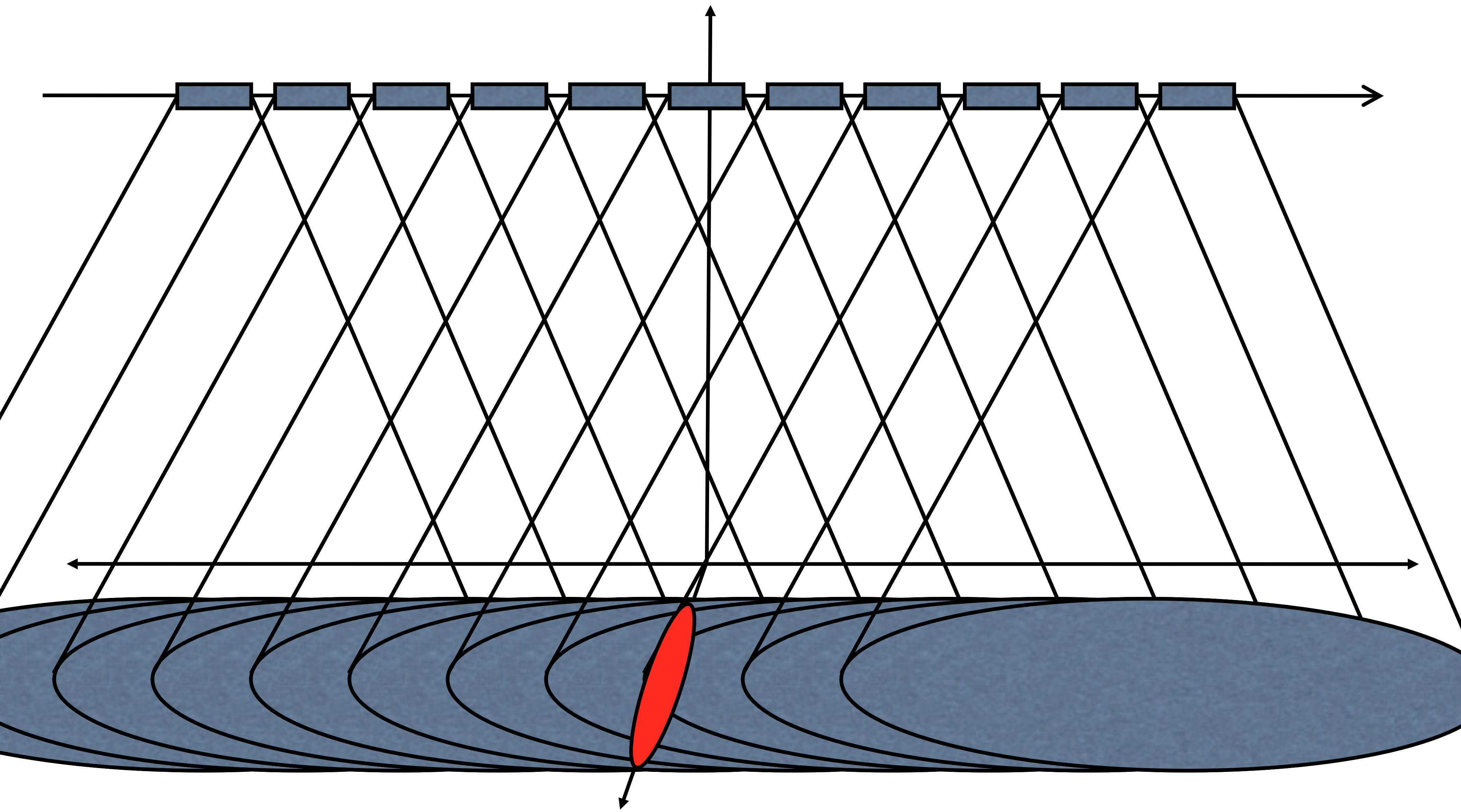

SAR Processing:
an alternate view using Doppler history

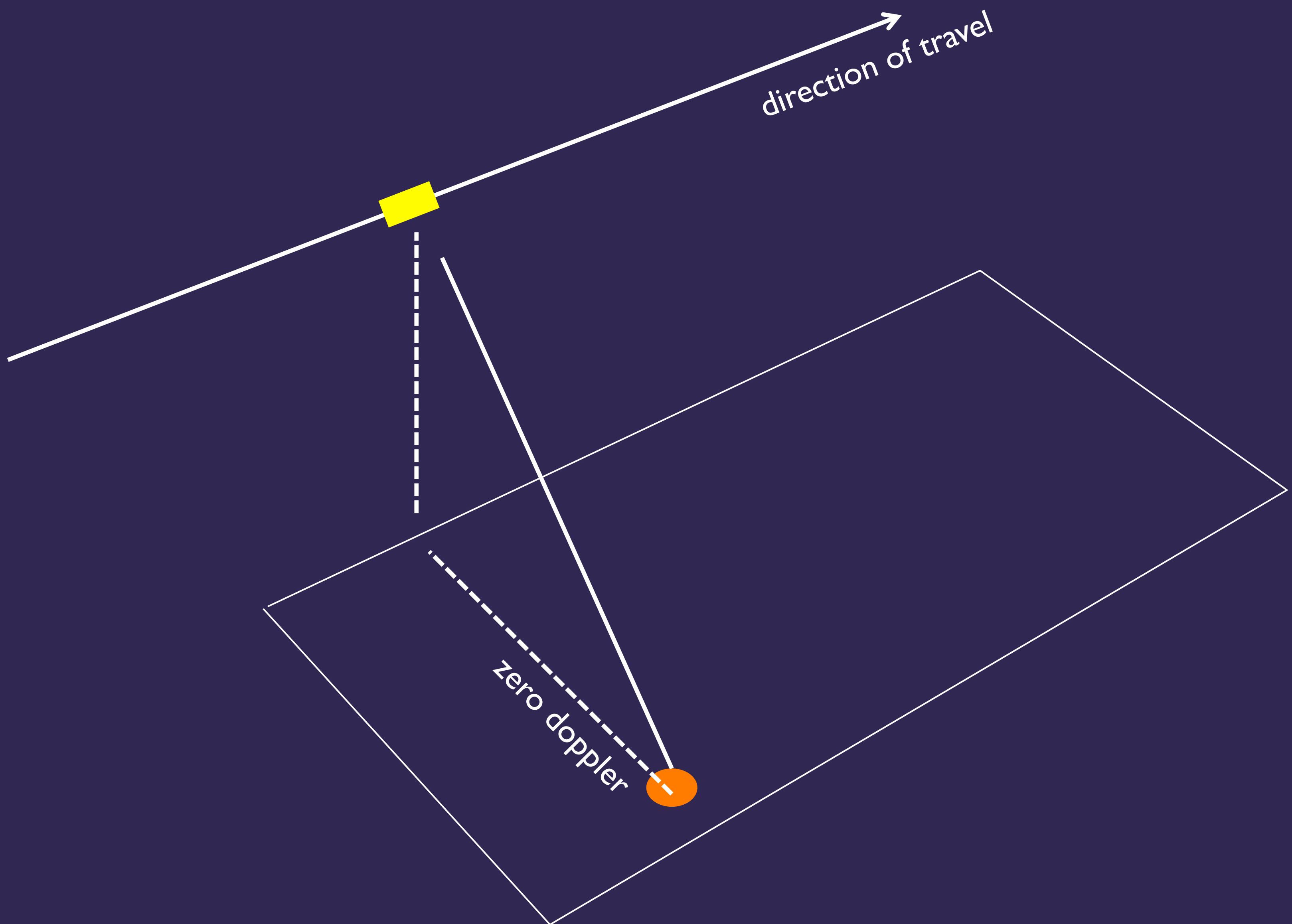

SAR Processing:
an alternate view using Doppler history

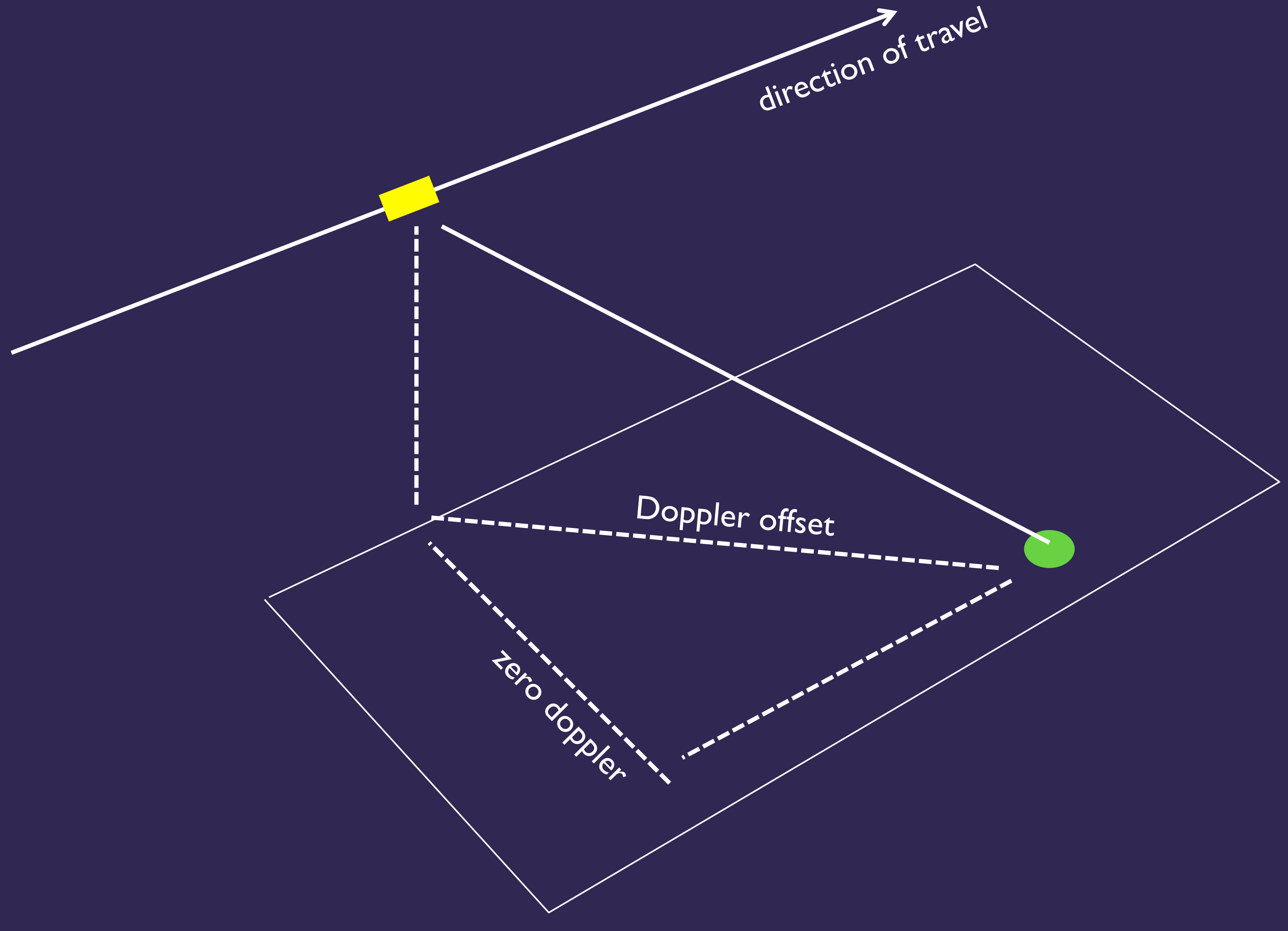

Range and Doppler Histories

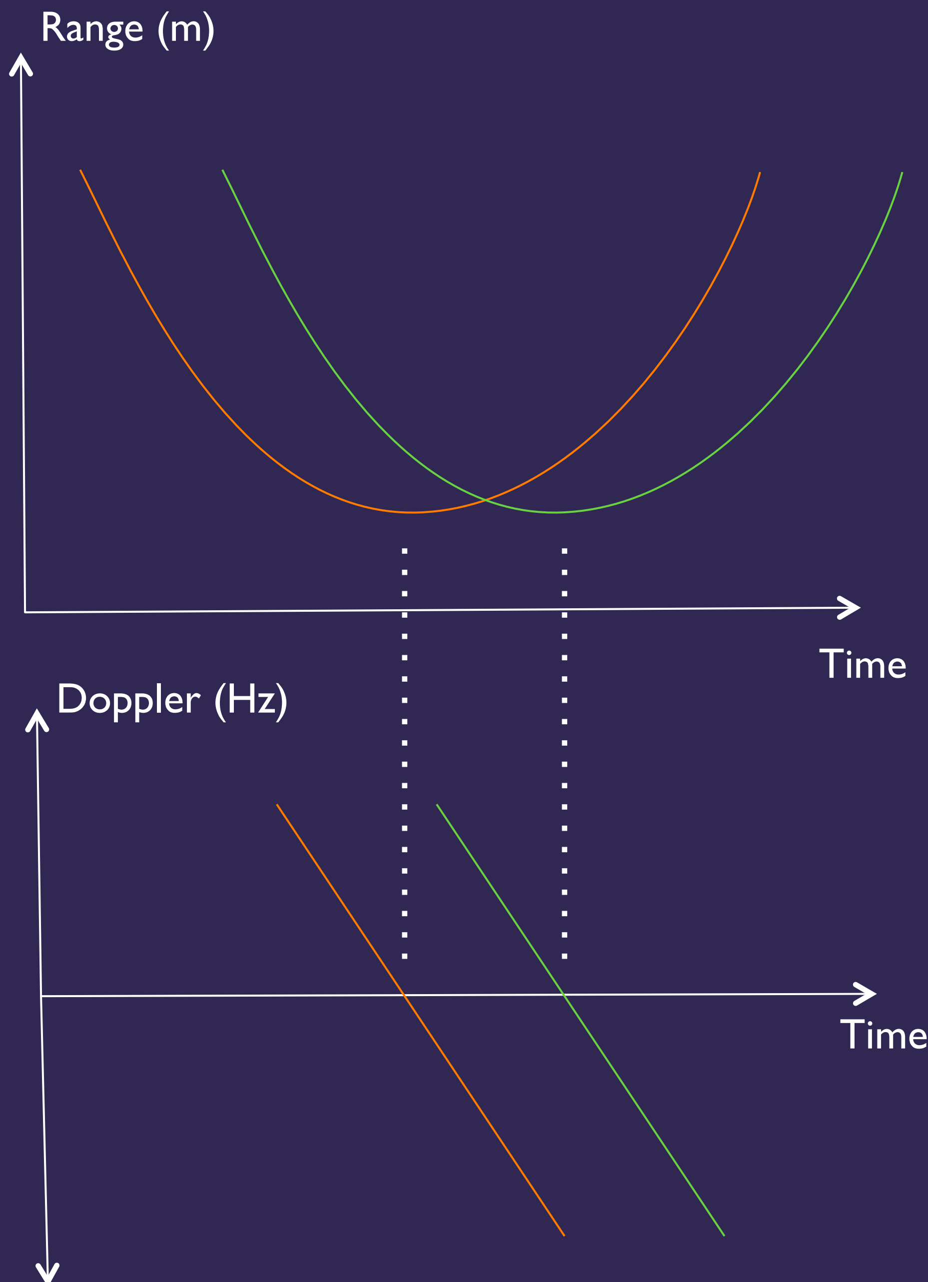

All targets in the imaged region will have unique range-doppler histories.

With matched filtering, these histories can be extracted to make a high-resolution image.

Results are based on well known metrics such as the Nyquist sampling theorem, and the relationship between bandwidth and resolution (Δf and Δt)

SAR Processing:
distributed targets

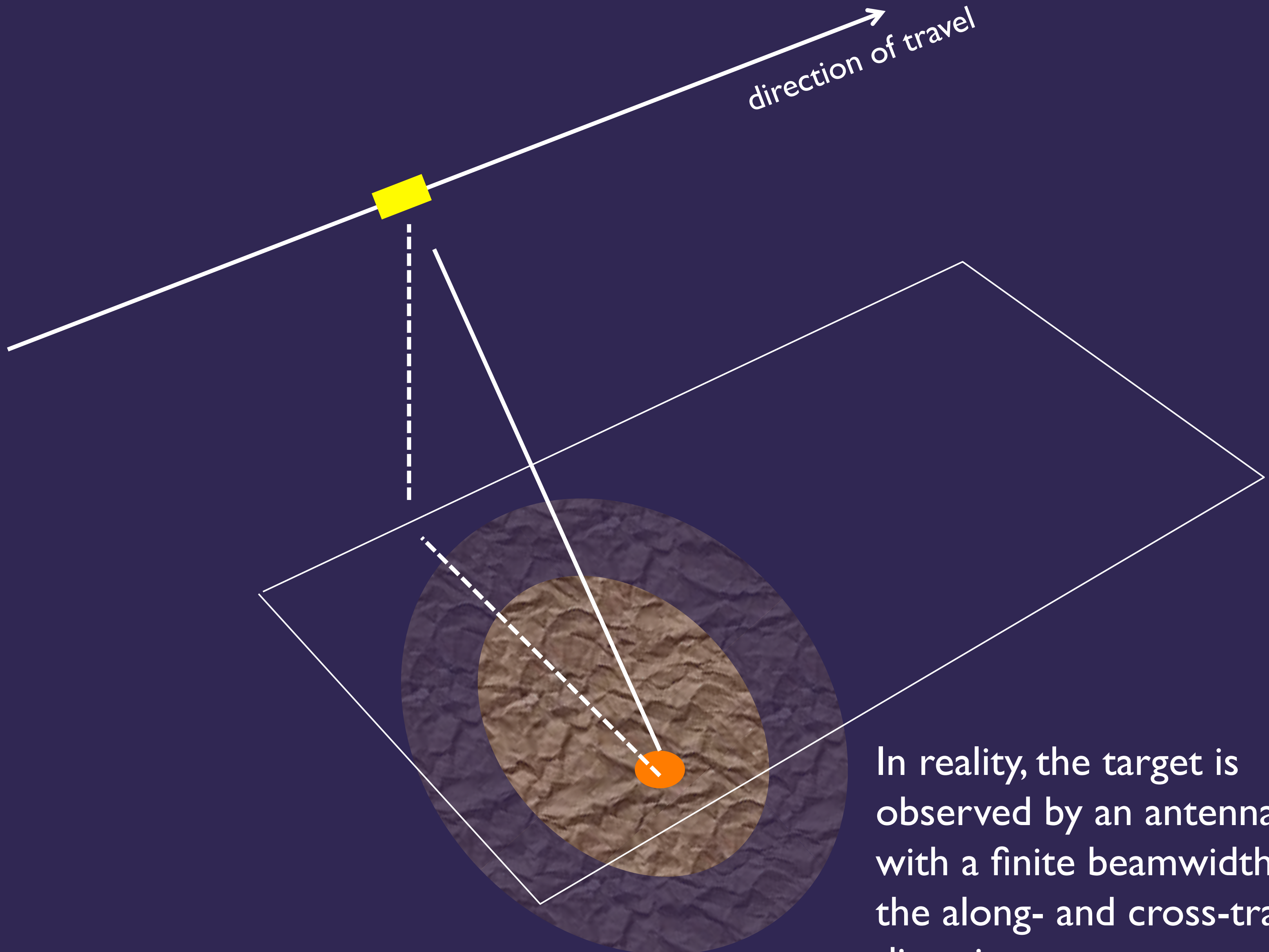

In reality, the target is observed by an antenna with a finite beamwidth in the along- and cross-track directions

Instantaneous Doppler Spectrum

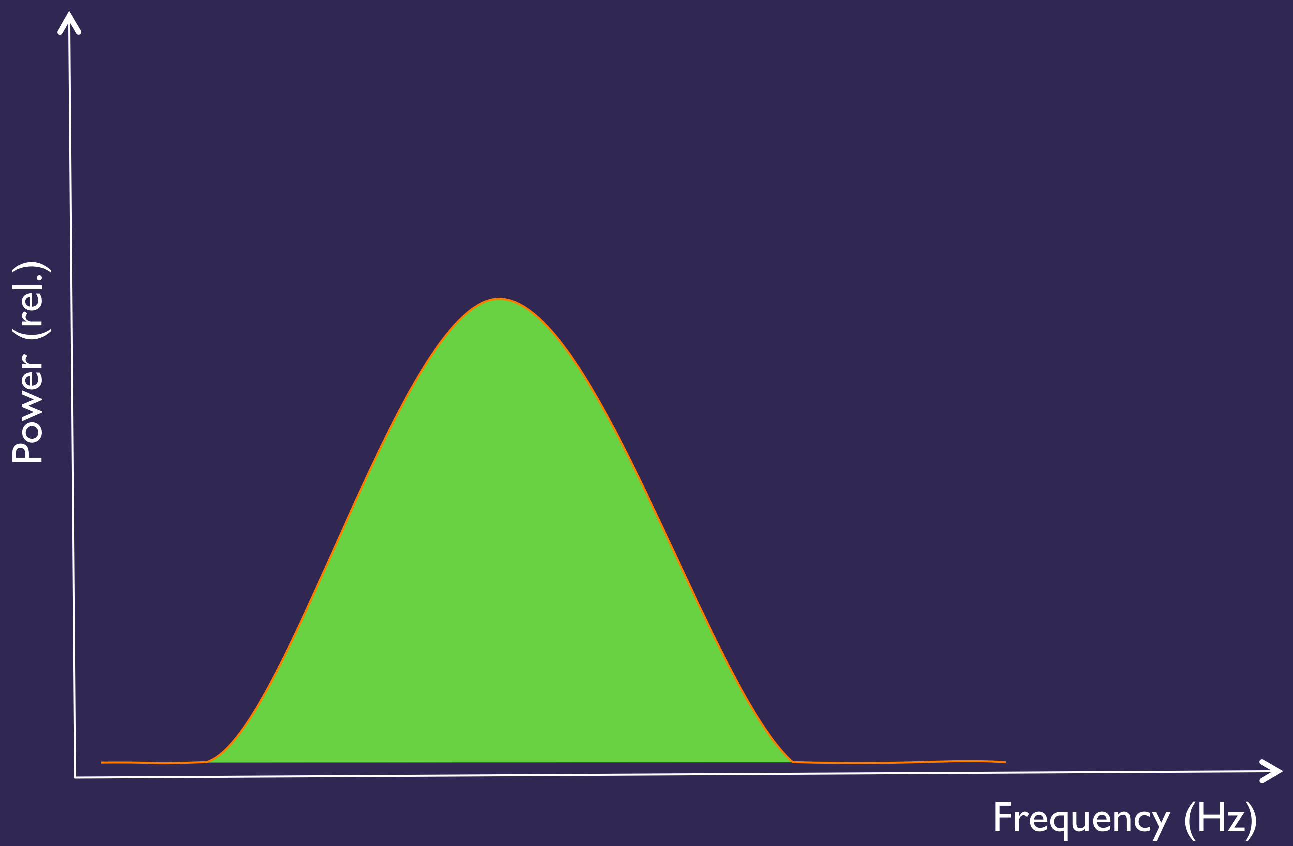

The spectrum of the received signal for any one particular range, is governed by the width of the azimuth antenna pattern

Instantaneous Doppler Spectrum

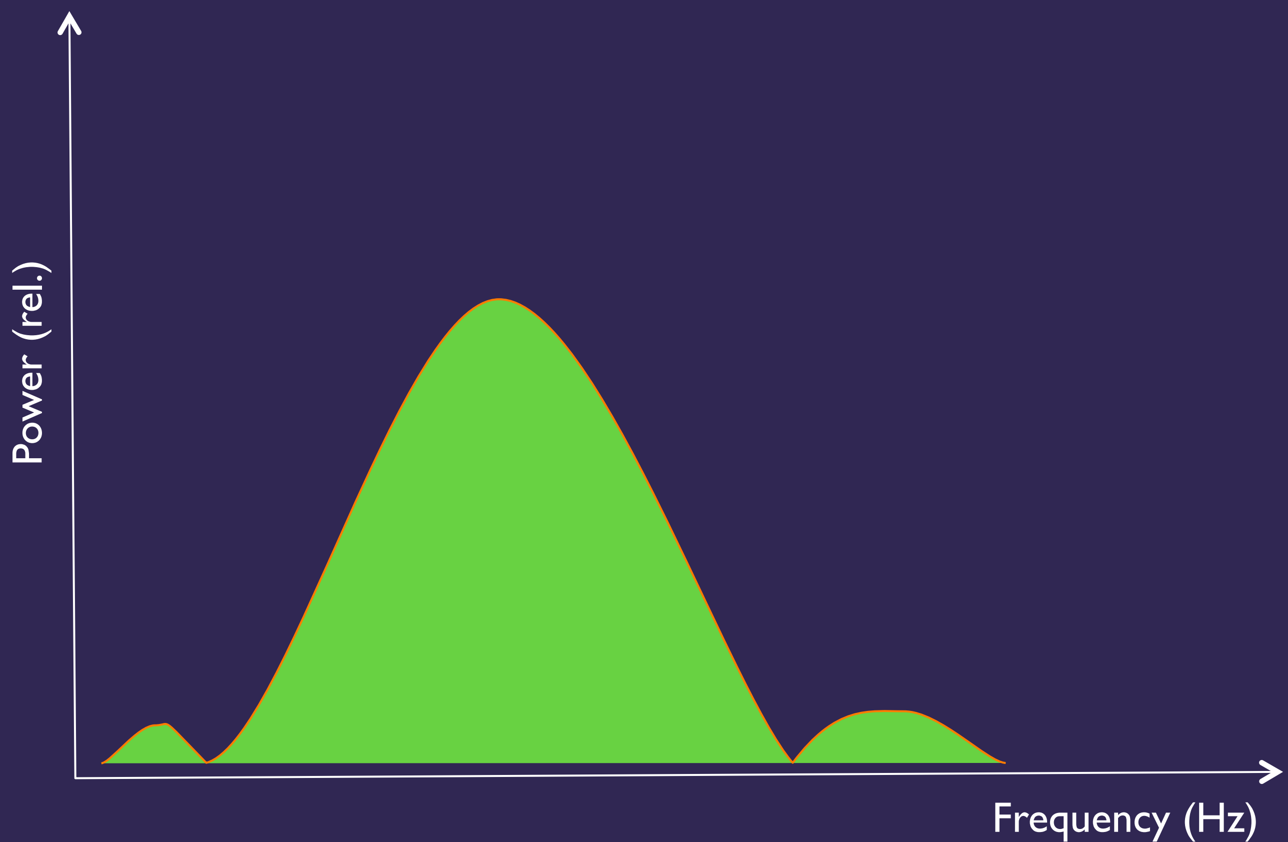

In reality, there are sidelobes in the azimuth pattern

Azimuth Sampling

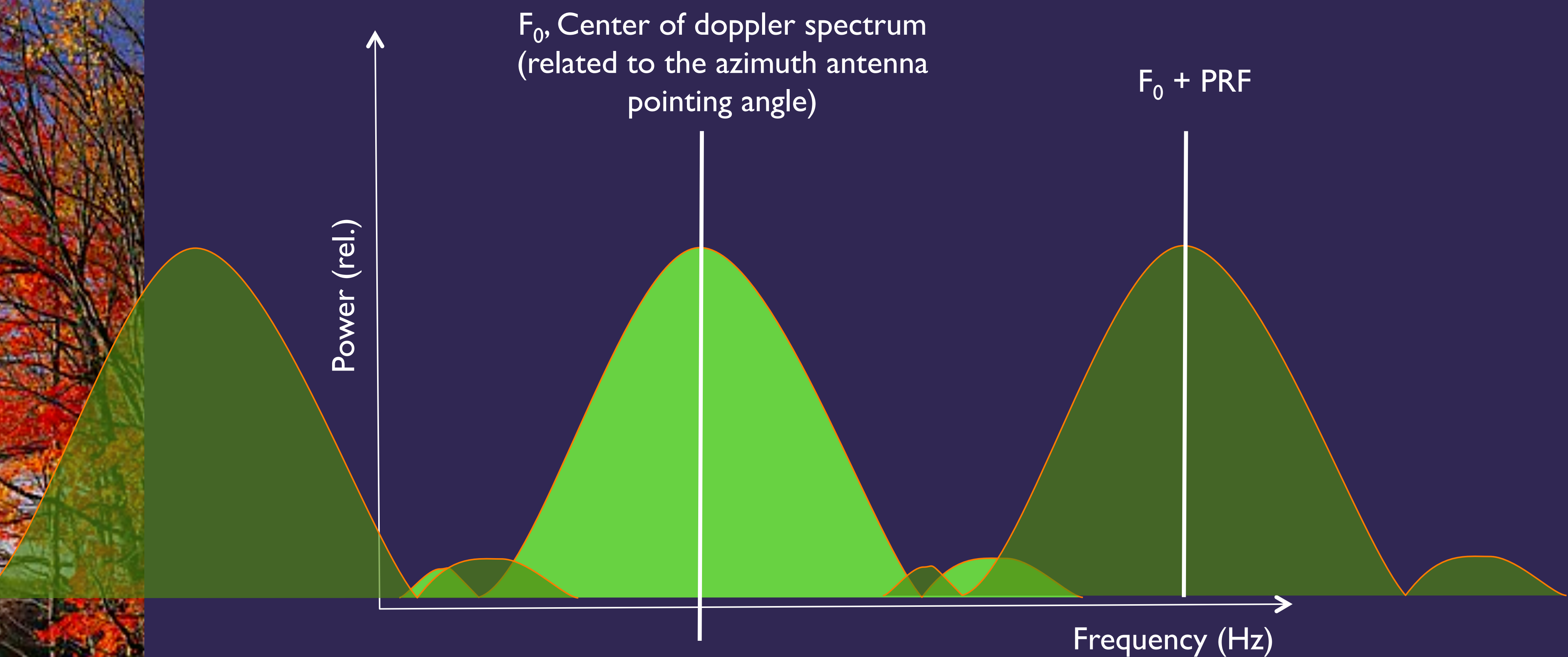

Since we are not continuously sampling the Doppler spectrum, we have the potential for aliasing the signal (Azimuth Alias)

This is the same phenomenon of underpopulating an antenna array

How Synthetic Aperture Radar Works

getting high resolution from a far distance

Azimuth Resolution

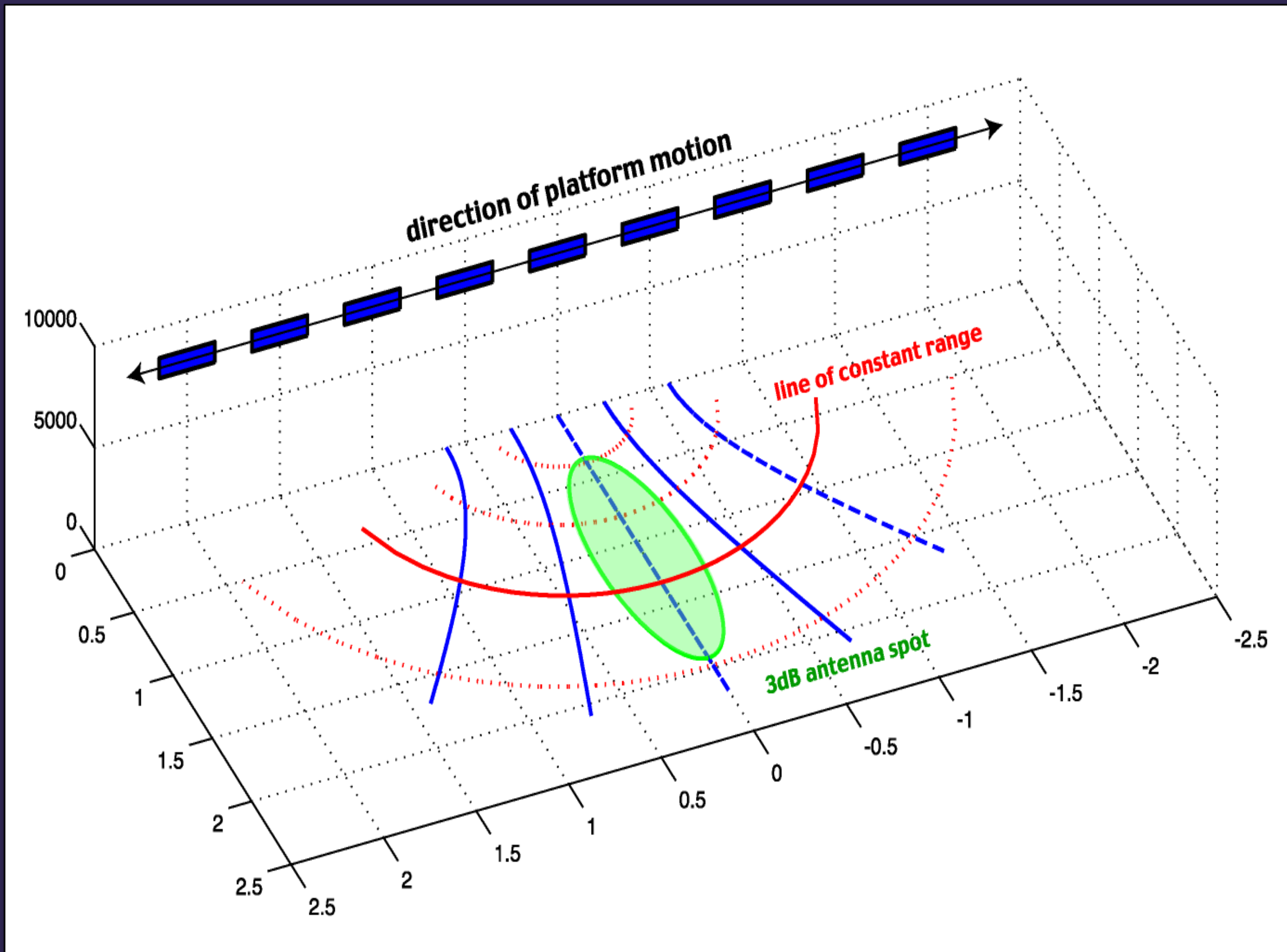

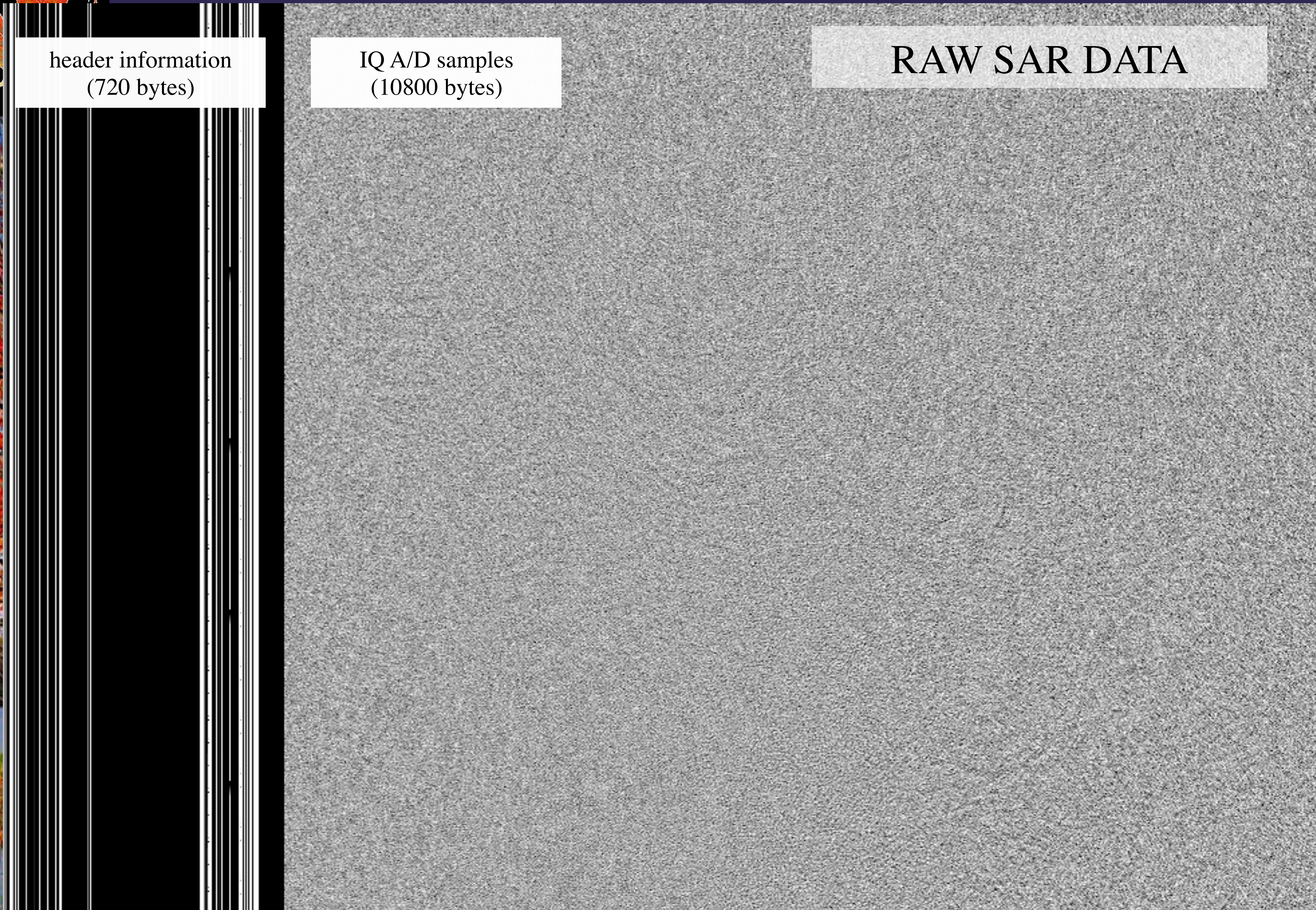
RAW SAR DATA
header information
(720 bytes)
IQ A/D samples
(10800 bytes)

RANGE COMPRESSED

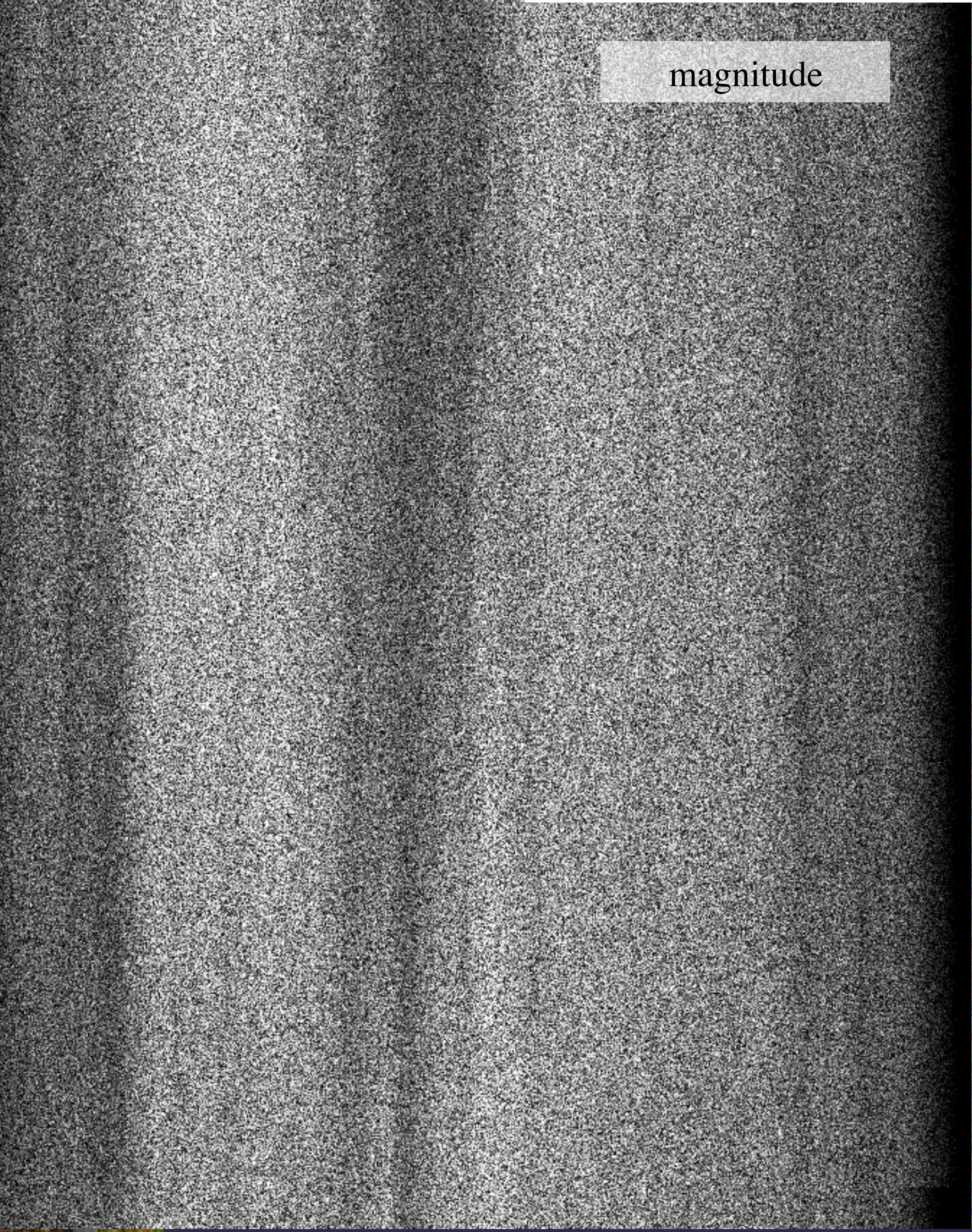

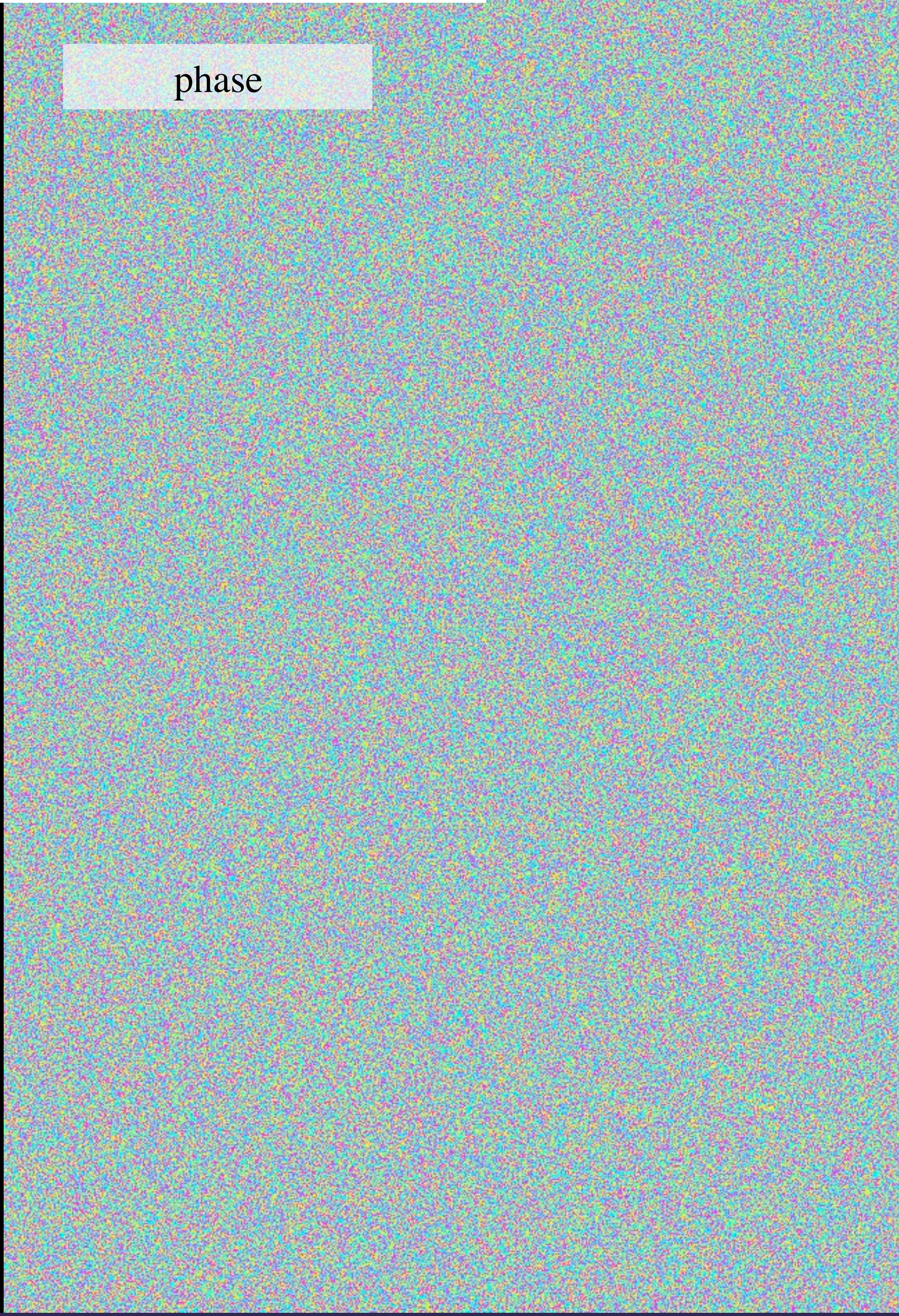

AZIMUTH (along track) COMPRESSED

magnitude

phase

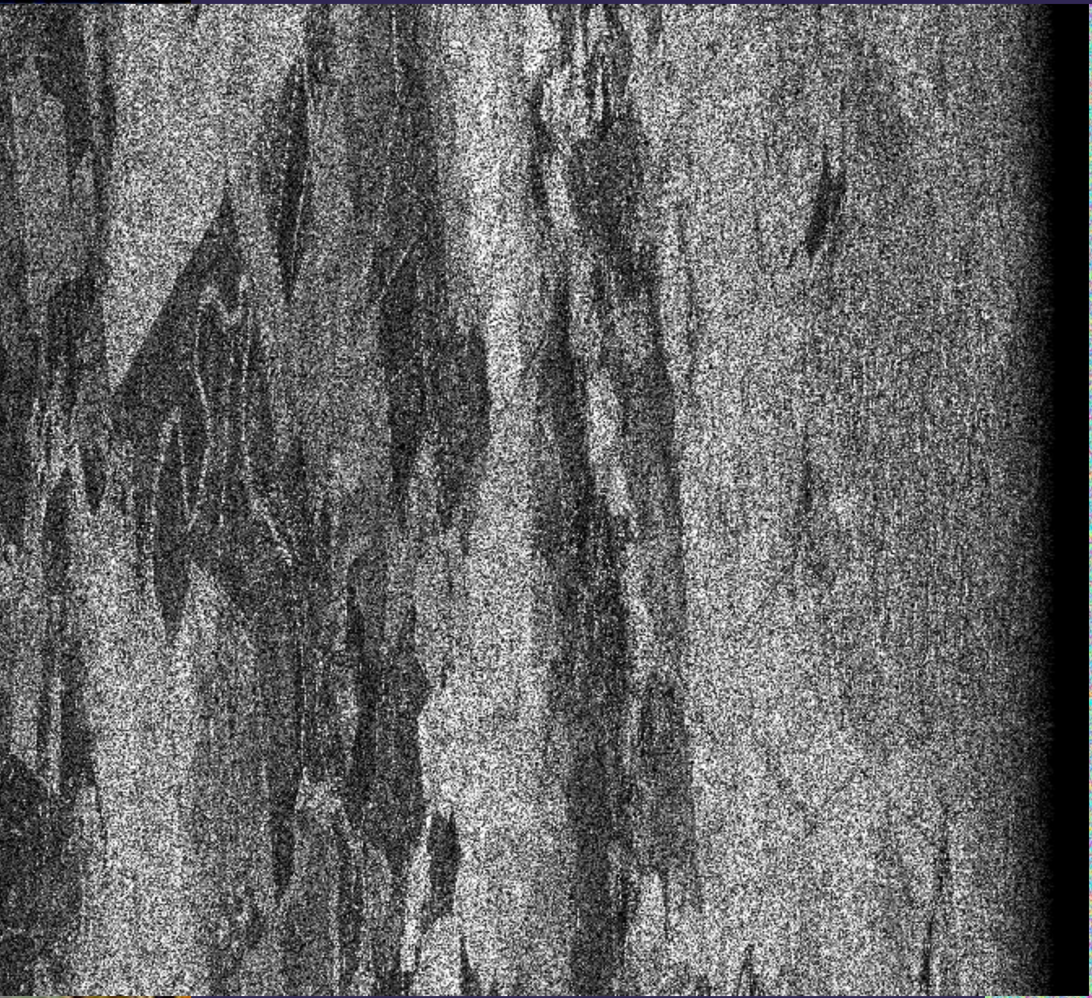

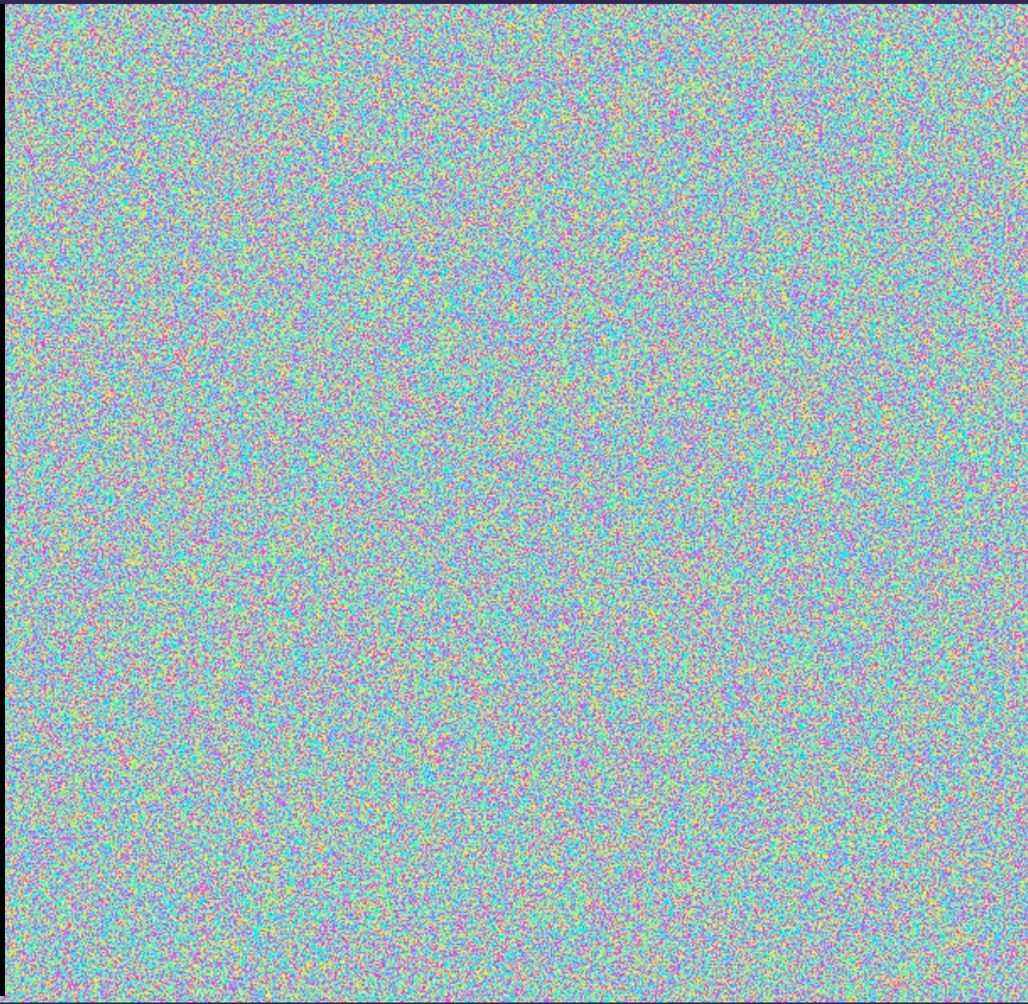

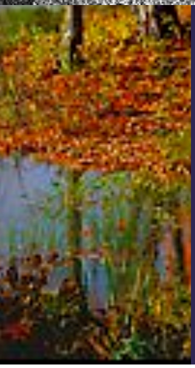

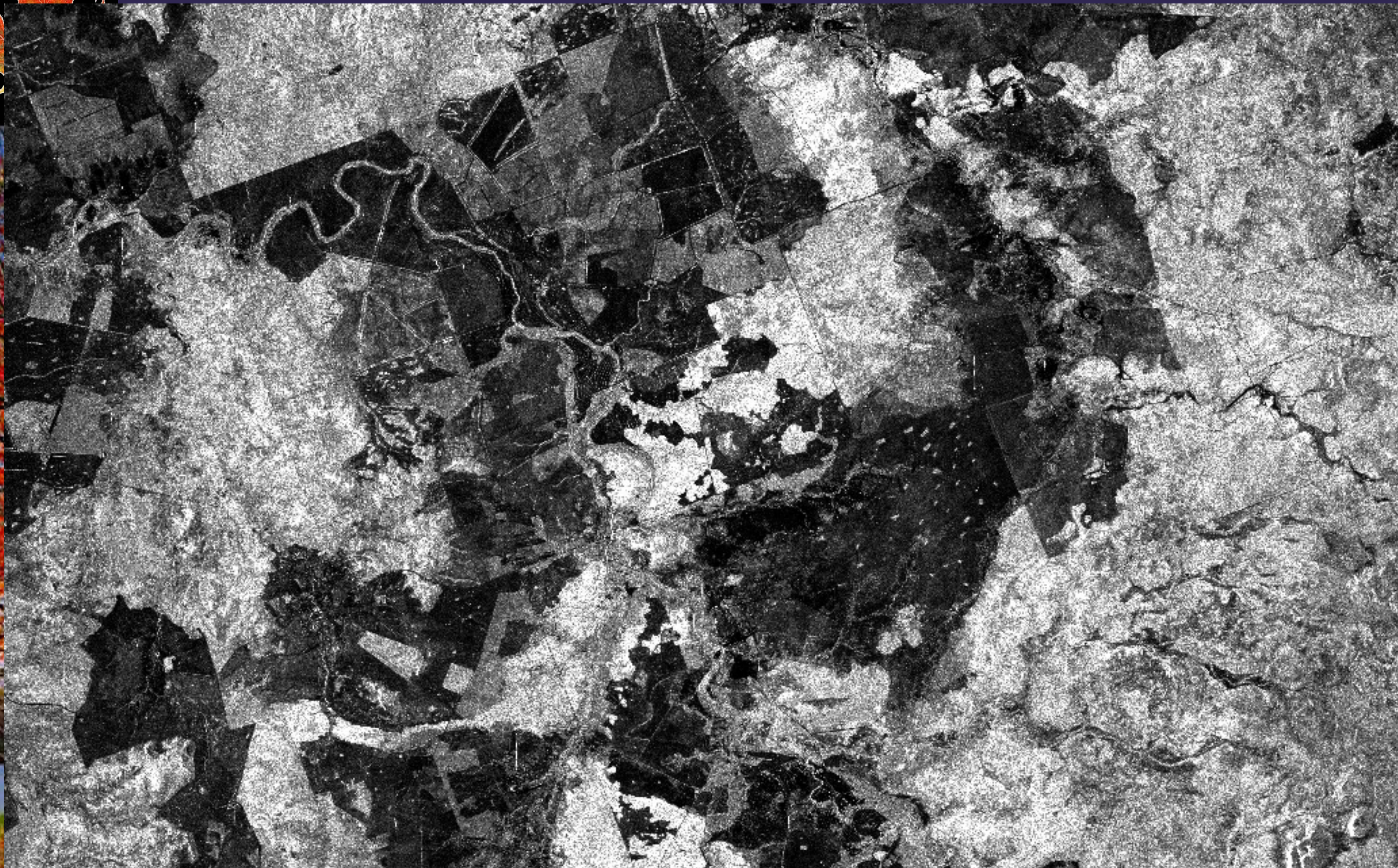

Magnitude after averaging in both azimuth and range

A Single SAR antenna

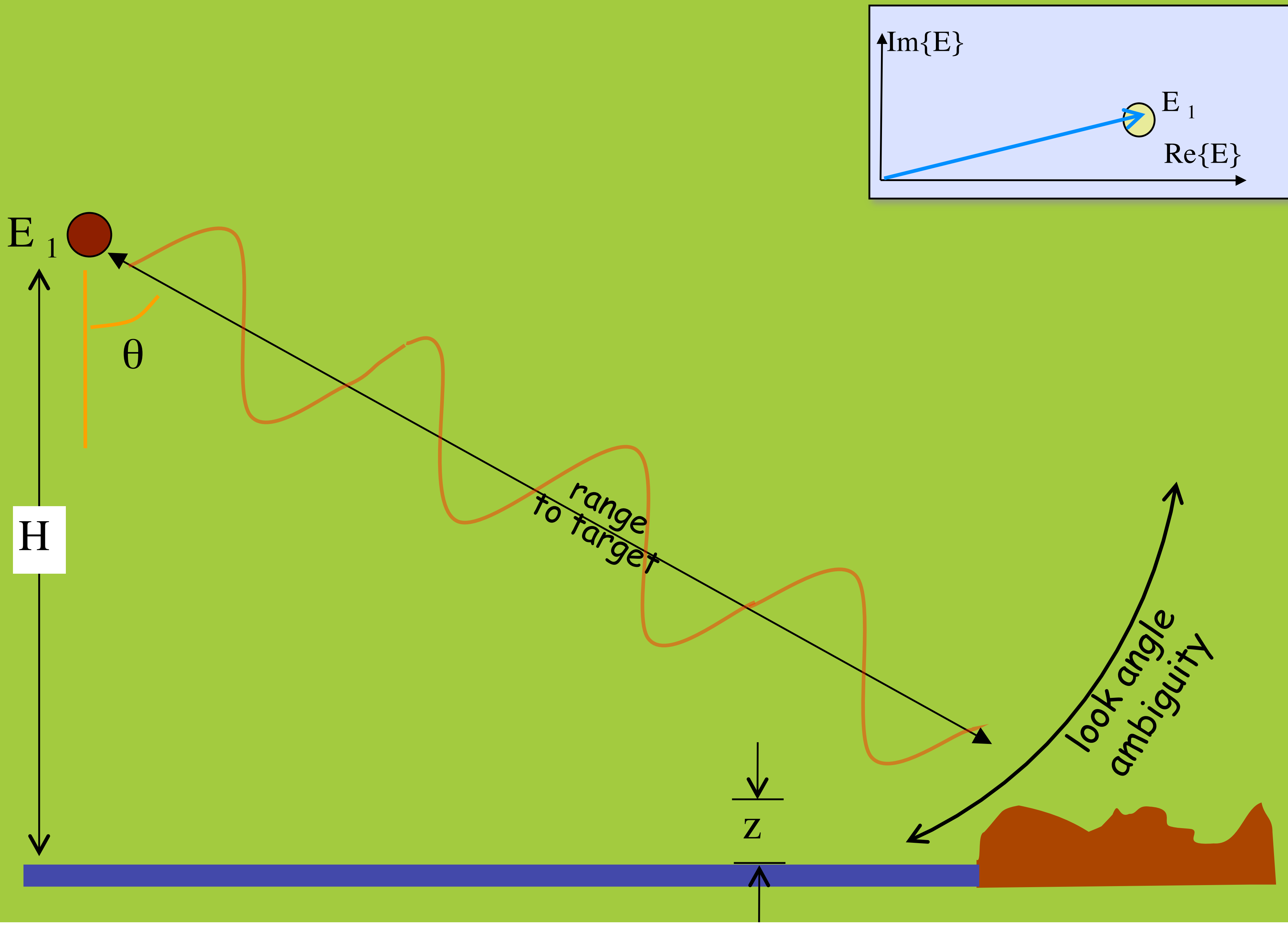

Interferometry Used to Measure Surface Topography and Deformation

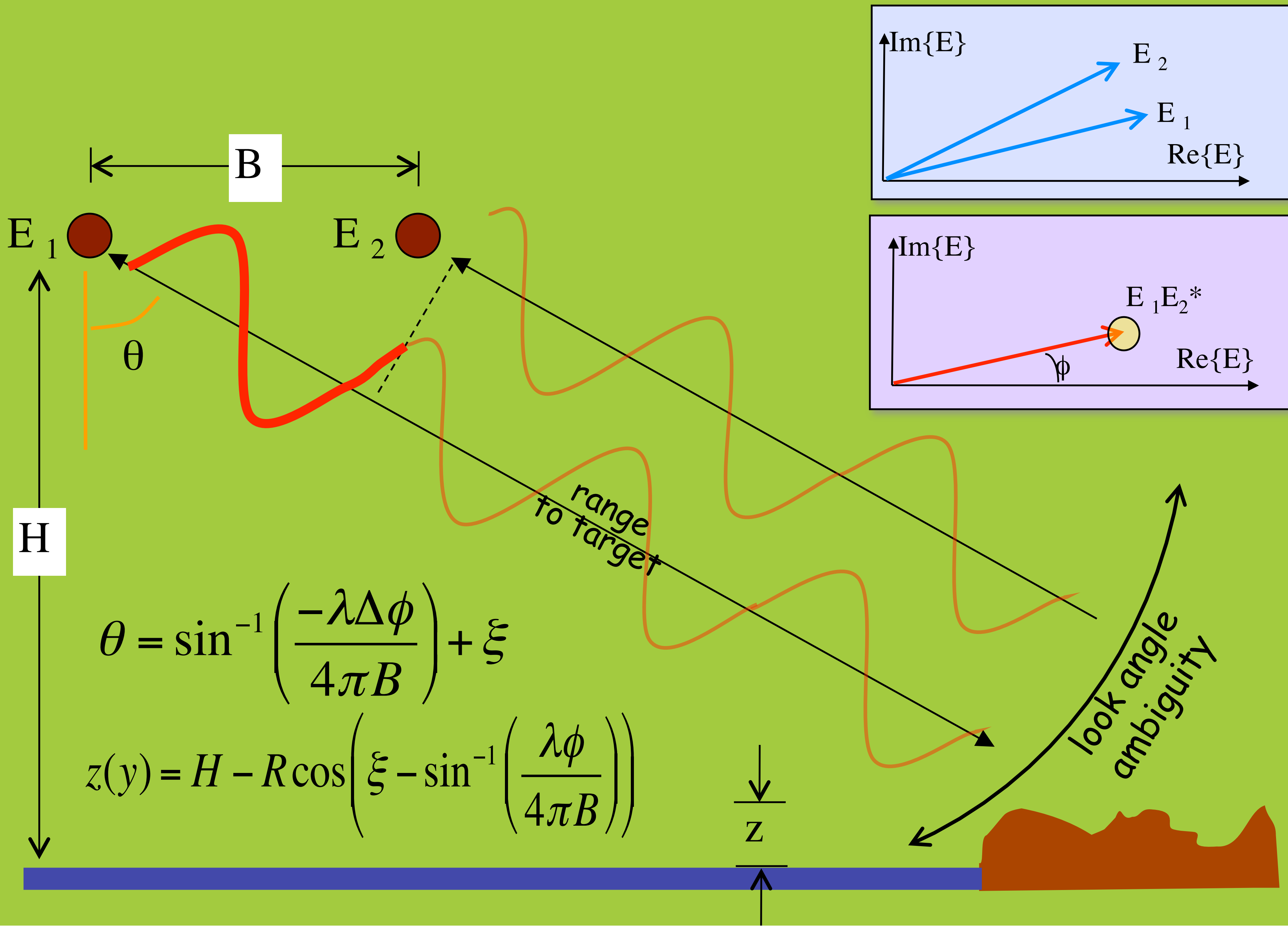

$$\theta = \sin^{-1}\left(\frac{-\lambda\Delta\phi}{4\pi B}\right) + \xi$$

$$z(y) = H - R\cos\left(\xi - \sin^{-1}\left(\frac{\lambda\phi}{4\pi B}\right)\right)$$

35 GHz Interferometry

Cessna 206 Stationair

Sample images

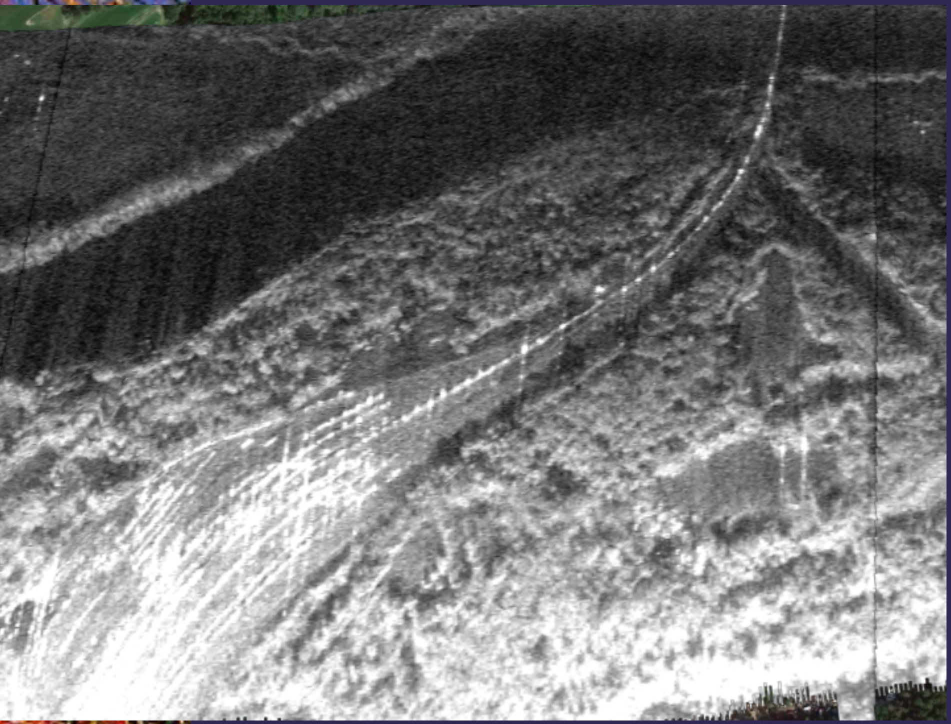

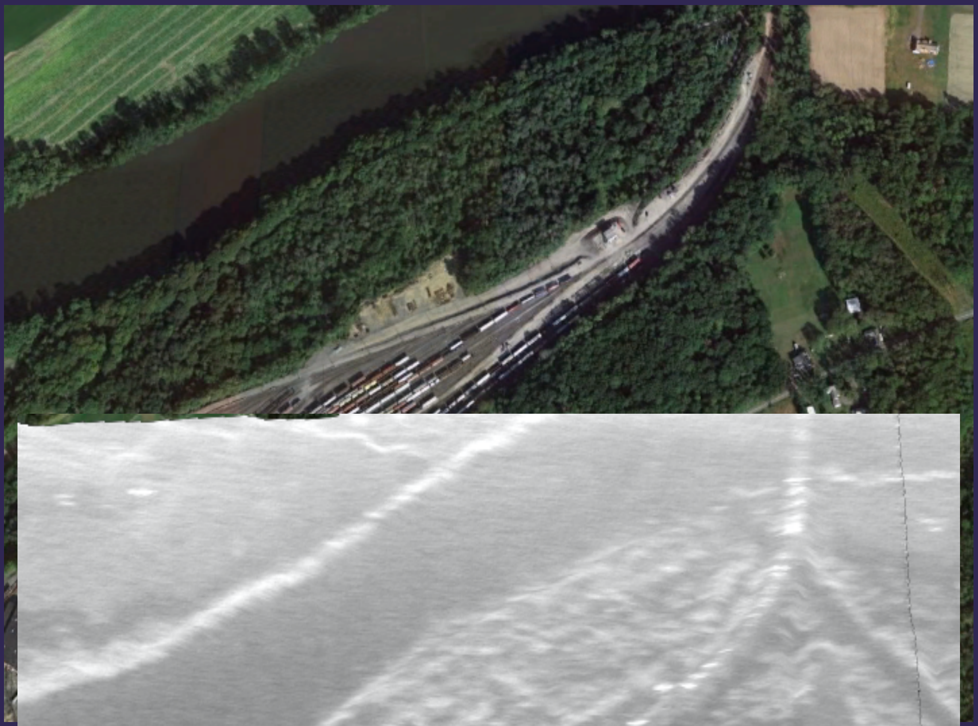

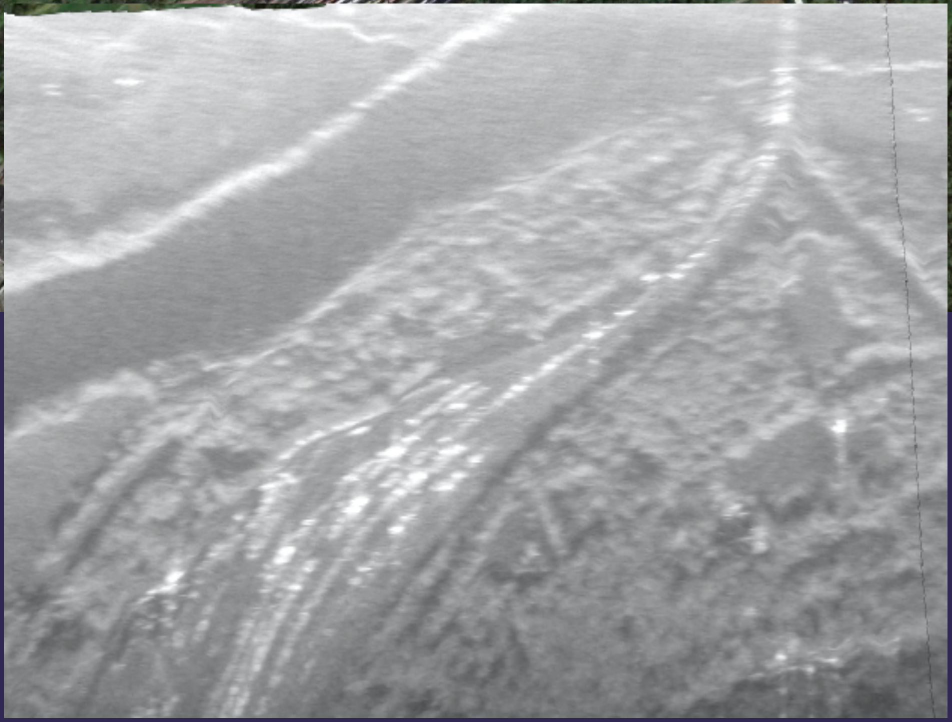

Cross track

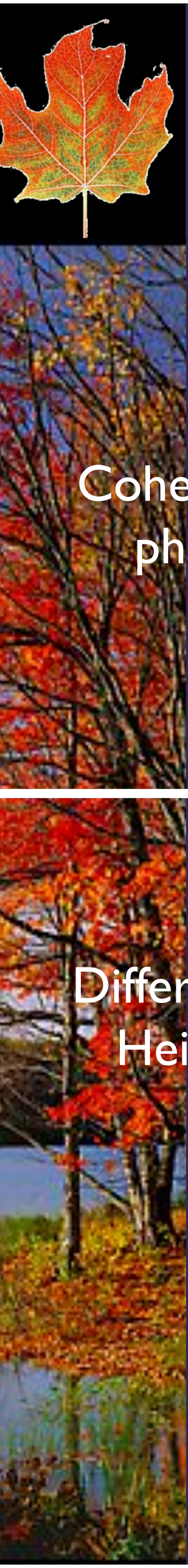

SAR interferometry

Coherence phase

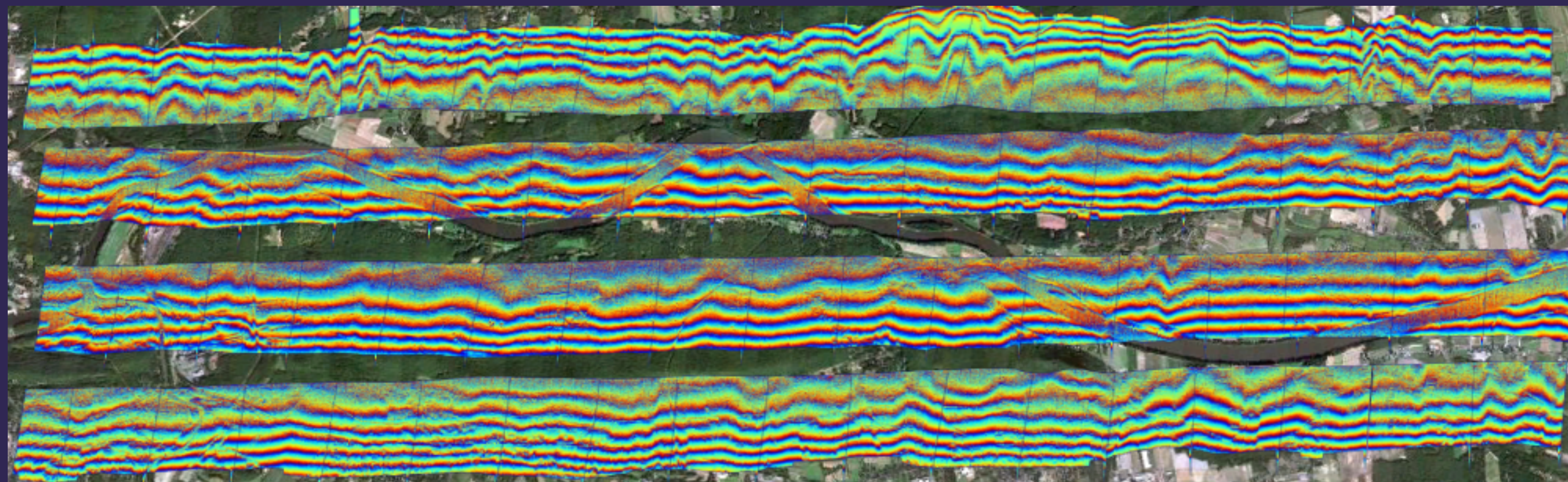

Differential Height

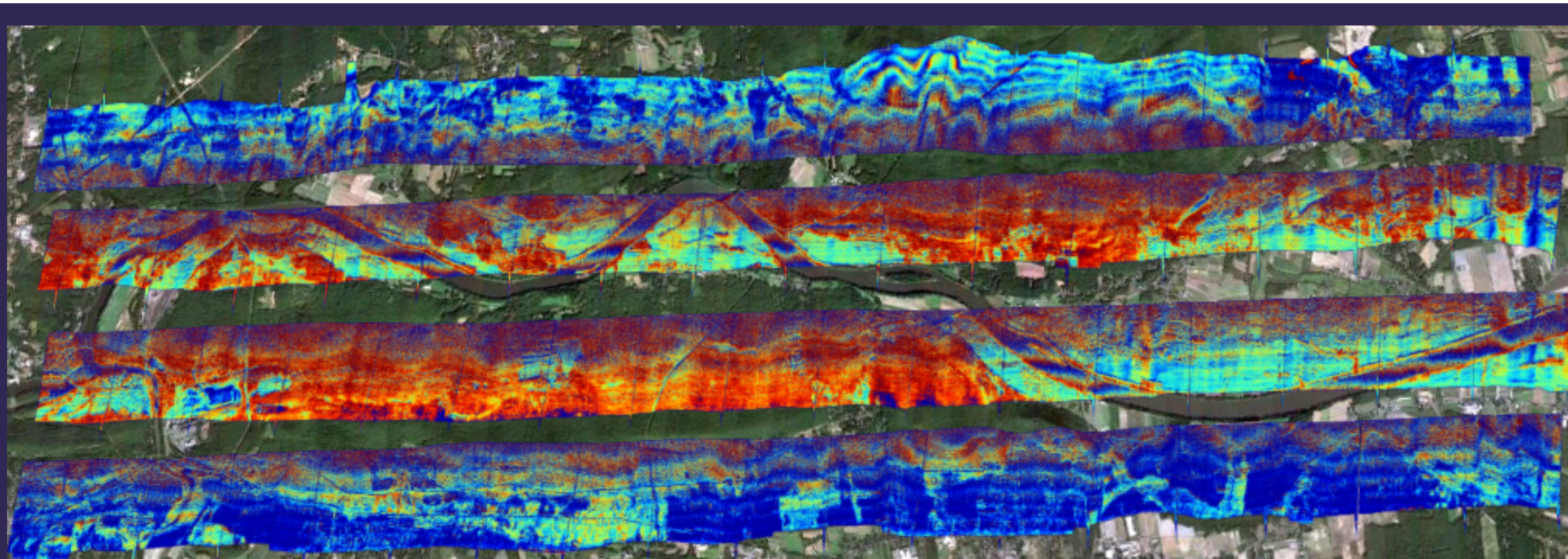

Differential Height Example

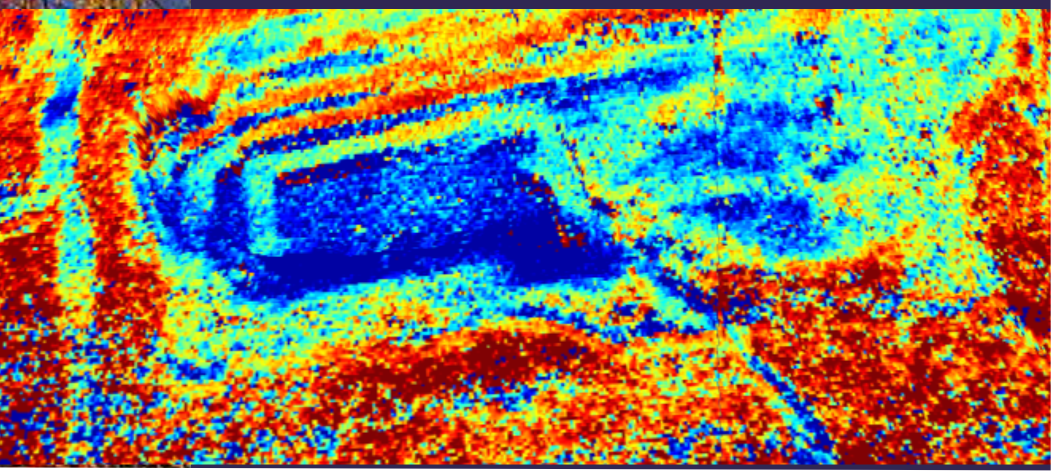

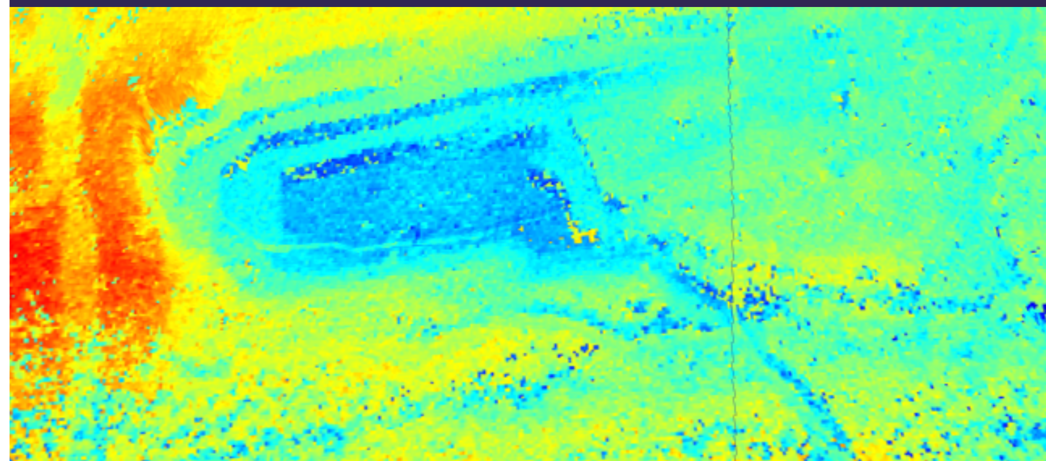

Differential Height

Final DEM

Optical (Google Earth)

SRTM (Shuttle Radar Topography Mission)

Mapped 80% of the Earth's landmass using C- and X-band Interferometry.

60 meter antenna baseline created by extending a boom from the Shuttle's cargo bay.

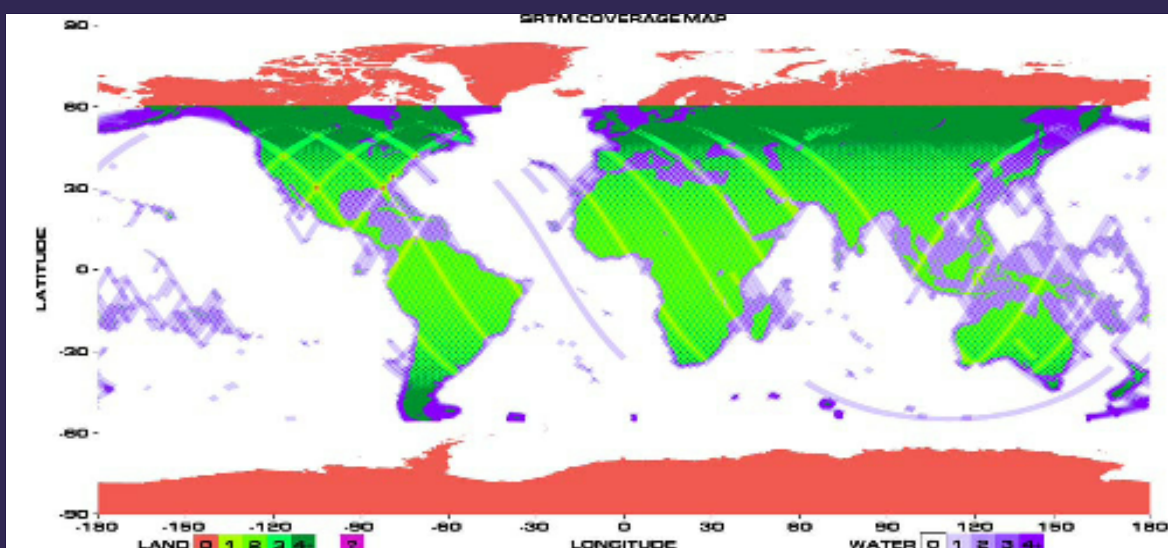

10 day mission executed in February 2000.

Topographic data products just now becoming available (~30 meter postings)

Ocean and Inland Waterways Topographic Mapping

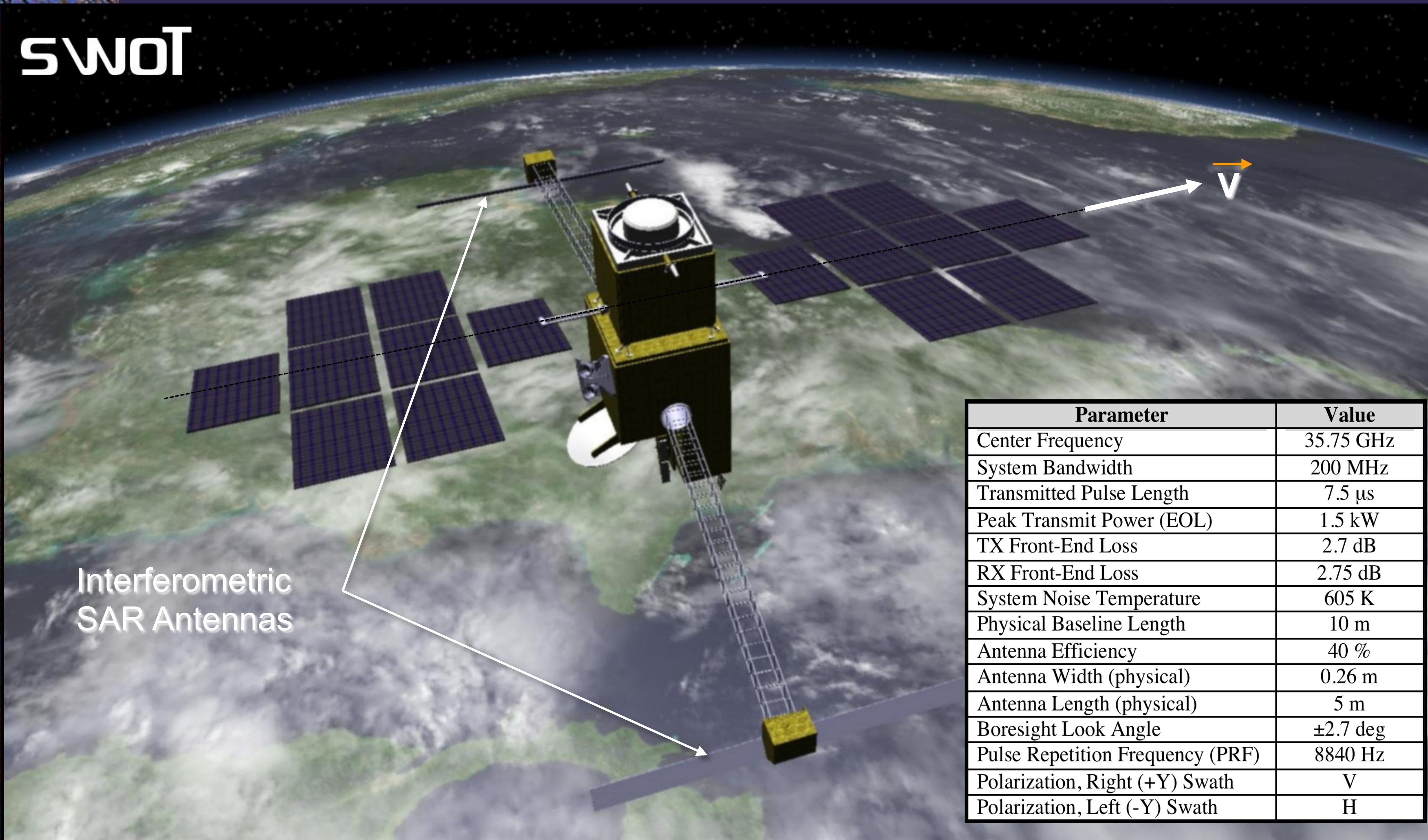

Parameter	Value
Center Frequency	35.75 GHz
System Bandwidth	200 MHz
Transmitted Pulse Length	7.5 μs
Peak Transmit Power (EOL)	1.5 kW
TX Front-End Loss	2.7 dB
RX Front-End Loss	2.75 dB
System Noise Temperature	605 K
Physical Baseline Length	10 m
Antenna Efficiency	40 %
Antenna Width (physical)	0.26 m
Antenna Length (physical)	5 m
Boresight Look Angle	±2.7 deg
Pulse Repetition Frequency (PRF)	8840 Hz
Polarization, Right (+Y) Swath	V
Polarization, Left (-Y) Swath	H

Satellite Radar Altimetry

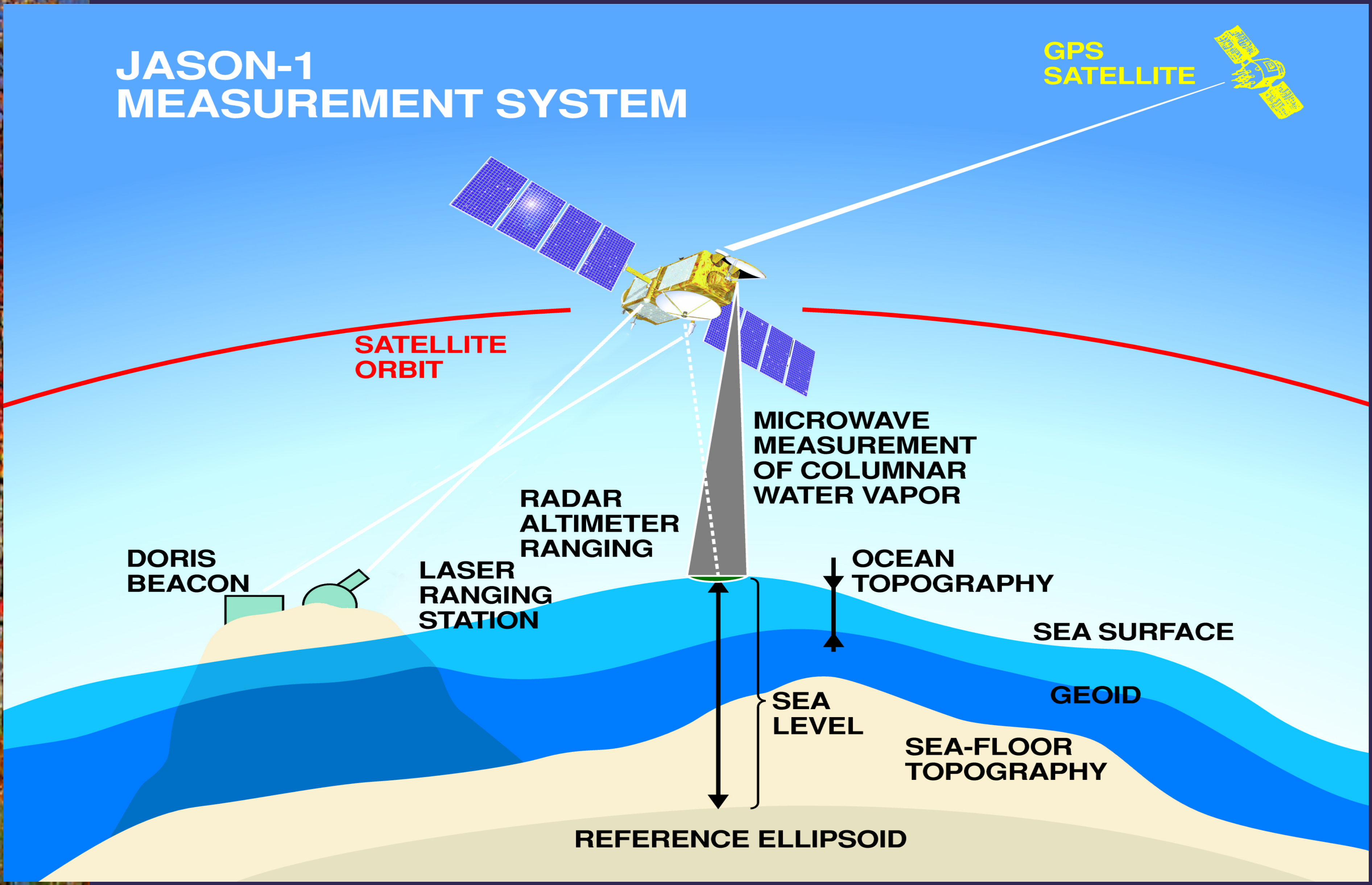

Ocean Topography Mapping

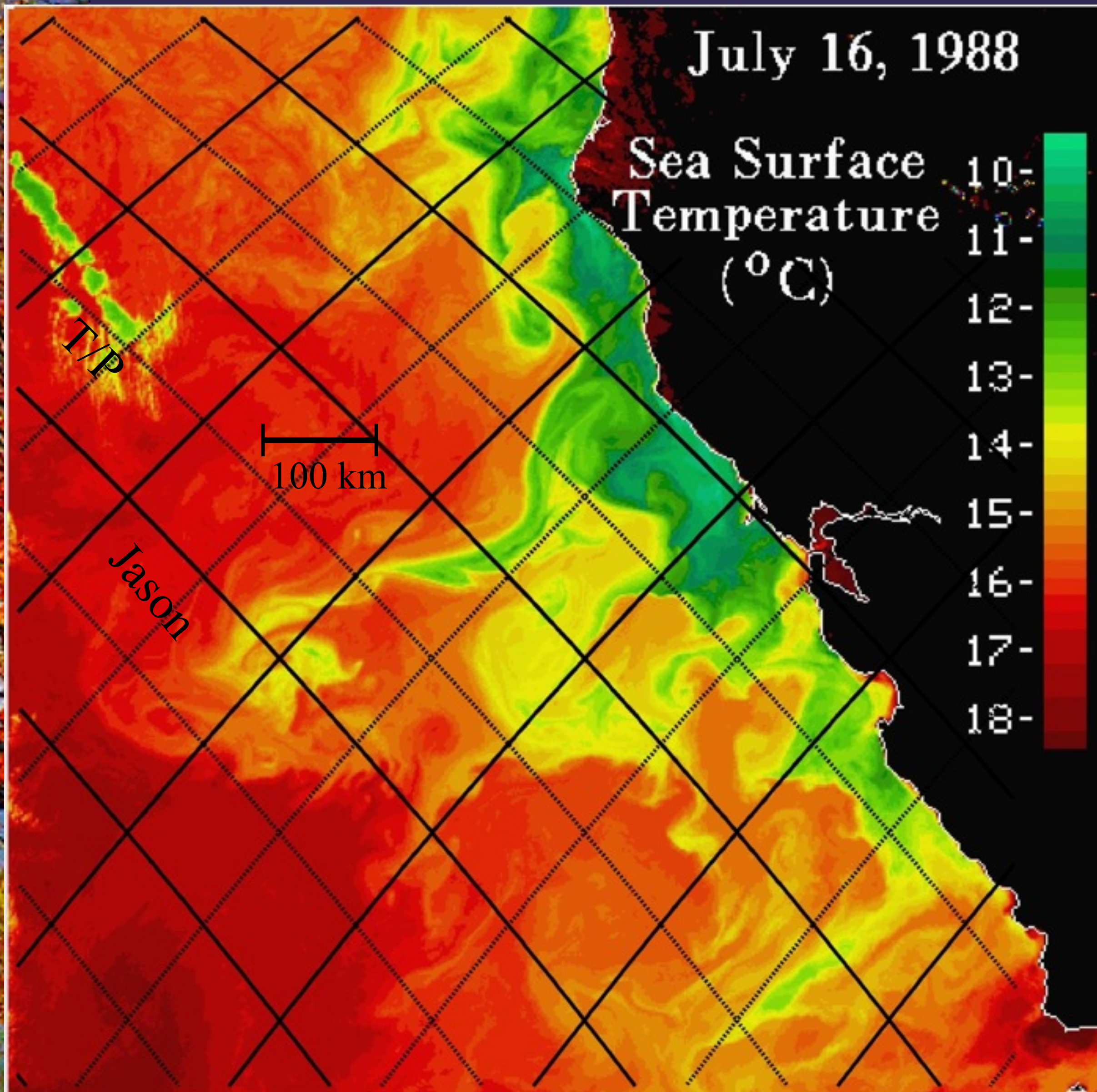

- Submesoscale phenomena exhibit rich spatial patterns characteristic of turbulent mixing down to small scales
- SWOT driving requirement: resolve submesoscale phenomena in space and height
- Spatial scales where SSH is diagnostic of circulation: 10km-20km
- Height accuracies characteristic of those scales: 1cm @ 1km white noise levels
- For submesoscales, noise at high-frequencies has a higher impact than noise at low frequencies

Identifying Critical Parts in the overall design

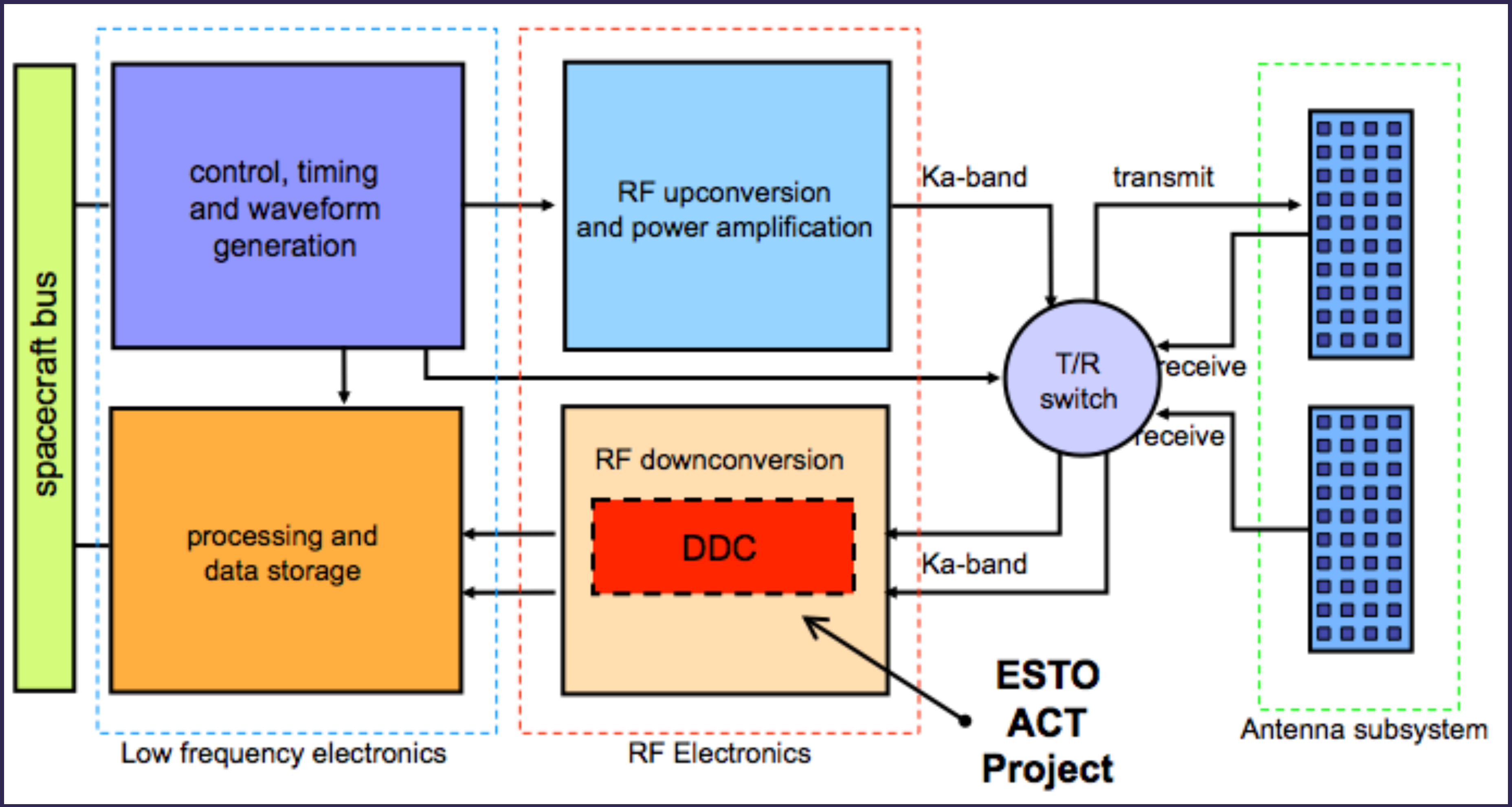

A critical component in the receive chain is the two-channel interferometric downconverter, also called the DDC

Ka-band Downconverter

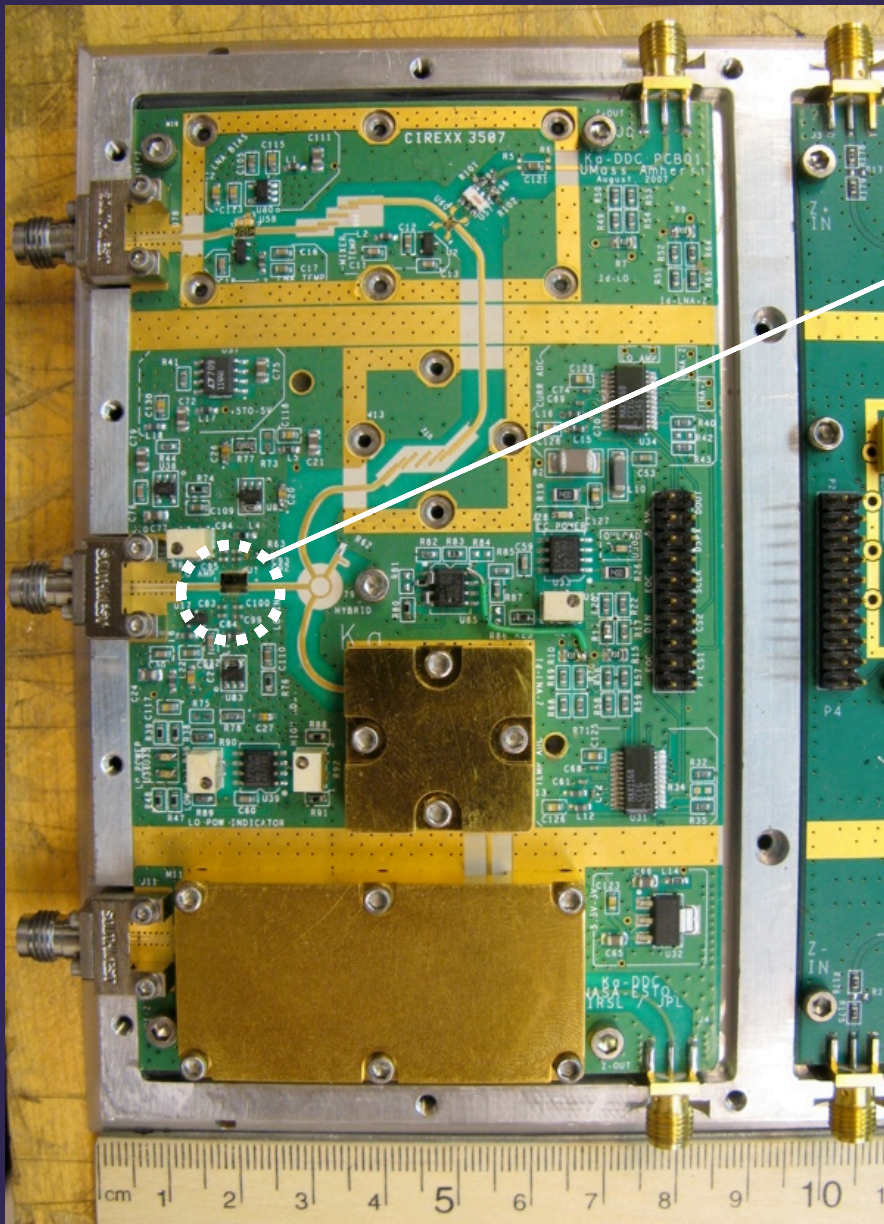

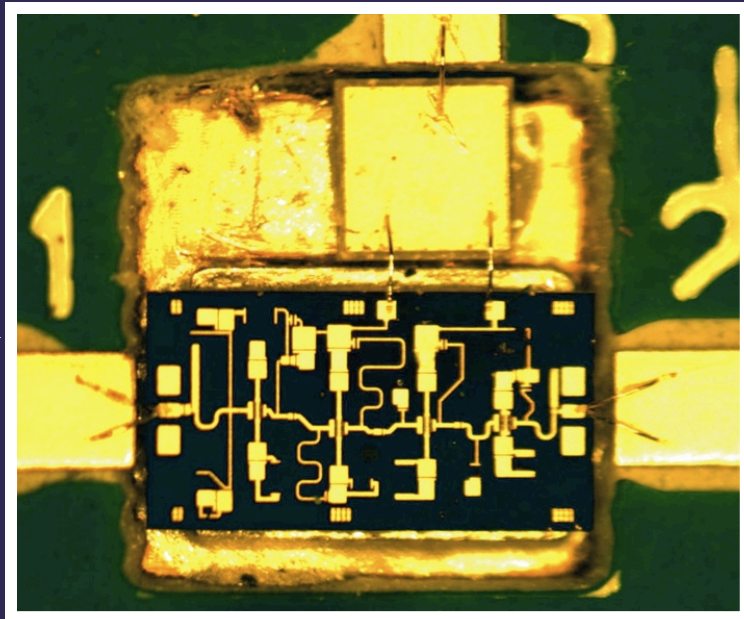

- As part of a NASA funded Advanced Component Technology (ACT) effort, UMass built and tested a high precision, high stability two-channel Ka-band downconverter.
- Temperature and phase stability were key components of the characterization, as was interchannel isolation
- UMass also developed a high precision method for measuring differential phase, able to meet theoretical limits in terms of SNR

Phase Difference, Temperature, and Best Fit Model

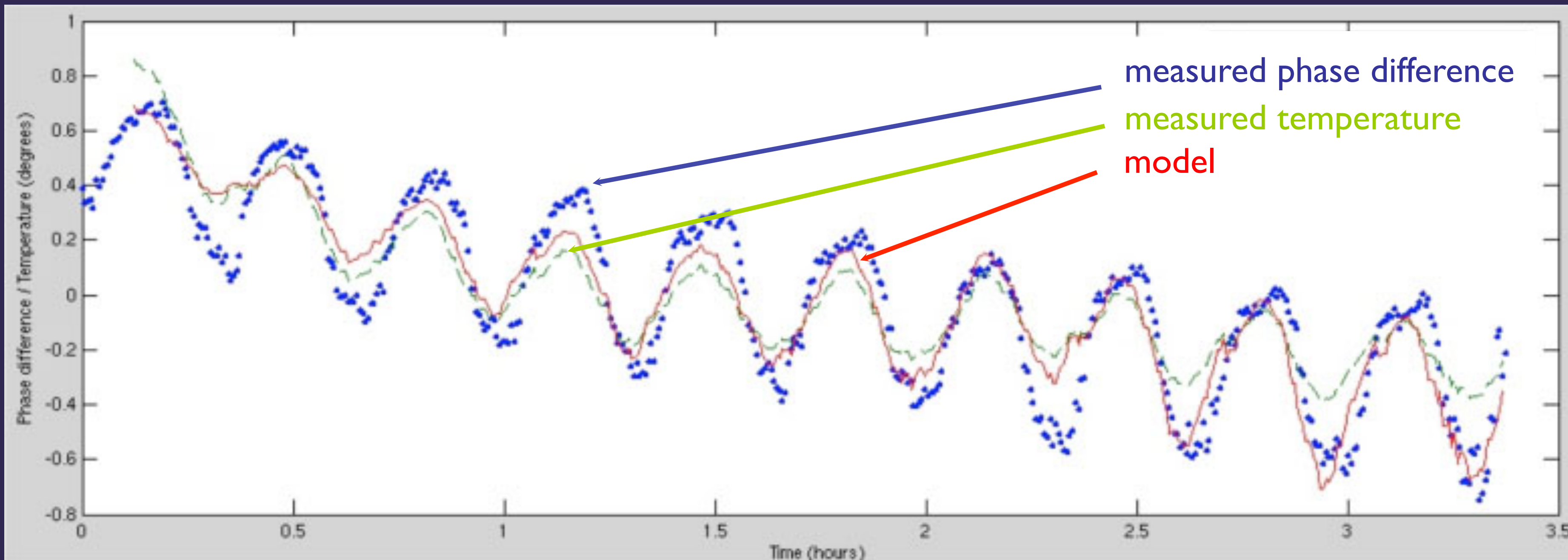

Thermal cycles (1 deg C) in building strongly effect differential phase. Measuring temperature and modeling the effect can remove some of the variation, but not sufficiently to meet the tight performance requirements.

Thermal Testing

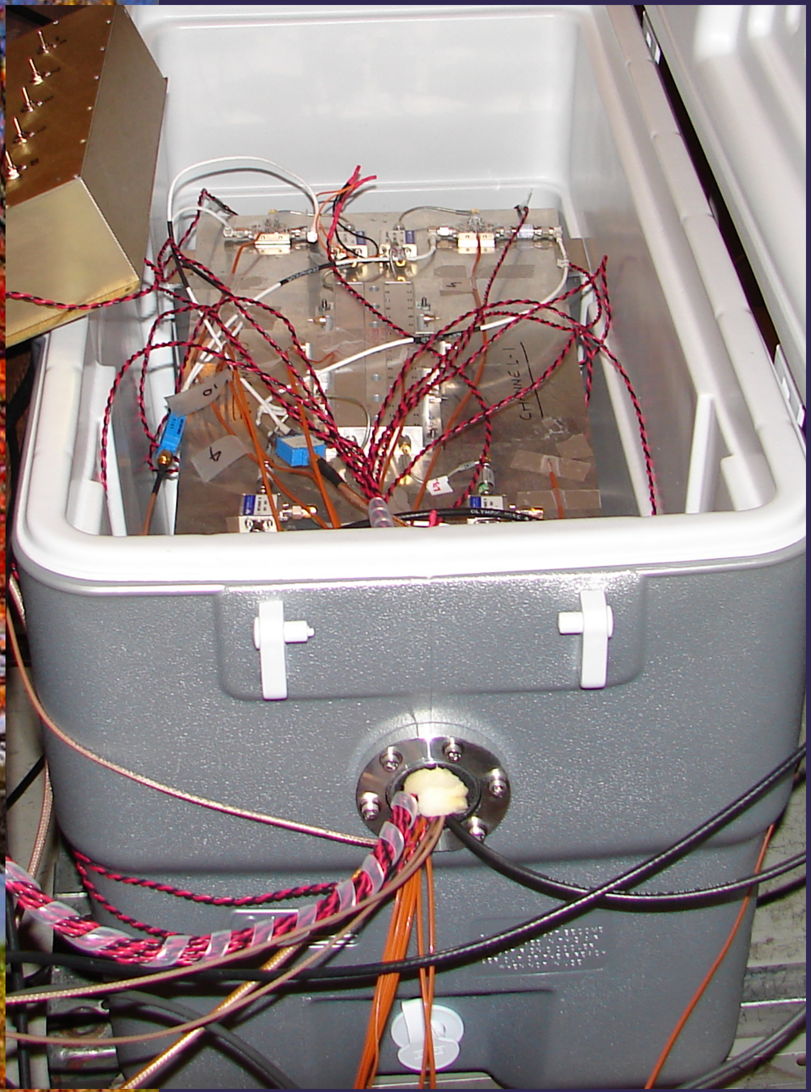

Thermally isolating the downconverter (breadboard model) leads to a 20 mdeg phase error over time.

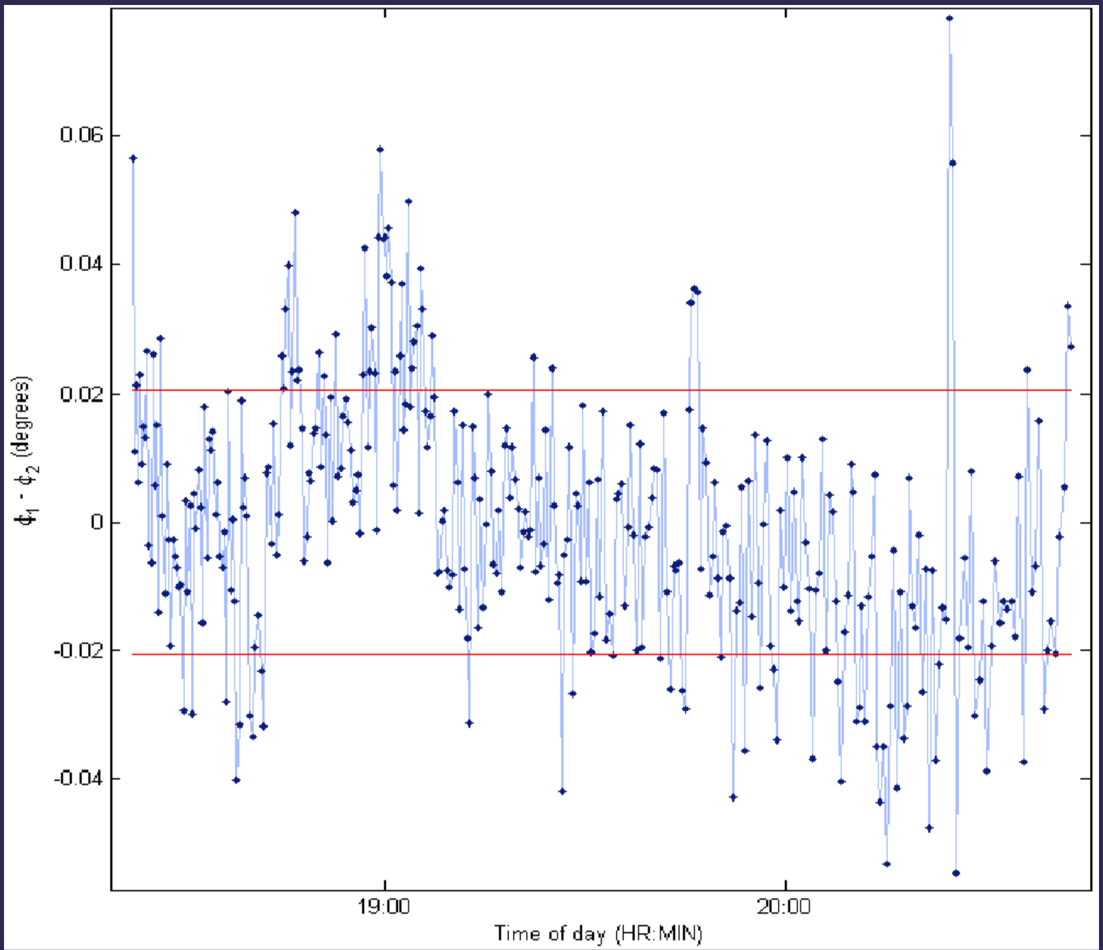

Work on High Performance Sensing Systems

For increasing reliability, systems have to be tested in the different environments of space.

Here, one system is shown where the frequency is so high (35 GHz), the wires no longer behave the way we are used to at lower frequencies
(e.g. 60 Hz)

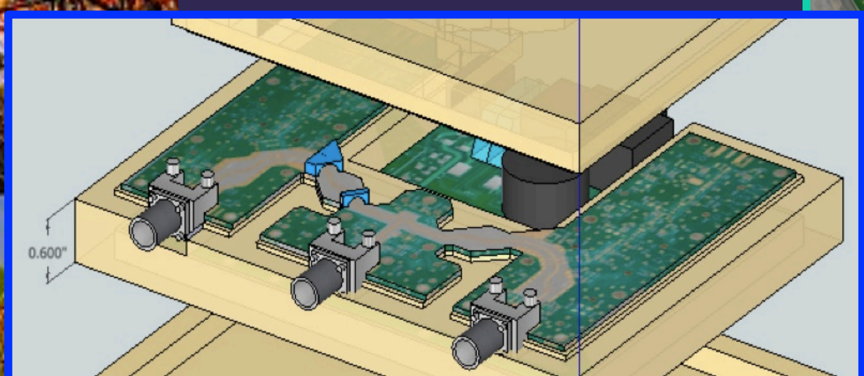

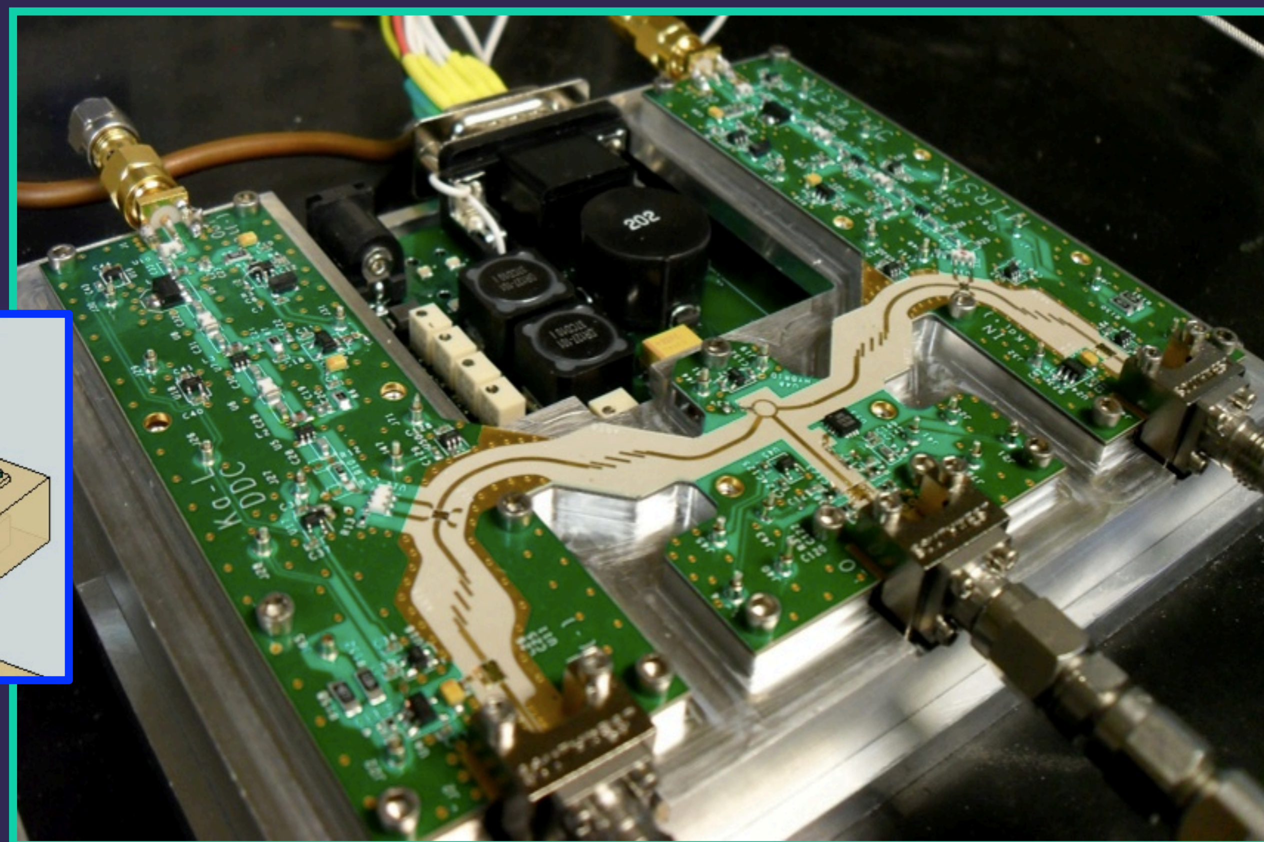

A Slotted Waveguide Antenna

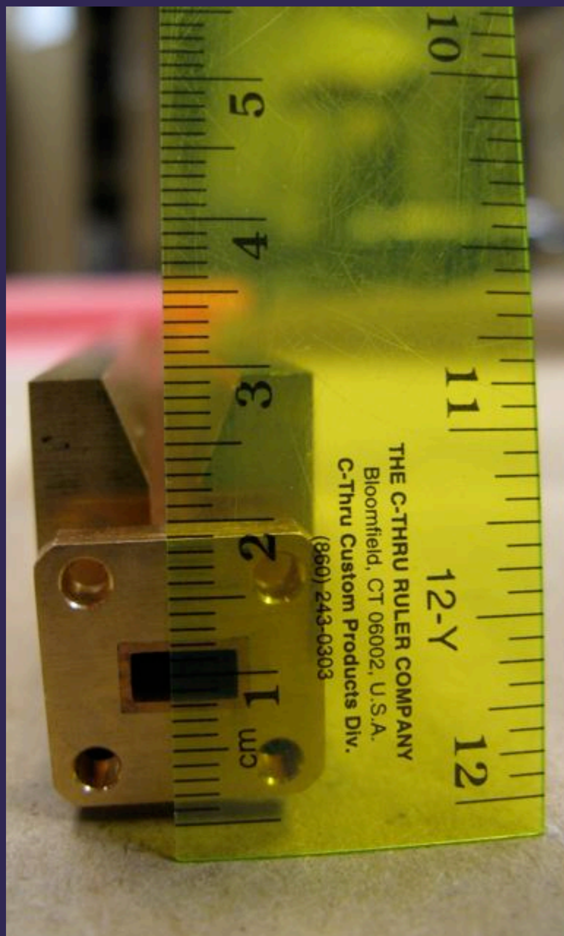

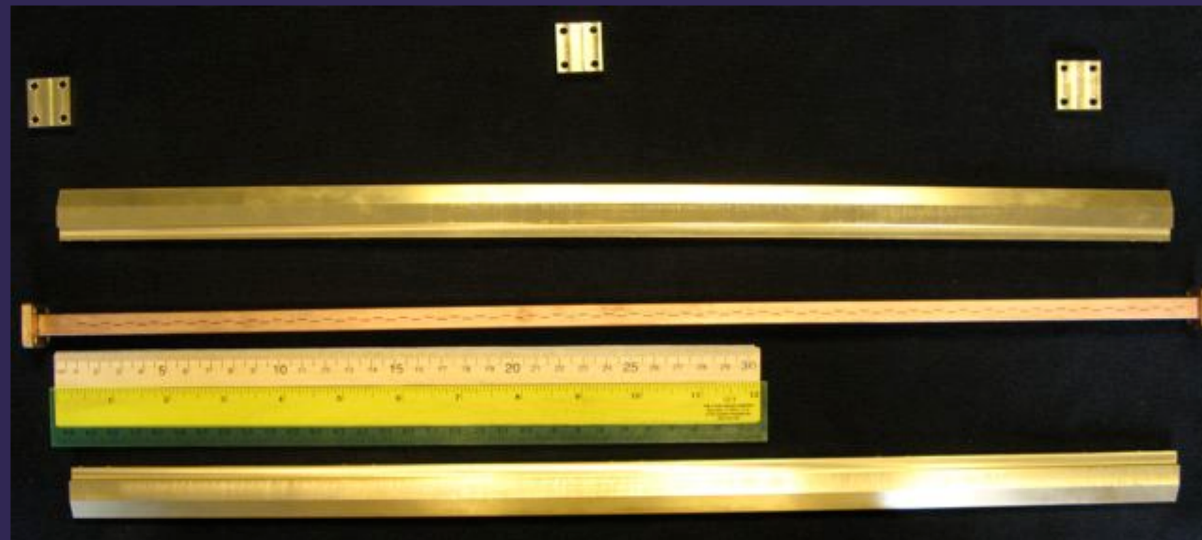

Interferometric Data Products

DEM from Interferometry

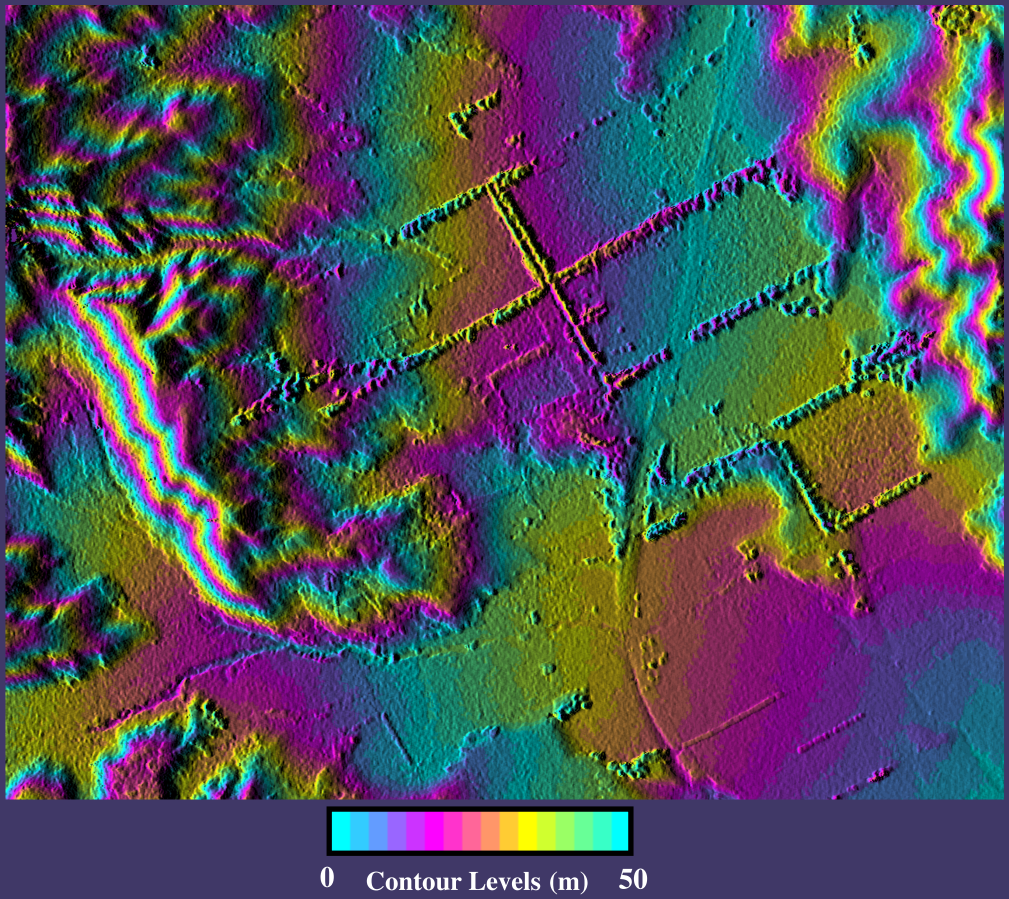

Correlation Map

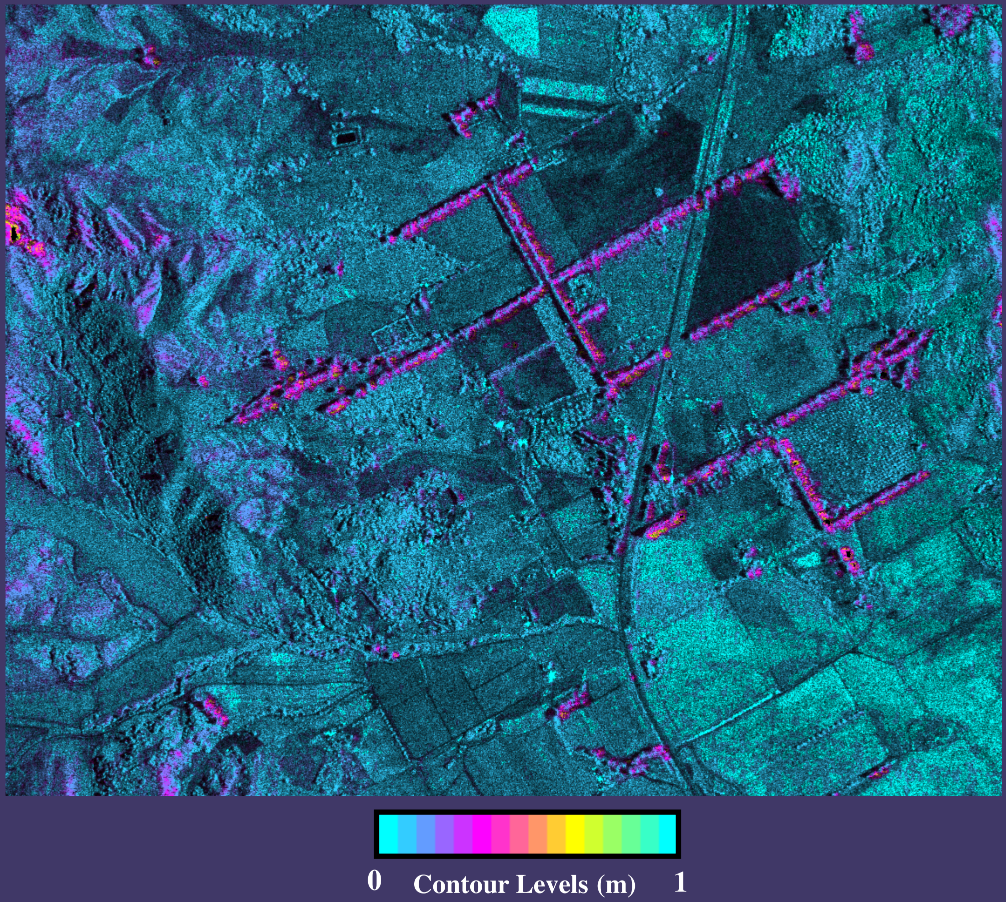

Sensitivity to Volume Scattering

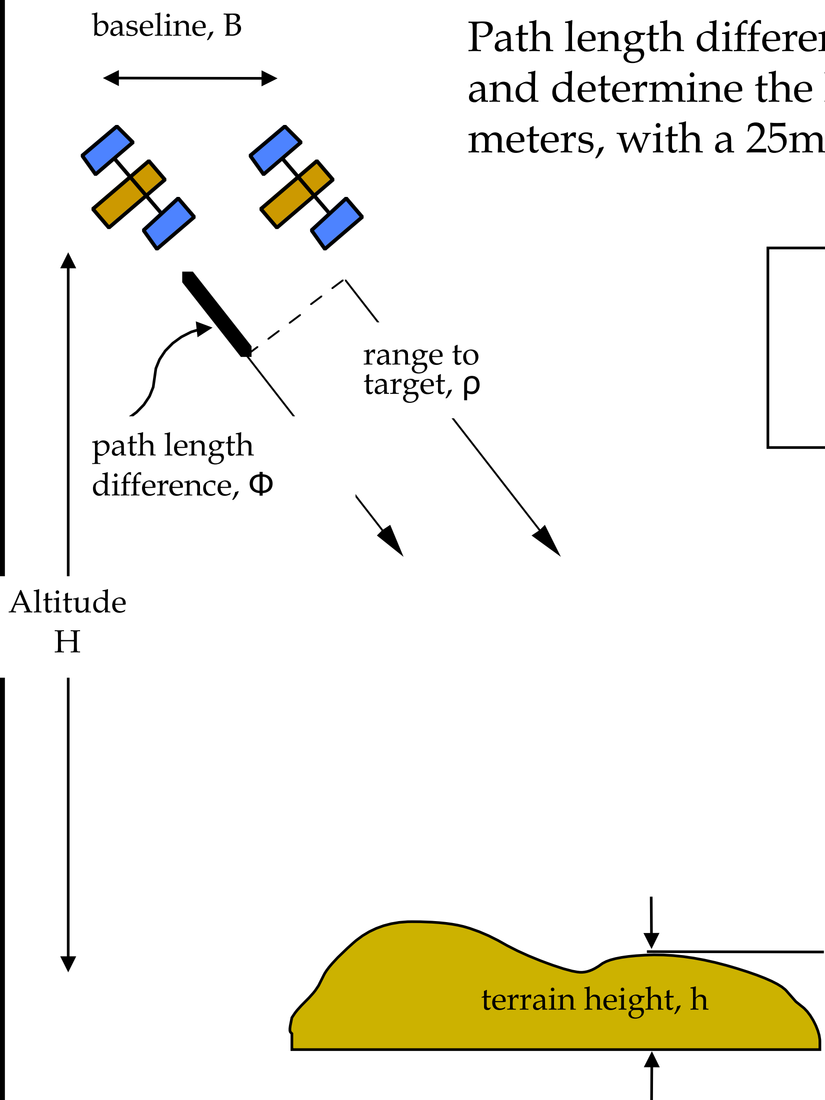

Path length difference can be used to resolve positional ambiguity and determine the height of the terrain. Accuracy is on the order of meters, with a 25m resolution

$$h = H - \rho \cos\left(\sin^{-1}\left(\frac{\lambda\phi}{4\pi B} \right) \right)$$

When the signal return comes from multiple heights, a unique signature is observed by the interferometer

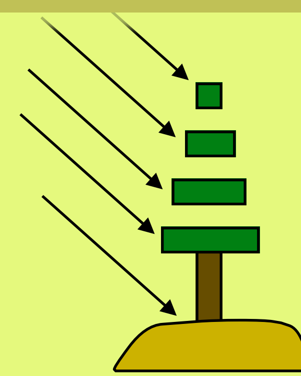

Modeling of the Interferometric Response to Volumes

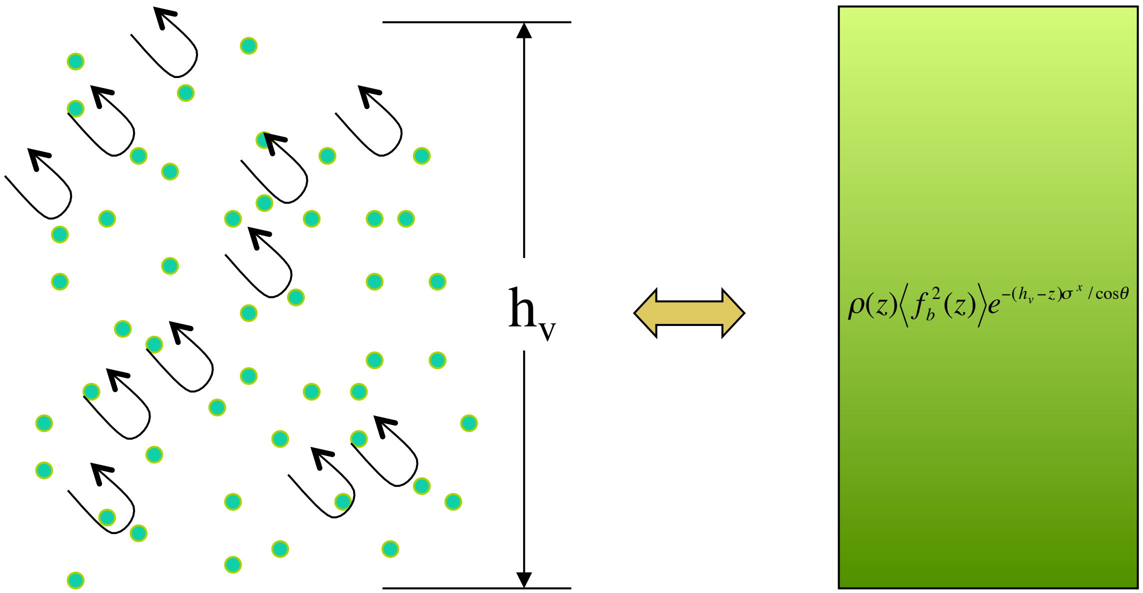

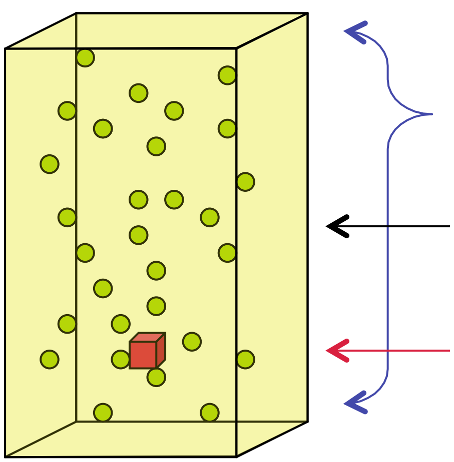

- range of possible scattering phase center locations
- mean of possible scattering phase center locations
- scattering phase center for one particular observation

$$\gamma = \frac{\left\langle E_1 E_2^* \right\rangle}{\sqrt{\left\langle \left|E_1\right|^2 \right\rangle \left\langle \left|E_2\right|^2 \right\rangle}}$$

$$k_z = \frac{kBa\cos(\theta - \alpha)}{r\sin\theta}$$

$$\sigma(z) = \rho(z)\left\langle f_b^2(z)\right\rangle e^{-(h_v - z) / \cos\theta}$$

$$\gamma_{vol} = \left|\gamma_{vol}\right| e^{i\phi_{vol}} = \frac{\int \sigma(z) e^{ik_z z} dz}{\int \sigma(z) dz}$$

$$f(z) = \frac{\sigma(z)}{\int \sigma(z) dz}$$

$$\gamma_{vol} = \int f(z) e^{ik_z z} dz$$

Volumetric Correlation Dependence on Structure

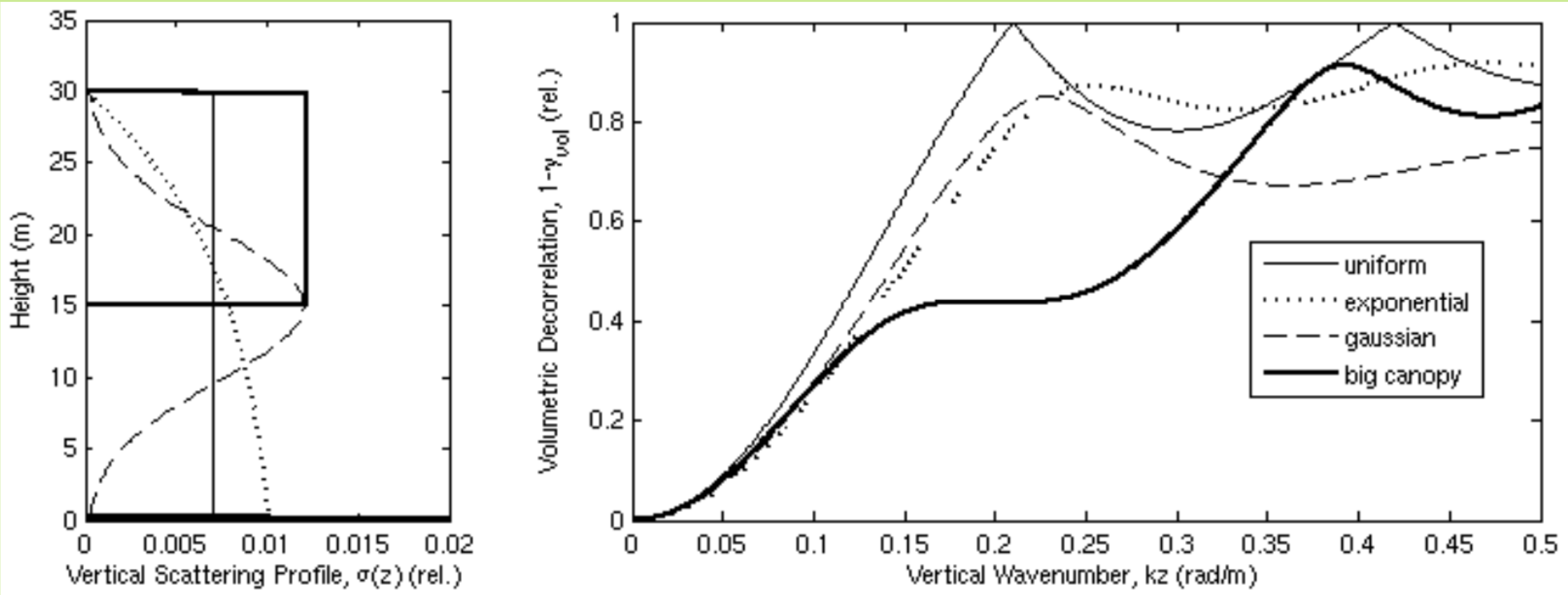

In general: $\gamma_{vol} \leq \mathrm{sinc}\left(k_z h_v / 2\right)$ random volume, no ground

Note: multiple baselines using the same polarization will have the same scattering phase center. This however does not take into effect extinction, which will raise the phase center slightly as a function of incidence angle.

Multibaseline diversity

Baseline diversity is used to distinguish one vertical profile from another

Plot shows inteferometric response to different types of uniform reflectivity

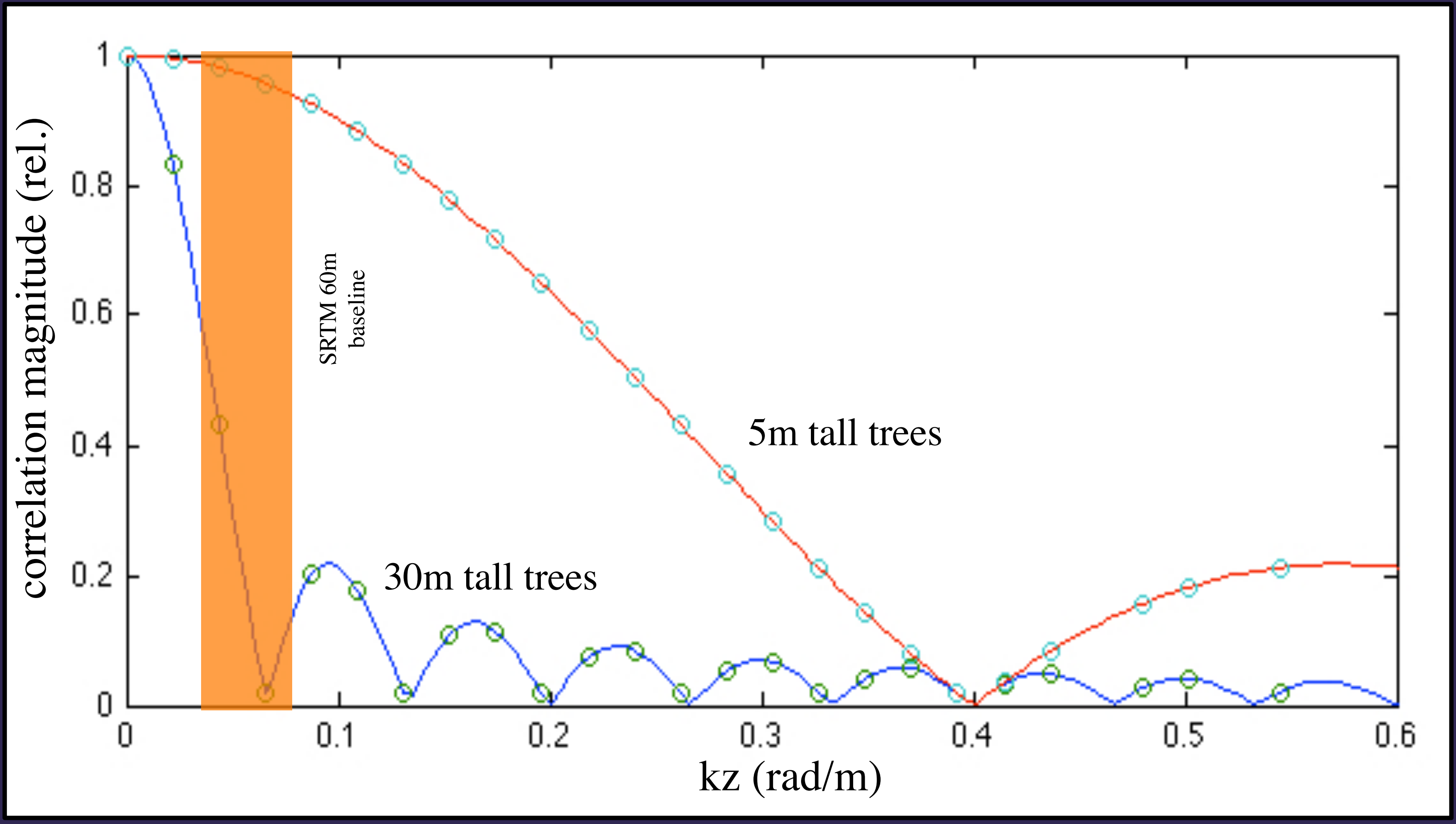

Ascending Pass

UAVSAR Flown over the region in August 2009

Four tracks per ascending/desending pass

Baseline offsets used to provide redundancy and multibaseline observations

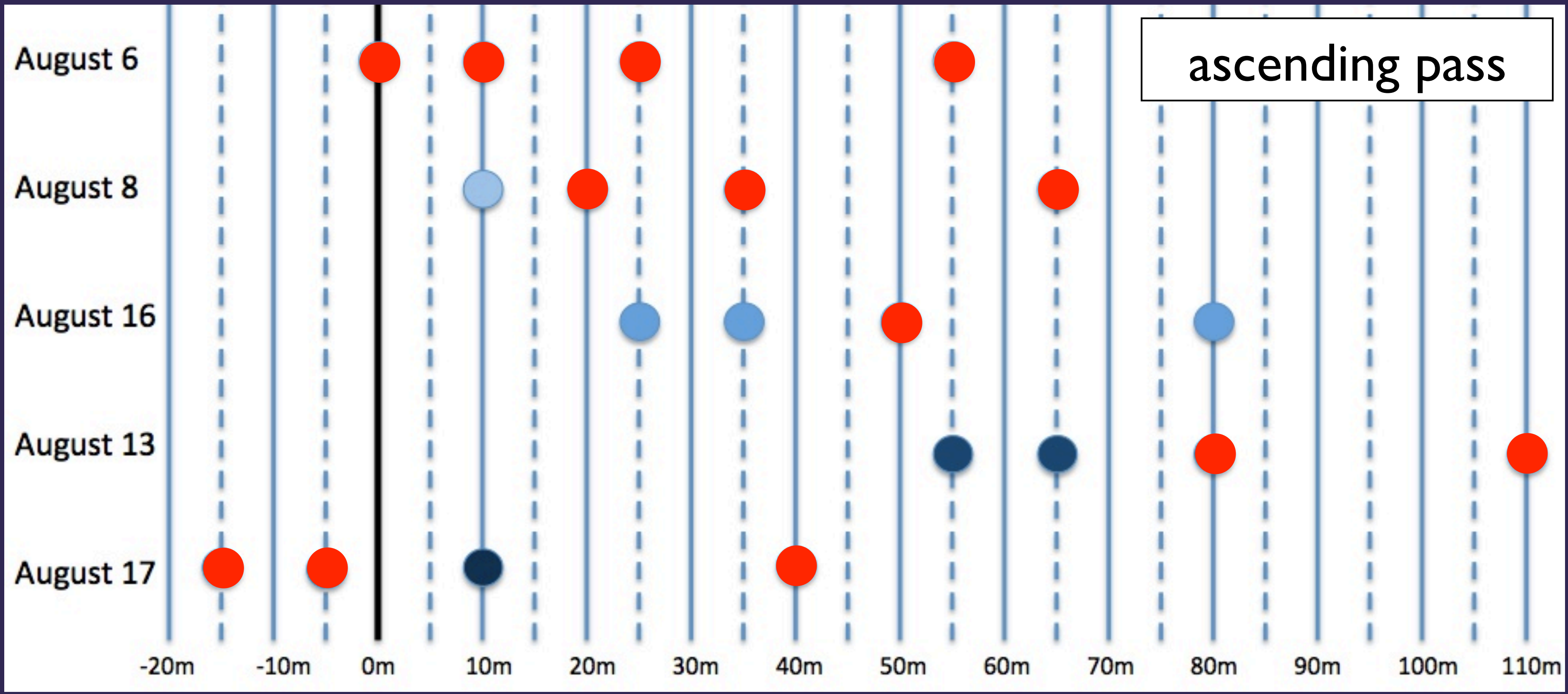

Repeat-pass repeat baselines

Redundant baselines can be used to

- explore the effects of temporal decorrelation
- ascending and descending passes should provide the same correlation measures
- choice of repeat tracks intended provide both baseline diversity and redundant baselines over a wide variety of combinations

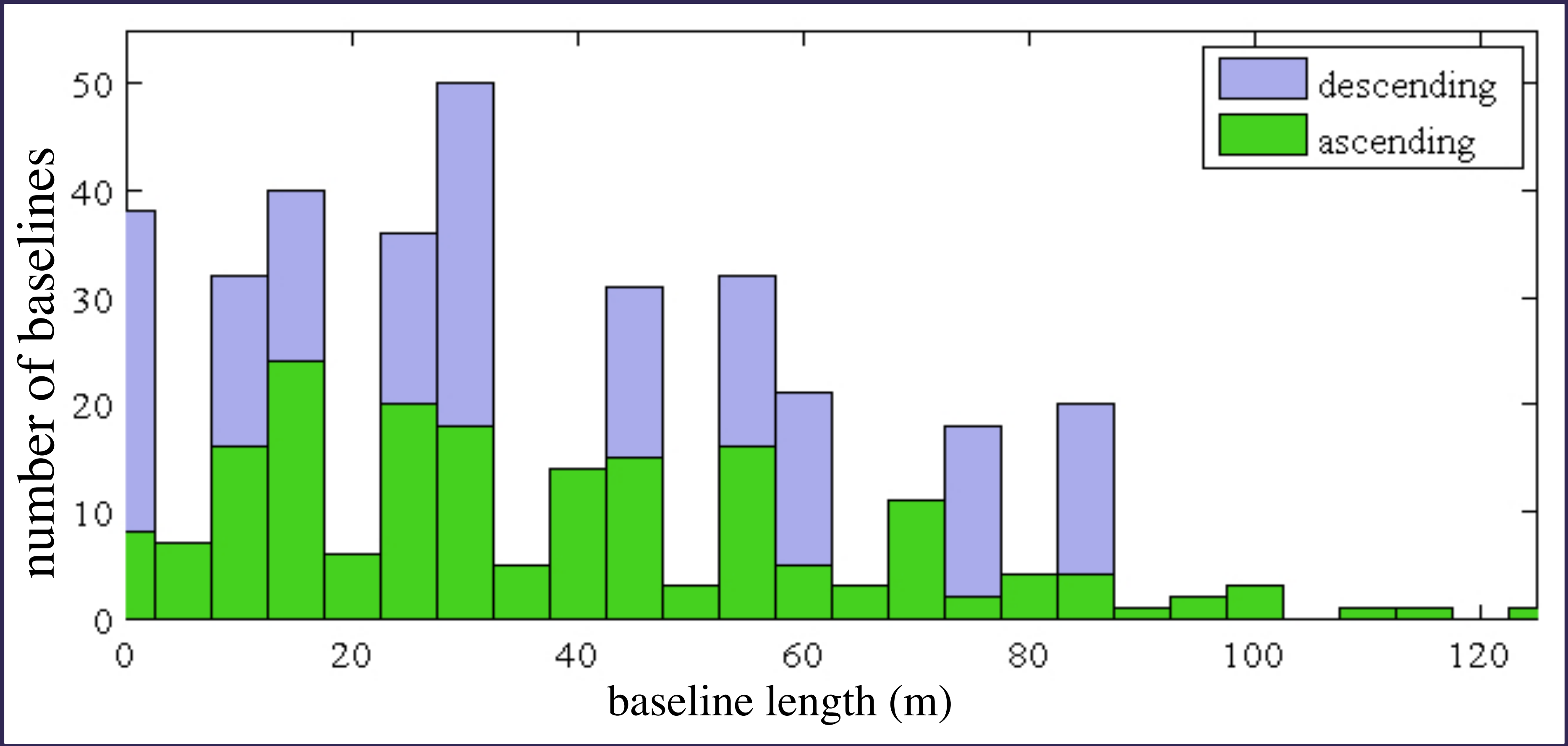

Height Maps as a Function of Frequency

L-band Minus P-band   C-band Minus P-band   X-band Minus P-band

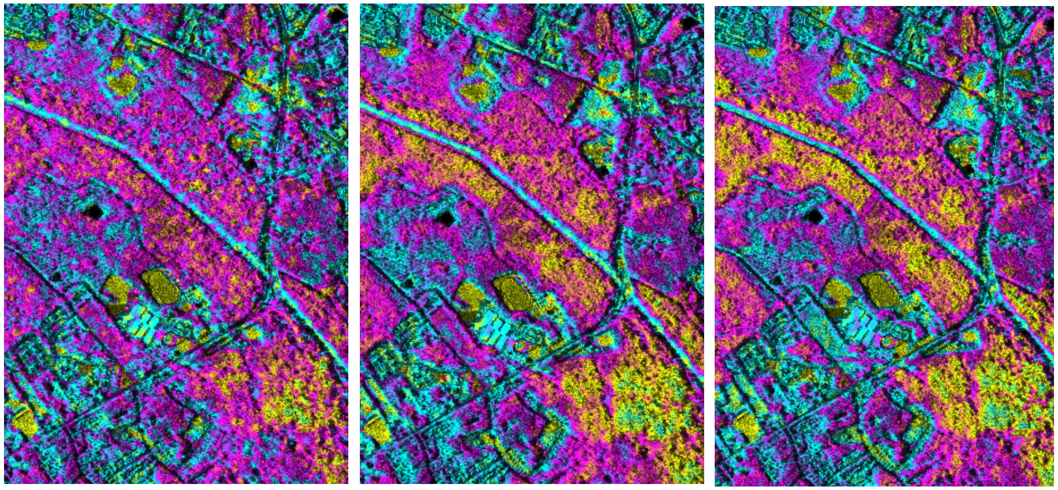

L-, C-, and X-band all penetrate into the canopy about the same distance. P-band phase center is at the canopy base

HGT on slicer track 506 top(green) and grnd(black) heights

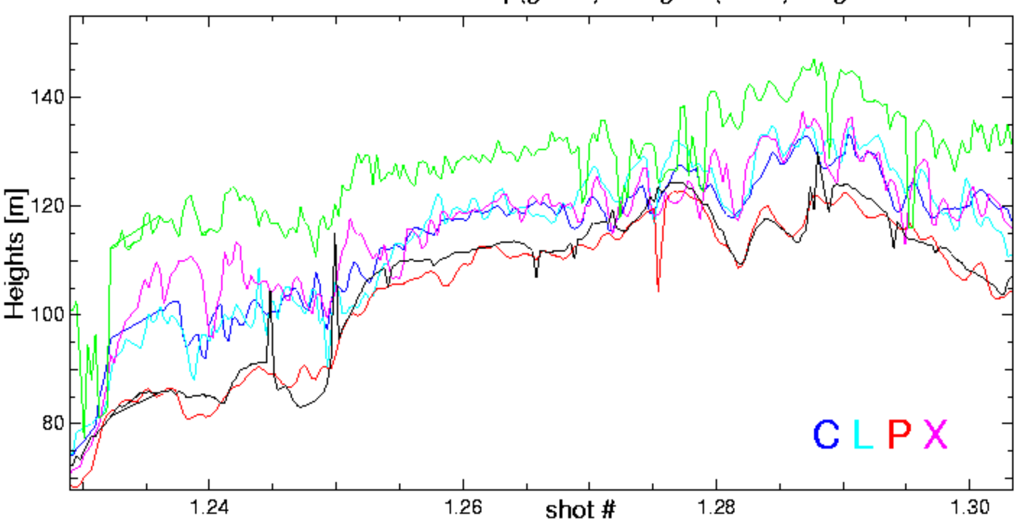

Multi-Baseline Interferometry for Forest Structure

L-band multibaseline (multi-pass) experiment conducted by the DLR, Germany

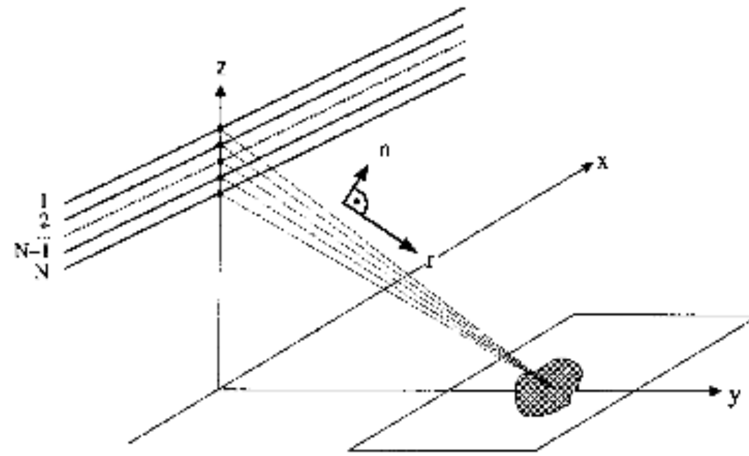

Reigber, A., Moreira, A., "First Demonstration of Airborne SAR Tomography Using Multibaseline L-Band Data," IEEE Trans. Geosci. Rem. Sens., 38(5), 2000.


this is the
End
… of the
presentation

Ka-band EIK (CPI) and HVPS (Pulse Systems)

- 1.5 kW 5% duty cycle extended interaction klystron (EIK) amplifier from CPI
- Modulator provided by Pulse Systems
- EIK Demand for large current from the HVPS at the PRF (4 kHz) causes an oscillation in the system phase performance

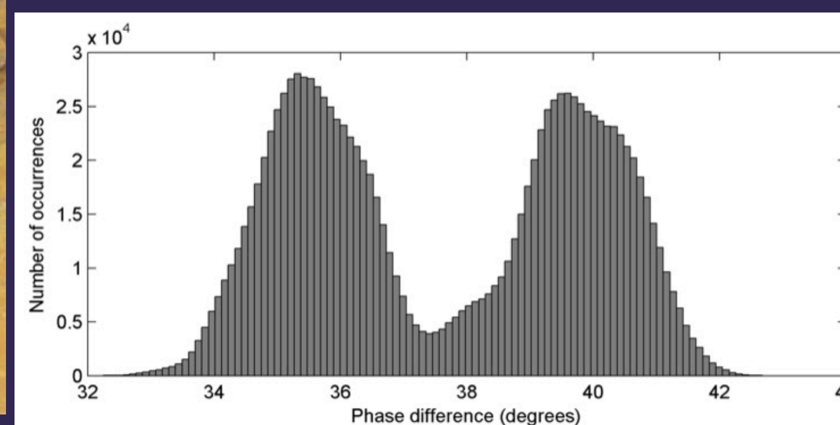

The Art of Engineering

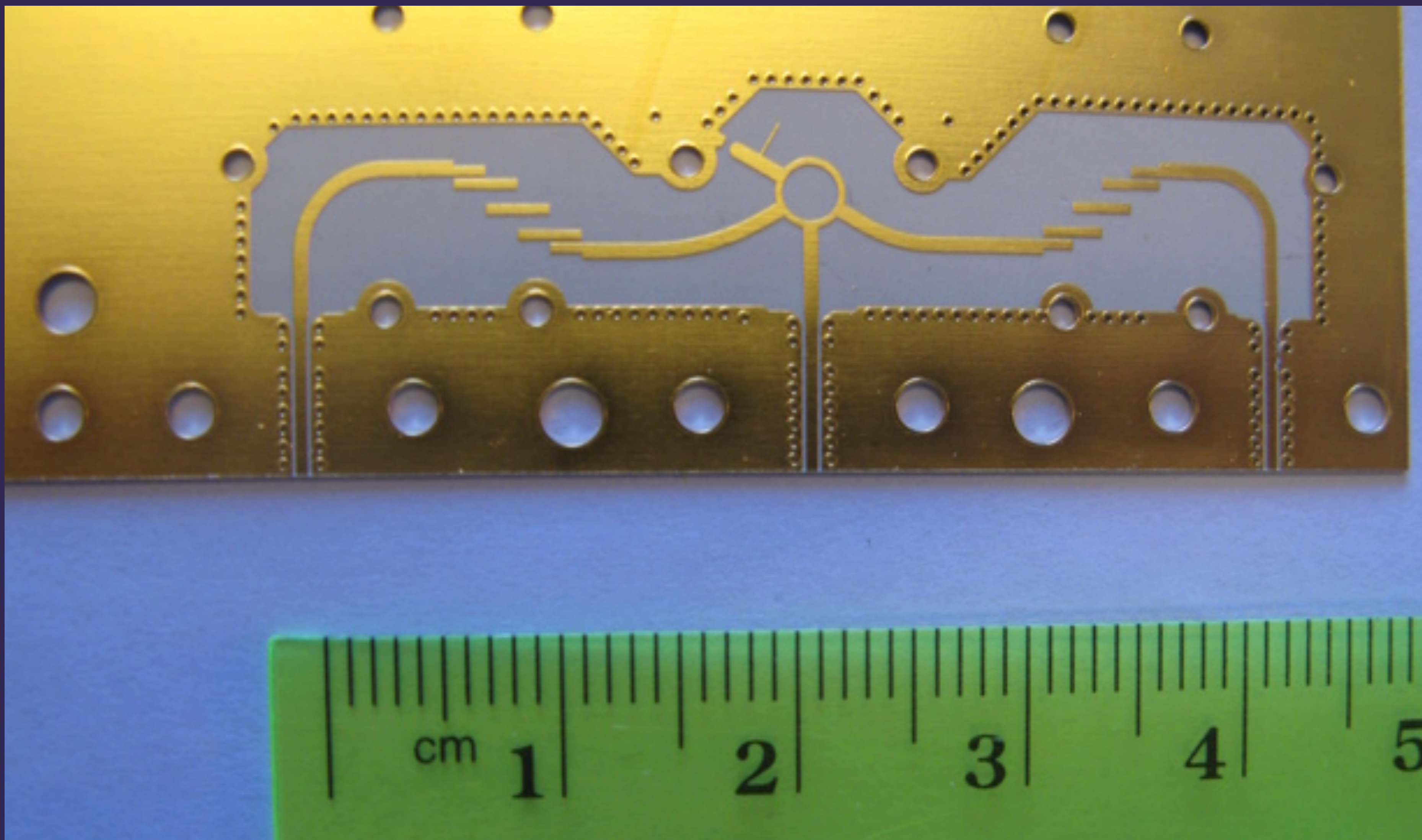

An Earthborne Version of the Instrument

The Ka-band interferometer is deployed locally, to test hardware and algorithms as well as to test new applications

Analysis of individual target behavior

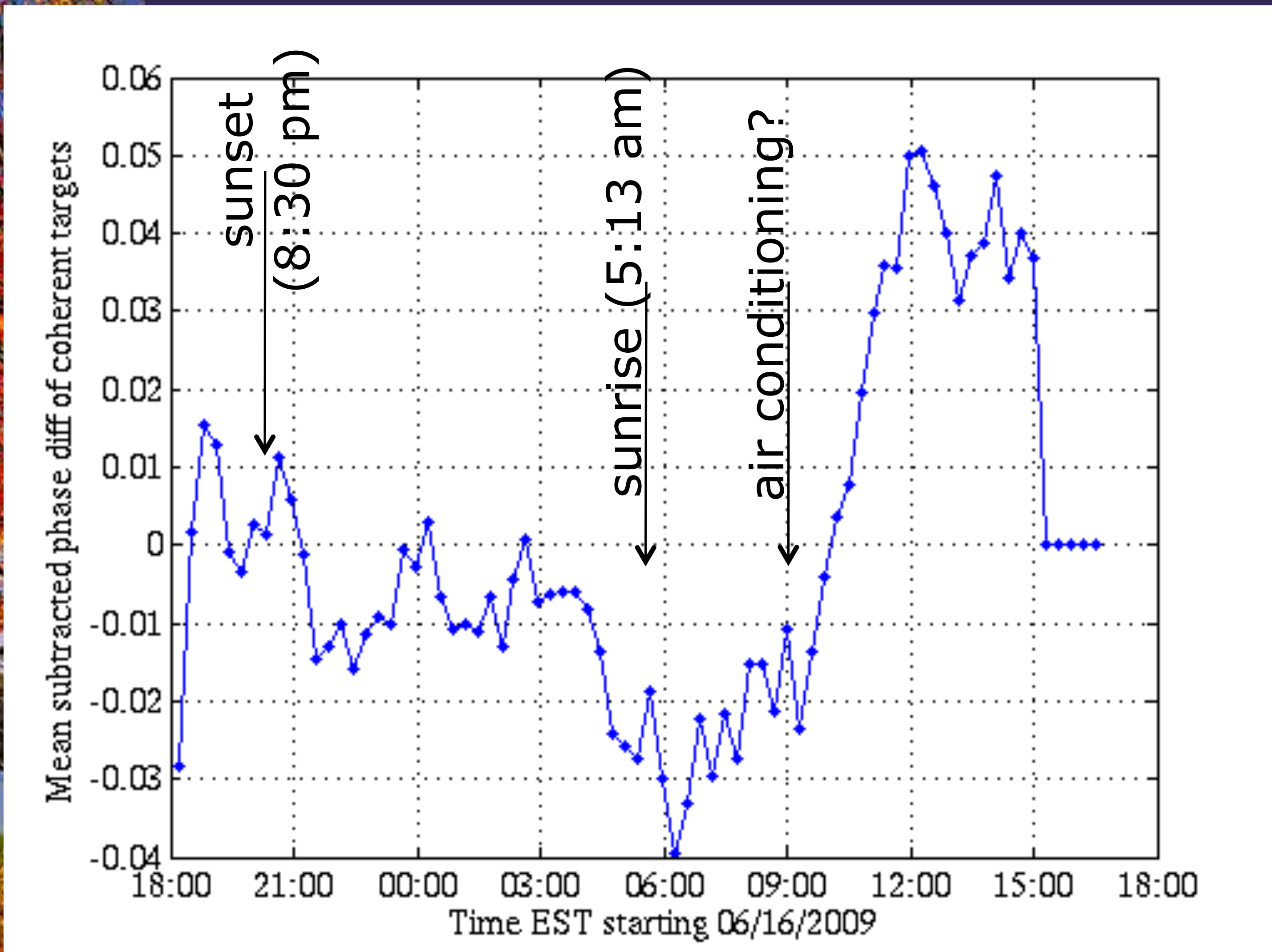

ase signatures of a
uilding on campus
ows an interesting
profile

Transition to an airborne platform

Shadowing and loss of sensitivity due to low grazing angle for ground based systems are the biggest error sources. Hence, an effort is underway to transition the instrument onto a Cessna 206 Aerial Survey platform.

This is being done with Thomas Millette, from the Geography Department at Mt. Holyoke College.

First airborne results

Map coordinates

Radar coordinates

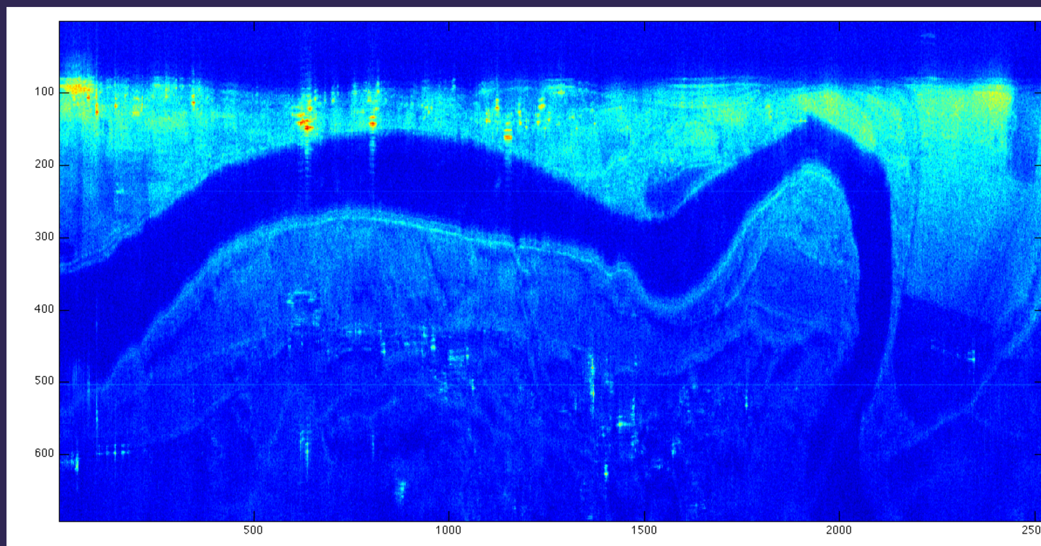

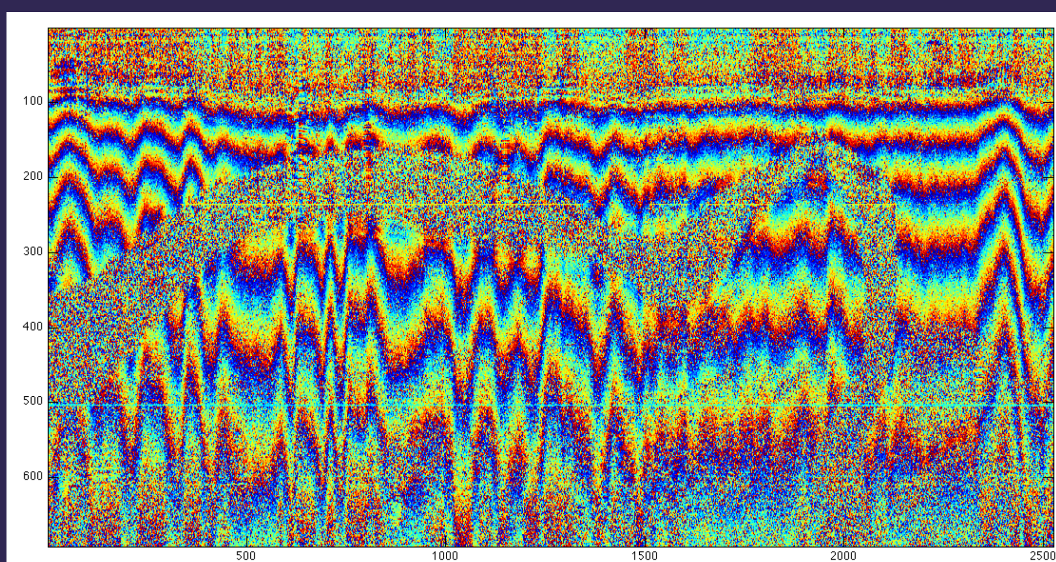

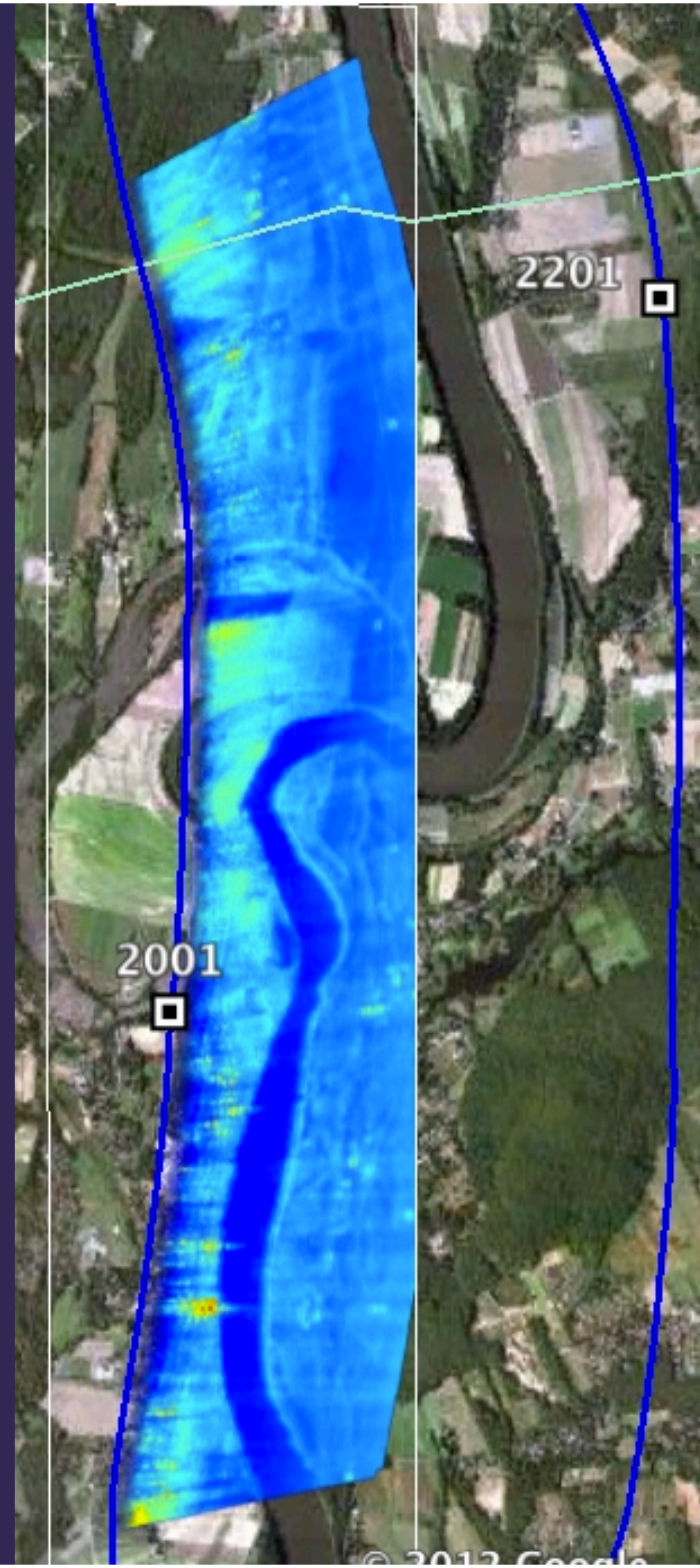

Real aperture results

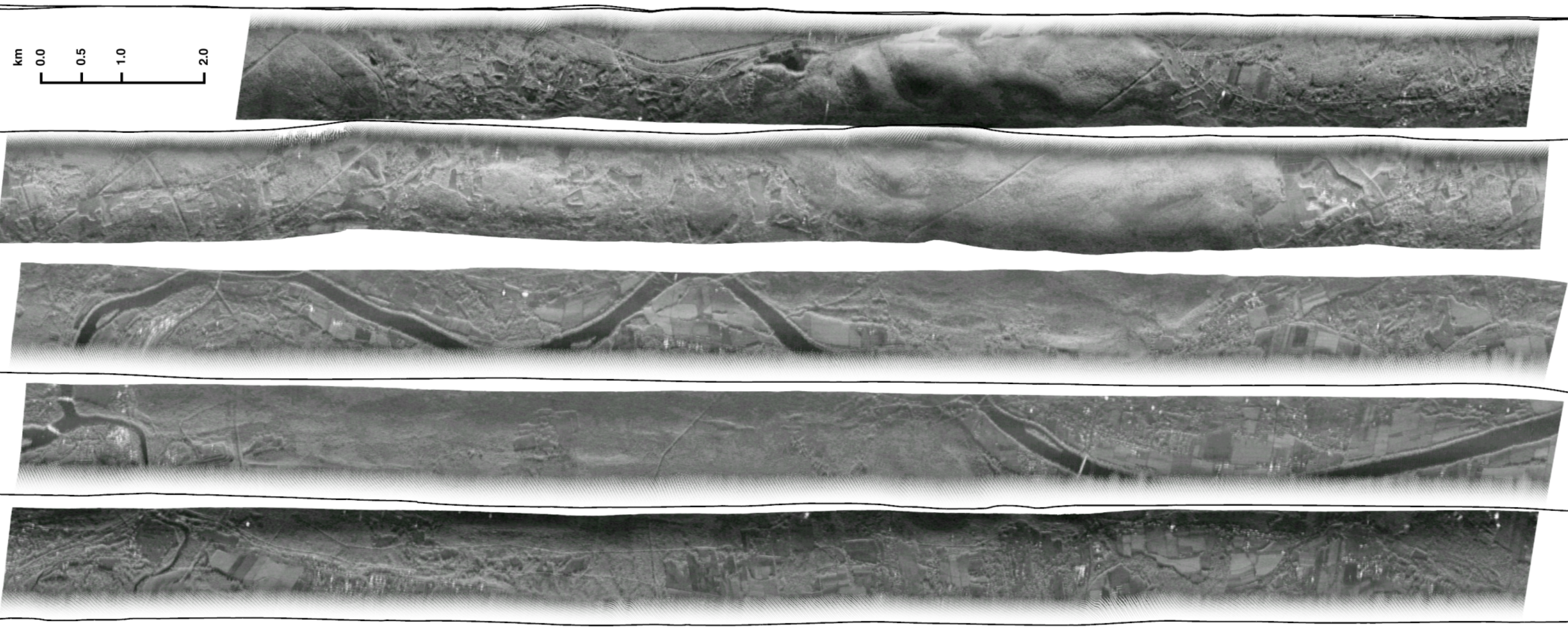

North ←

Results of SAR (2)

Flight direction

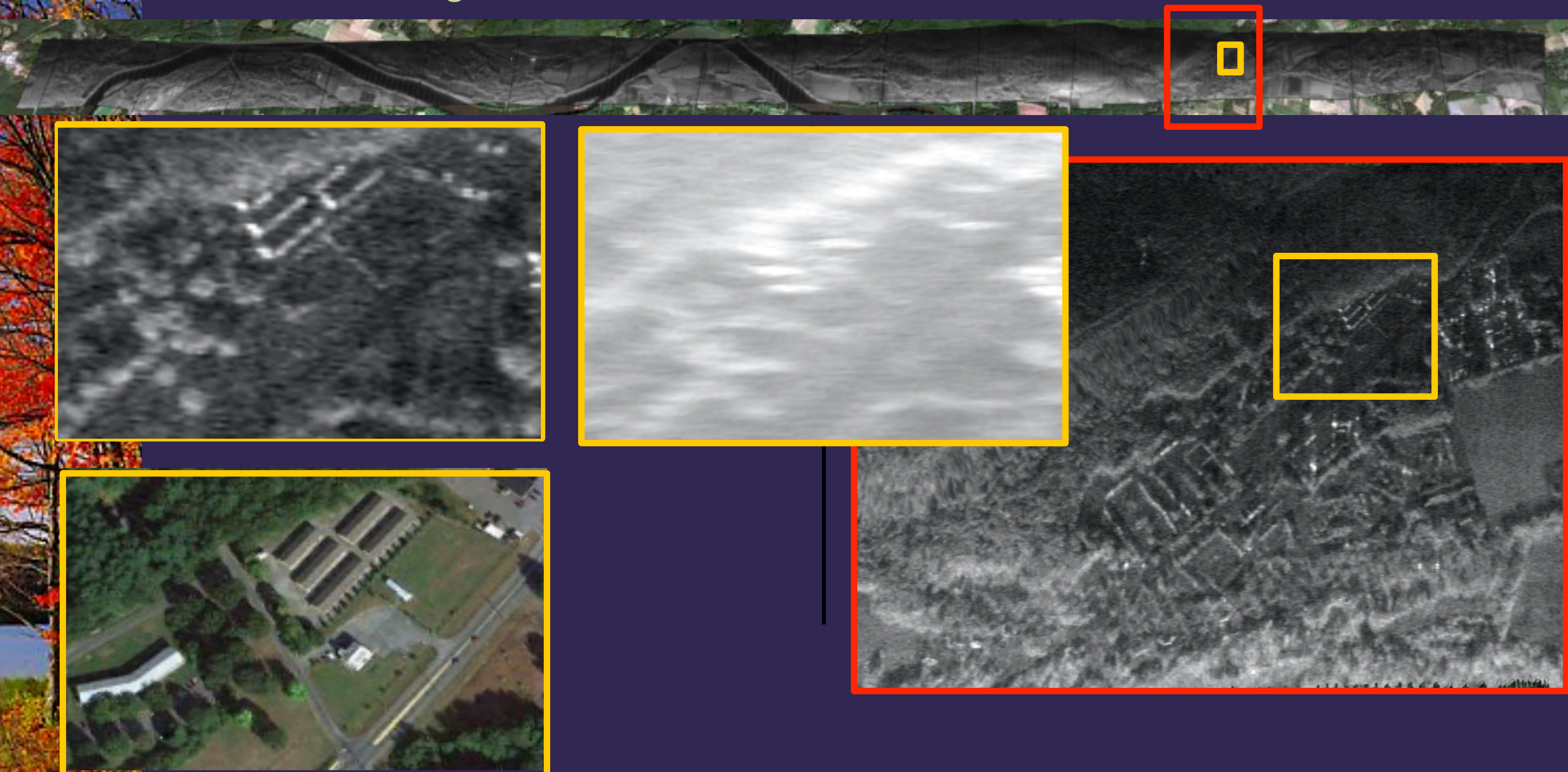

Thermal characterization

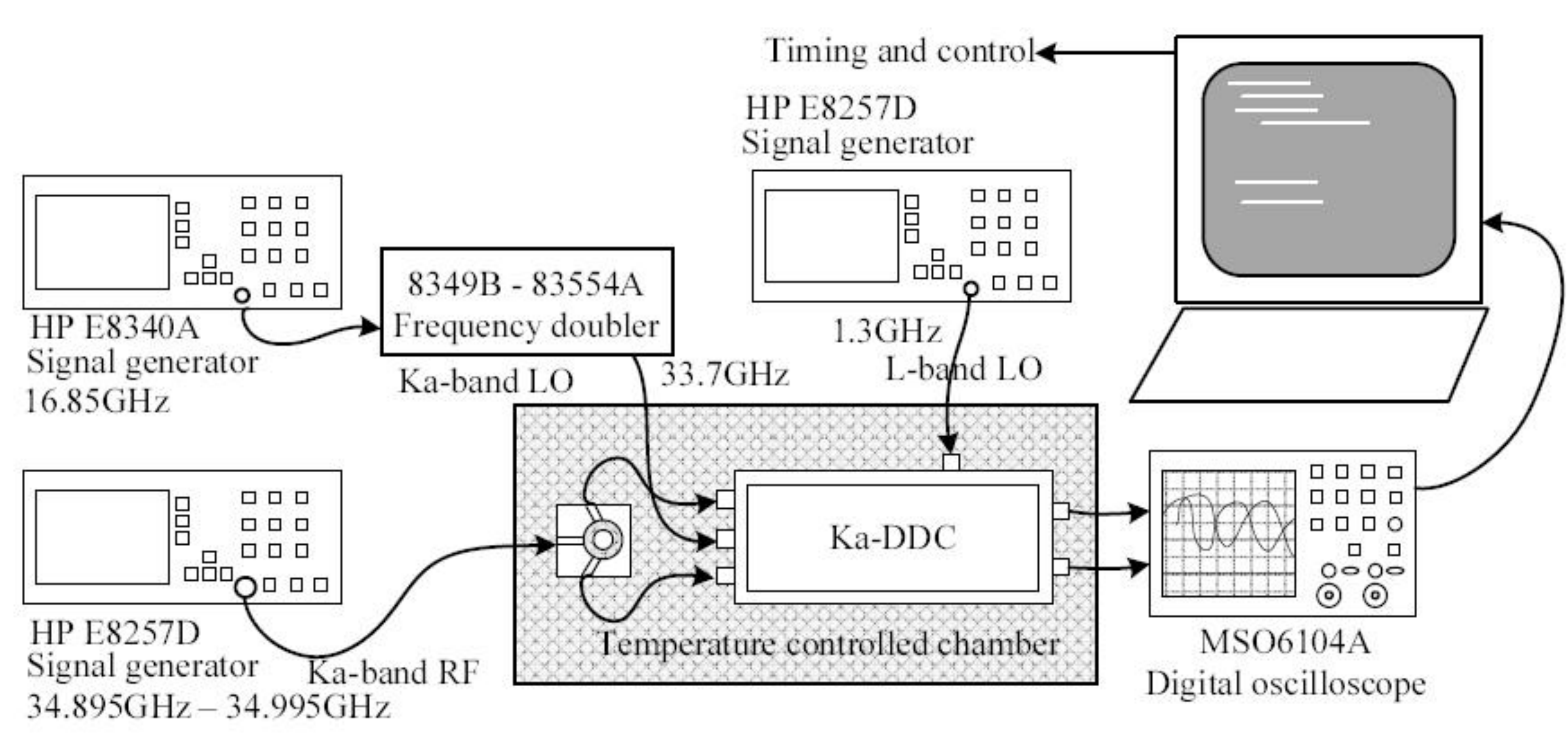

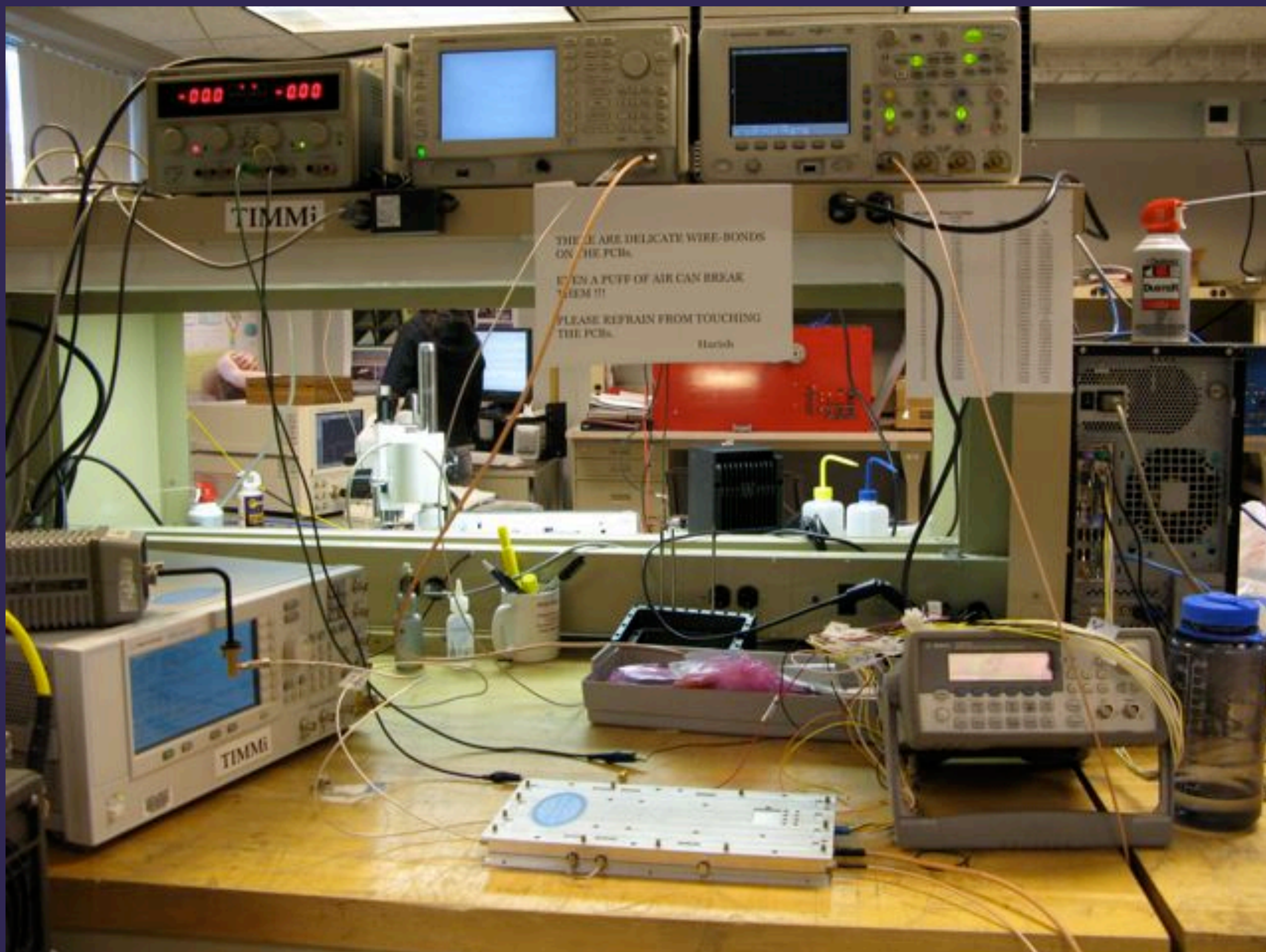
TIMMi
PLEASE REFRAIN FROM TOUCHING
THE PCBs.
Harish
TIMMi

A 3D-relief of previous Ka-band board

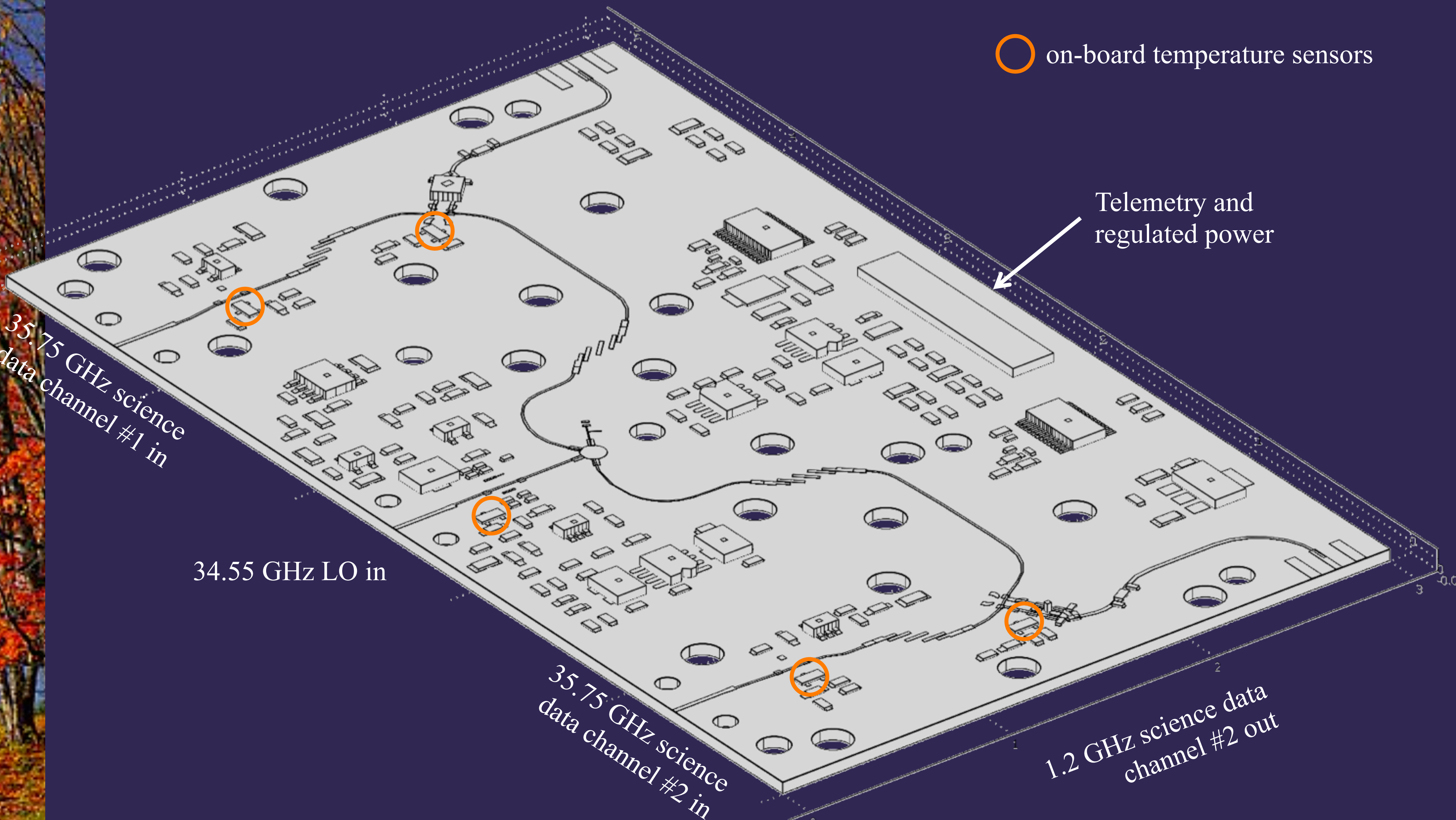

Used for COMSOL FEM modeling

ARGO Profiler Array for Measuring Sea Surface Height

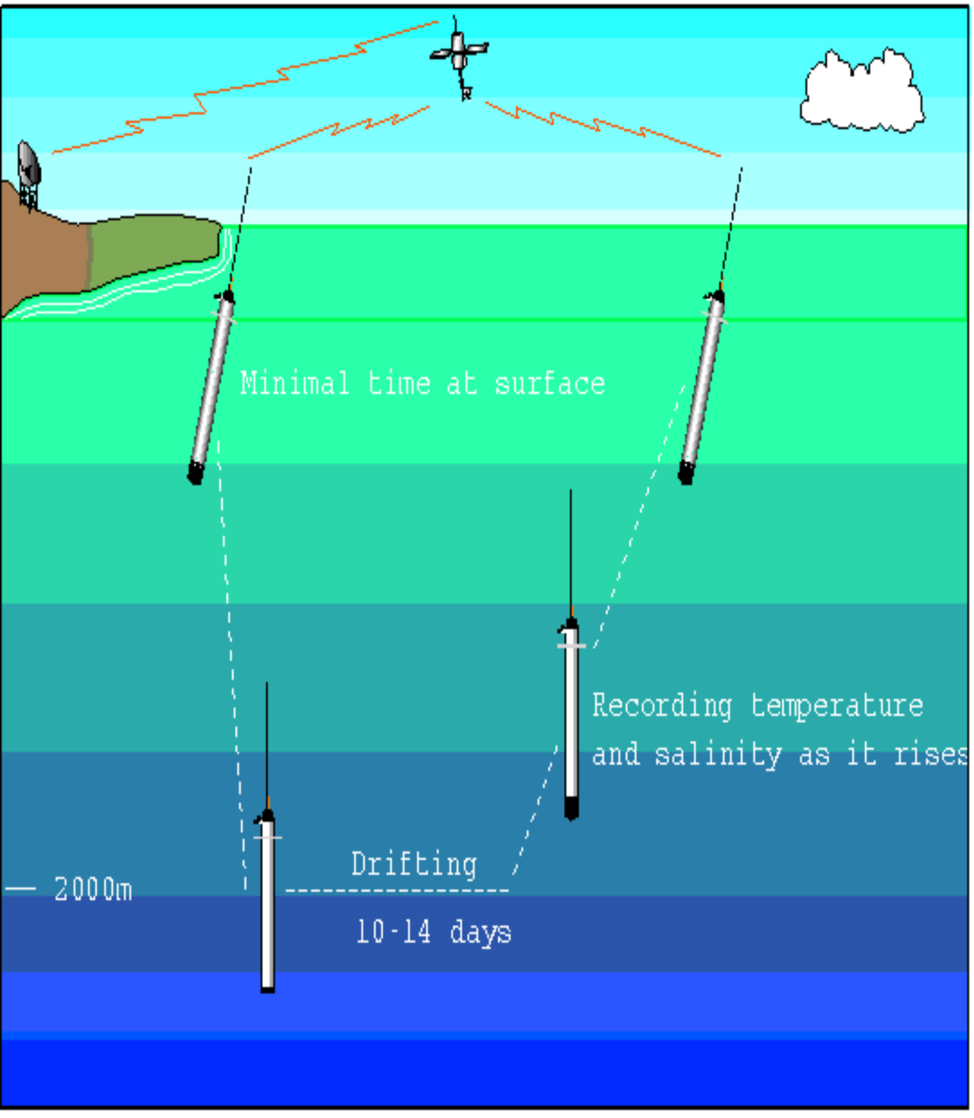

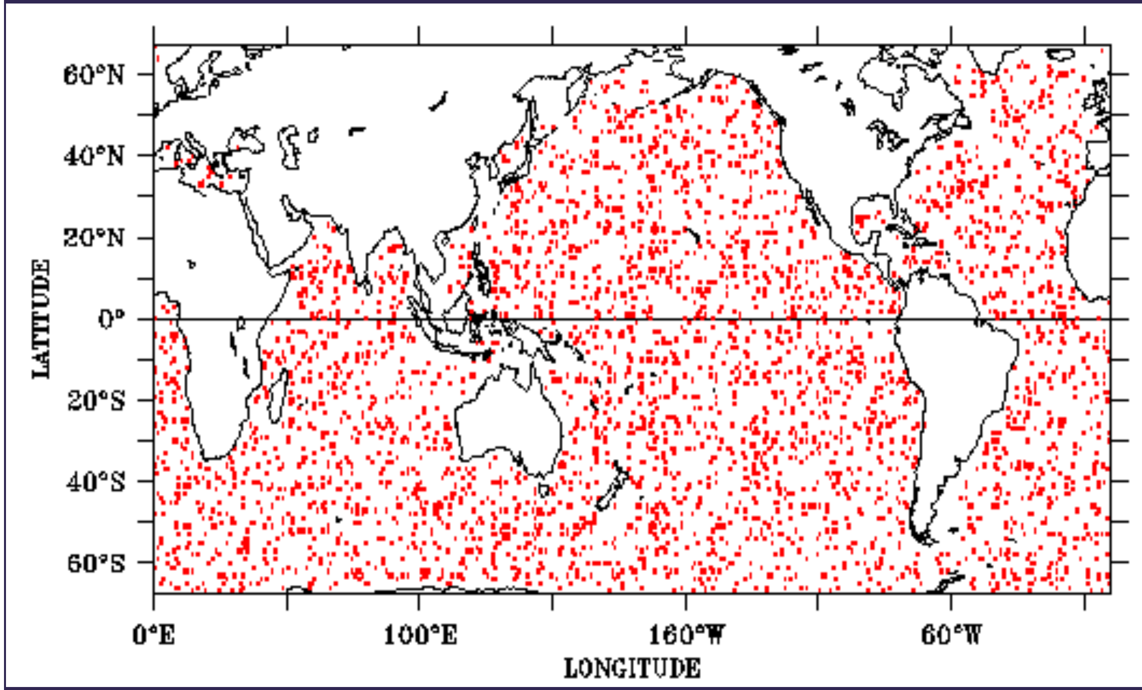

Sea Ice & Phase Change

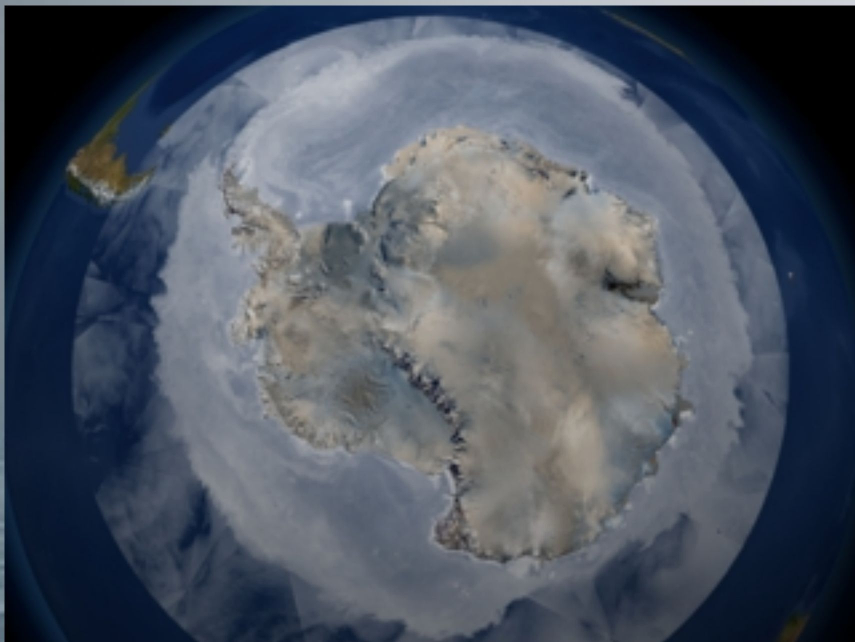

Modeled Thermal Imbalance

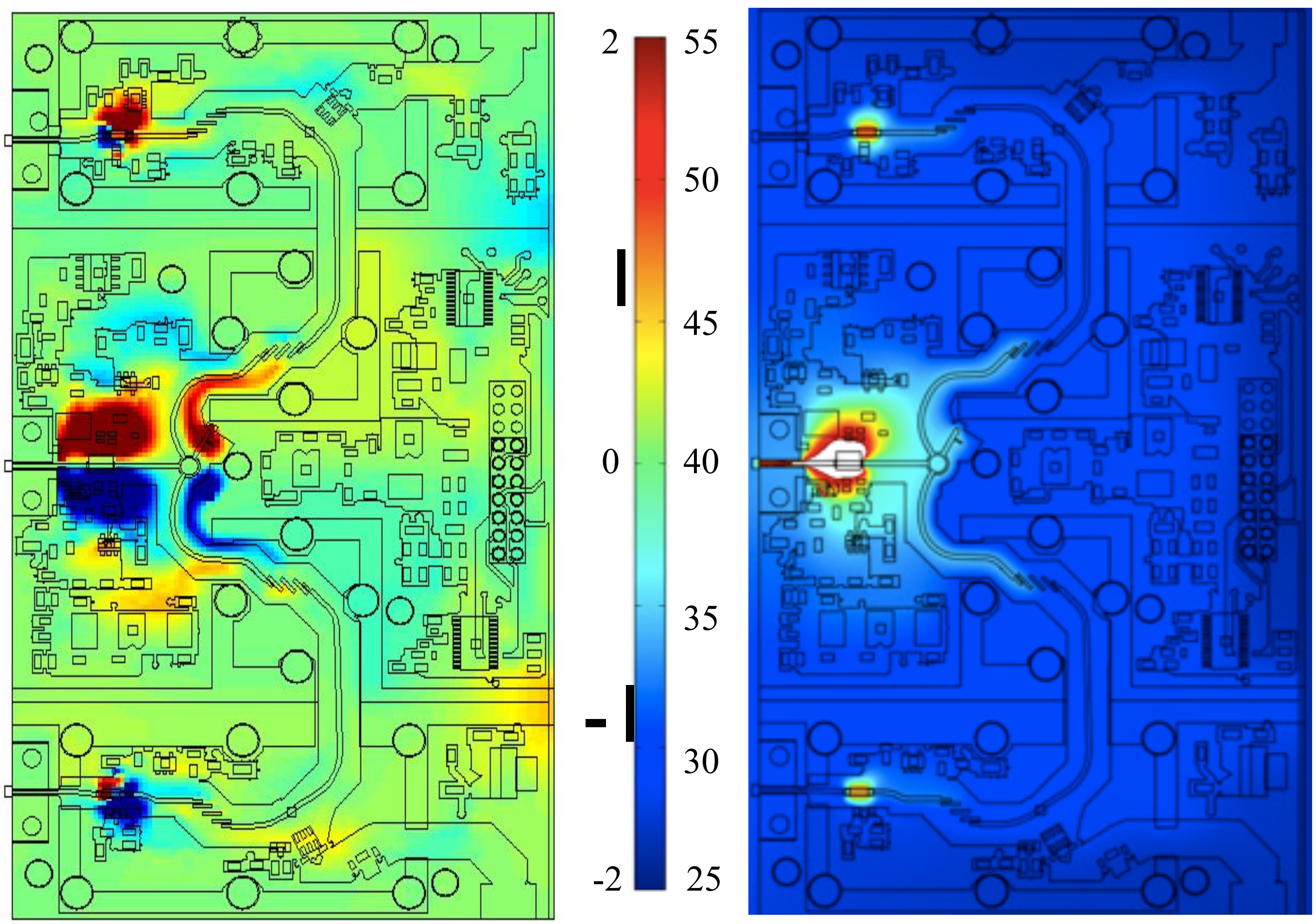

Temperature imbalance (°C)   Temperature (°C)

- COMSOL used to solve the heat equation and estimate board temperture and thermal imbalances.

- Thermal assymetry in the downconverter design will lead to an assymetry in the electrical path length.

- While this is not a bad thing in of itself, in a dynamic temperature environment, it will create a bias in the phase measurements, and hence the inferred height.

SWOT
(Surface Water and Ocean Topography Mission)

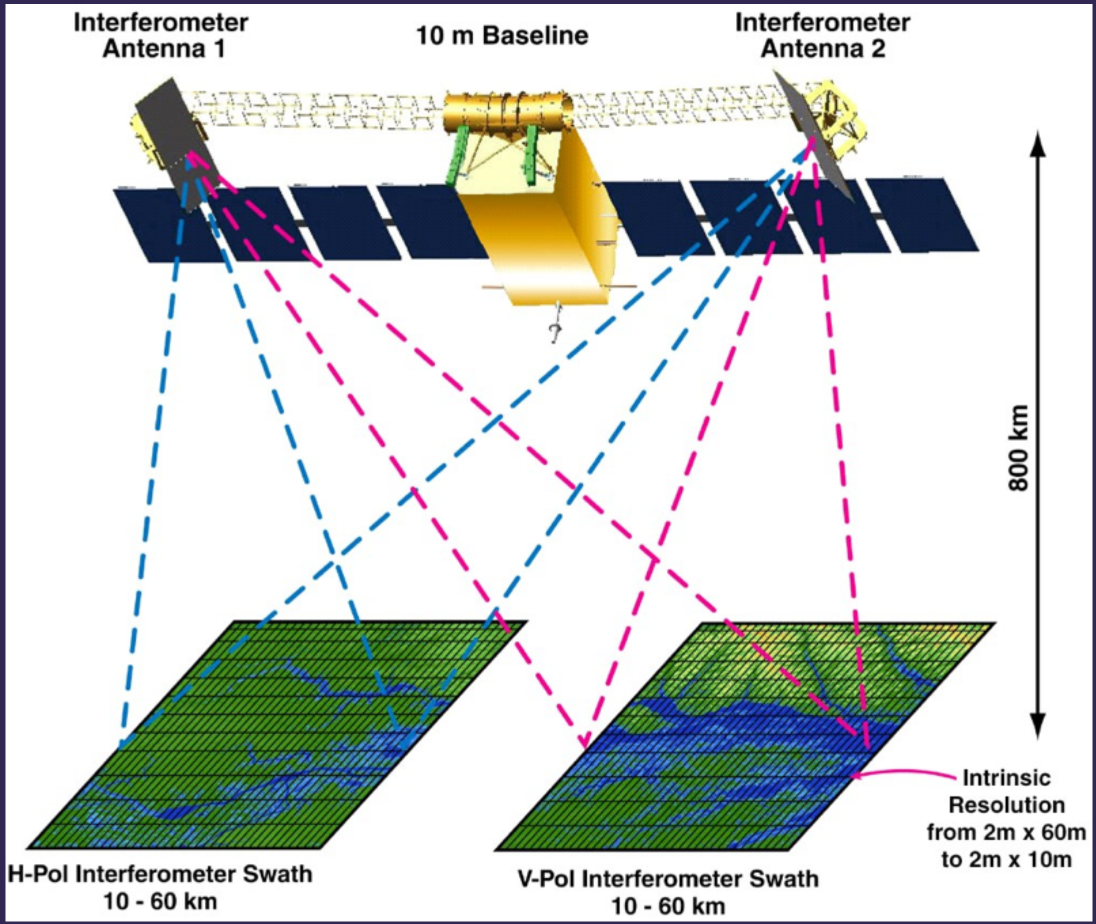

- Intended to launch in 2017
- Mission goal is to measure water height to within 7 cm accuracy, at a resolution between 50 and 100 m.
- Applications are for ocean topography and inland water monitoring

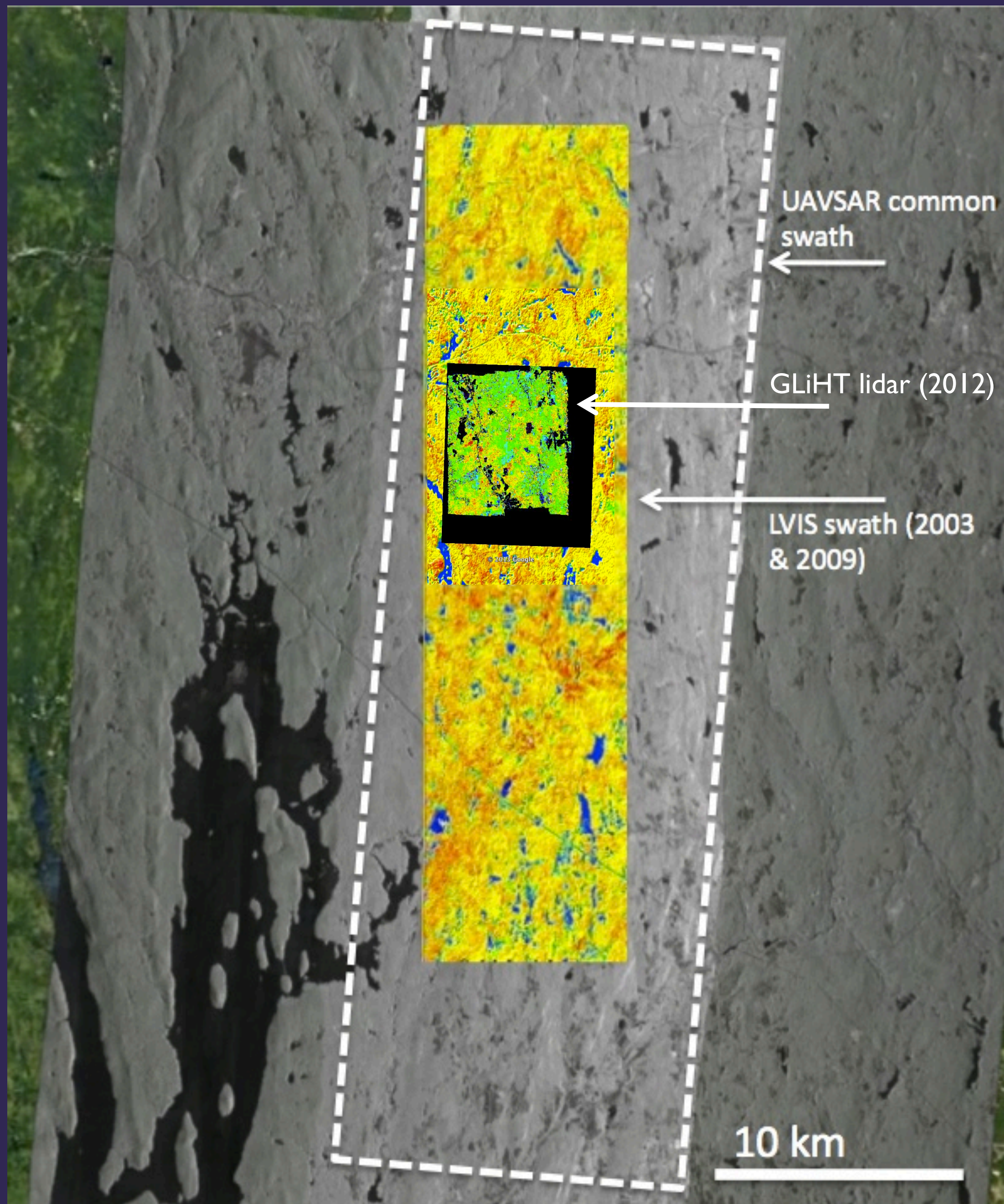
UAVSAR common swath
GLiHT lidar (2012)
LVIS swath (2003 & 2009)
10 km

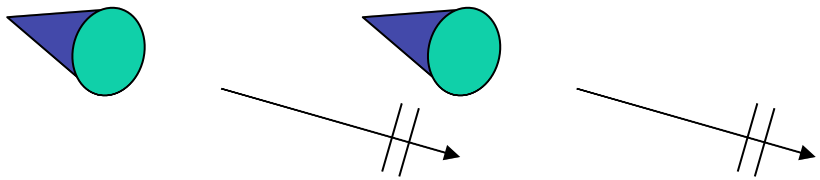

Single Antenna Backscatter

$$\left\langle \left|E_1\right|^2 \right\rangle = A^4 \int_{vol} W_r^{\,2} W_\eta^{\,2} e^{-\kappa z/\cos\theta} \rho(z) \left\langle f_b^{\,2} \right\rangle d^3 r$$

Two Antenna Interferometry

$$\gamma = \left\langle E_1 E_2^* \right\rangle = A^4 \int_{vol} e^{-ik_z z} W_r^{\,2} W_\eta^{\,2} e^{-\kappa z/\cos\theta} \left\langle f_b^{\,2} \right\rangle d^3 r$$

height dependent
phase term

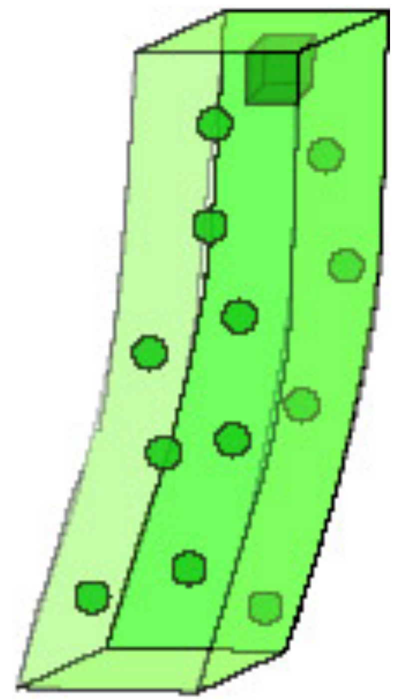

Thermal Testing and Characterization is a tricky affair

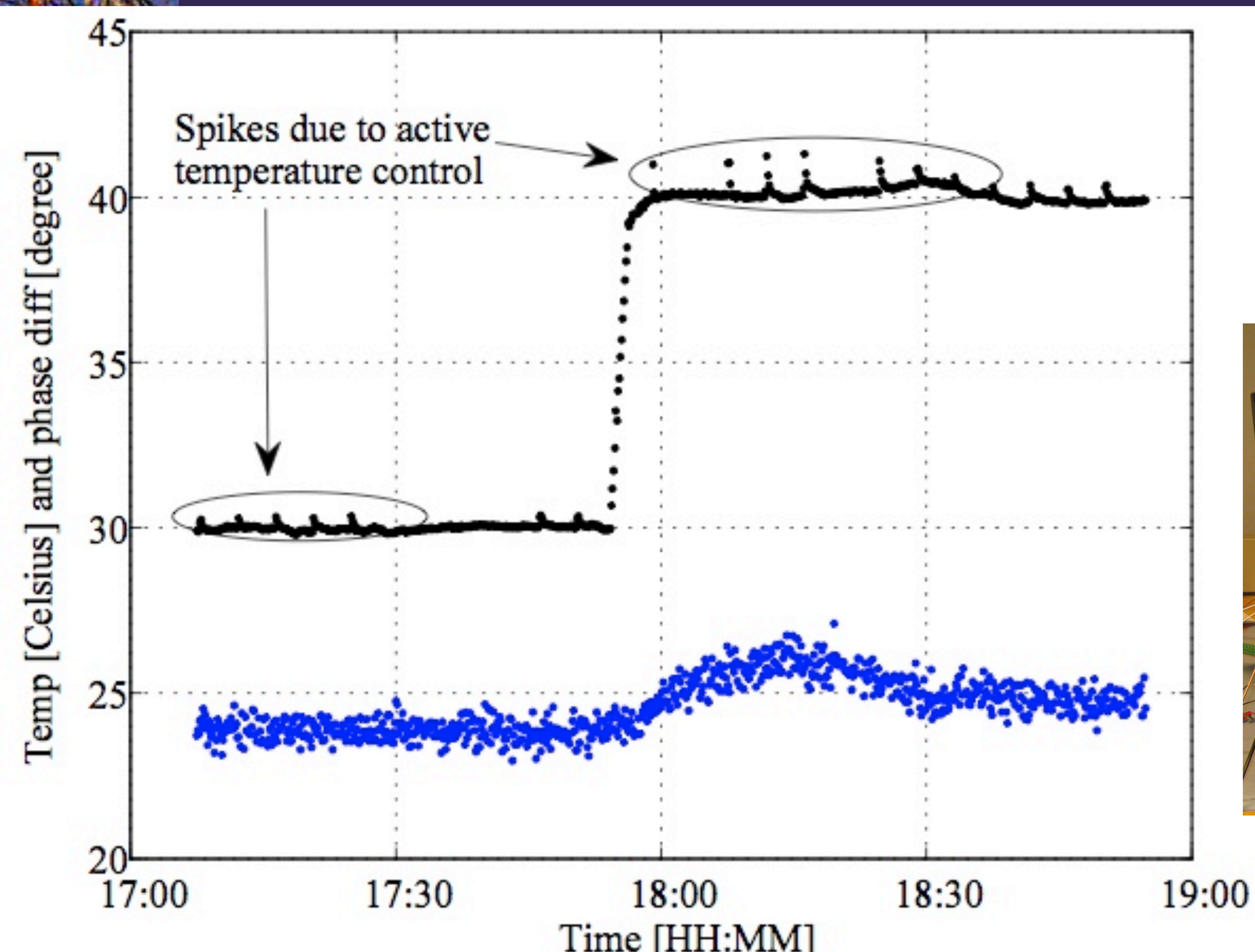

0.25°C/second, 15°C/min; -100°C to 300°C temperature range

Remote operation via serial port or IEEE-488 bus

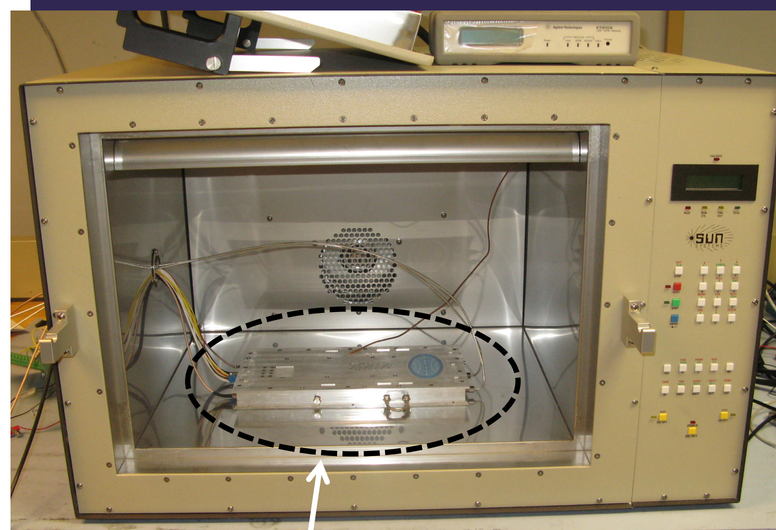

downconverter